PHOTOPHYSICS OF C_{60} COLLOIDS

A Dissertation Submitted to the Faculty of the
COLLEGE OF OPTICAL SCIENCES
In Partial Fulfillment of the Requirements For the Degree of
DOCTOR OF PHILOSOPHY
In the Graduate College
THE UNIVERSITY OF ARIZONA

Andrew F. Clements

November 28, 2012

Report Documentation Page

Form Approved
OMB No. 0704-0188

1. REPORT DATE **28 NOV 2012**	2. REPORT TYPE **Briefing Charts**	3. DATES COVERED **17-03-2012 to 22-10-2012**
4. TITLE AND SUBTITLE **Photophysics of C60 Colloids**		5a. CONTRACT NUMBER
		5b. GRANT NUMBER
		5c. PROGRAM ELEMENT NUMBER
6. AUTHOR(S) **Andrew Clements**		5d. PROJECT NUMBER
		5e. TASK NUMBER
		5f. WORK UNIT NUMBER
7. PERFORMING ORGANIZATION NAME(S) AND ADDRESS(ES) **U.S. Army TARDEC,6501 East Eleven Mile Rd,Warren,Mi,48397-5000**		8. PERFORMING ORGANIZATION REPORT NUMBER **#23508**
9. SPONSORING/MONITORING AGENCY NAME(S) AND ADDRESS(ES) **U.S. Army TARDEC, 6501 East Eleven Mile Rd, Warren, Mi, 48397-5000**		10. SPONSOR/MONITOR'S ACRONYM(S) **TARDEC**
		11. SPONSOR/MONITOR'S REPORT NUMBER(S) **#23508**

12. DISTRIBUTION/AVAILABILITY STATEMENT
Approved for public release; distribution unlimited

13. SUPPLEMENTARY NOTES

14. ABSTRACT
Briefing Charts

15. SUBJECT TERMS

16. SECURITY CLASSIFICATION OF:			17. LIMITATION OF ABSTRACT	18. NUMBER OF PAGES	19a. NAME OF RESPONSIBLE PERSON
a. REPORT **unclassified**	b. ABSTRACT **unclassified**	c. THIS PAGE **unclassified**	**Public Release**	**115**	

Standard Form 298 (Rev. 8-98)
Prescribed by ANSI Std Z39-18

Outline

- Intro to C_{60} Colloids
- Desired NLO Response
- Overview of Nonlinear Scattering and Absorption
- Previous Scholarship/Context
- Thesis Question
- Overview of Research
- Discussions of Experiments and Findings
  - Basic Characterization
  - Transient Absorption Spectroscopy
  - Z-Scan
  - Total Scattering
  - Computer Modeling
- Conclusions

Description of C_{60} Colloids

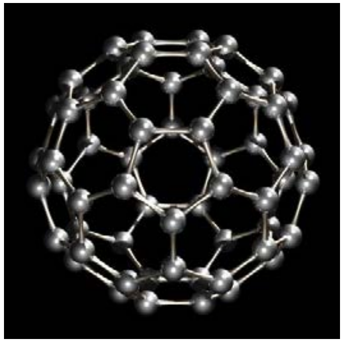

C_{60} Molecules

- Cage molecules composed of 60 carbon atoms
- Diameter: 0.88 nm
- NLO Response Mechanism: Nonlinear absorption

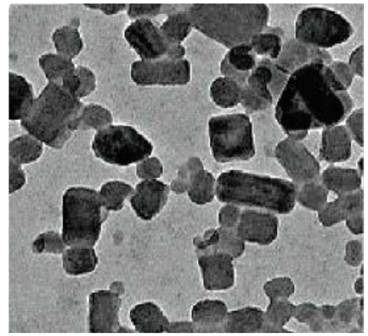

C_{60} Colloids

- Aggregates of C_{60} molecules
- Diameter: A few nm to microns
- Morphology: Fractal to crystalline
- NLO Response Mechanism: Expected to have both nonlinear absorption and nonlinear scattering

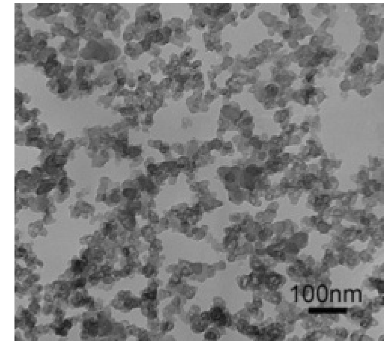

Carbon Black

- Aggregates of carbon atoms
- Diameter: 10 nm to microns
- Morphology: Amorphous (can be spheroidal, ellipsoidal, linear, or branched)
- NLO Response Mechanism: Nonlinear scattering

Images from:
- www.webelements.com/carbon/allotropes.html
- J. D. Fortner, D. Y. Lyon, C. M. Sayes, A. M. Boyd, J. C. Falkner, E. M. Hotze, L. B. Alemany, Y. J. Tao, W. Guo, K. D. Ausman, V. L. Colvin and J. B. Hughes, Environ. Sci. Technol. **39** (11), 4307-4316 (2005).
- http://openi.nlm.nih.gov/detailedresult.php?img=3211877_1556-276X-6-457-2&query=the&fields=all&favor=none&it=none&sub=none&uniq=0&sp=none&req=4&simCollection=1074344_1476-9255-1-2-2&npos=18&prt=3

Description of C_{60} Colloids

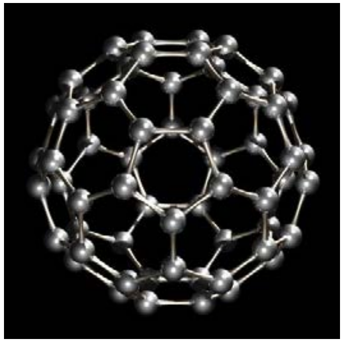

C_{60} Molecules

- Cage molecules composed of 60 carbon atoms
- Diameter: 0.88 nm
- NLO Response Mechanism: Nonlinear absorption

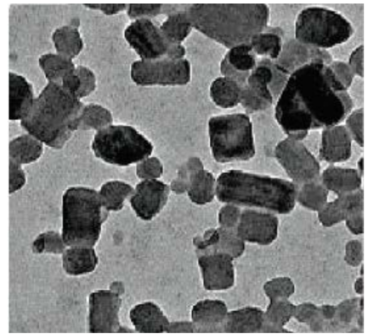

C_{60} Colloids

- Aggregates of C_{60} molecules
- Diameter: A few nm to microns
- Morphology: Fractal to crystalline
- NLO Response Mechanism: Expected to have both nonlinear absorption and nonlinear scattering

Could this result in stronger NLO response?

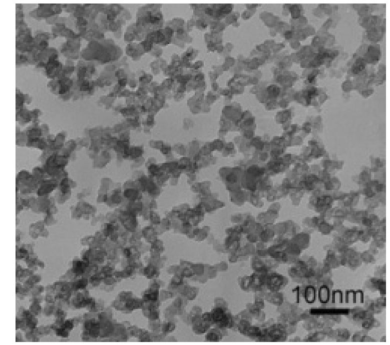

Carbon Black

- Aggregates of carbon atoms
- Diameter: 10 nm to microns
- Morphology: Amorphous (can be spheroidal, ellipsoidal, linear, or branched)
- NLO Response Mechanism: Nonlinear scattering

Images from:
- www.webelements.com/carbon/allotropes.html
- J. D. Fortner, D. Y. Lyon, C. M. Sayes, A. M. Boyd, J. C. Falkner, E. M. Hotze, L. B. Alemany, Y. J. Tao, W. Guo, K. D. Ausman, V. L. Colvin and J. B. Hughes, Environ. Sci. Technol. **39** (11), 4307-4316 (2005).
- http://openi.nlm.nih.gov/detailedresult.php?img=3211877_1556-276X-6-457-2&query=the&fields=all&favor=none&it=none&sub=none&uniq=0&sp=none&req=4&simCollection=1074344_1476-9255-1-2-2&npos=18&prt=3

Desired Nonlinear Optical Response

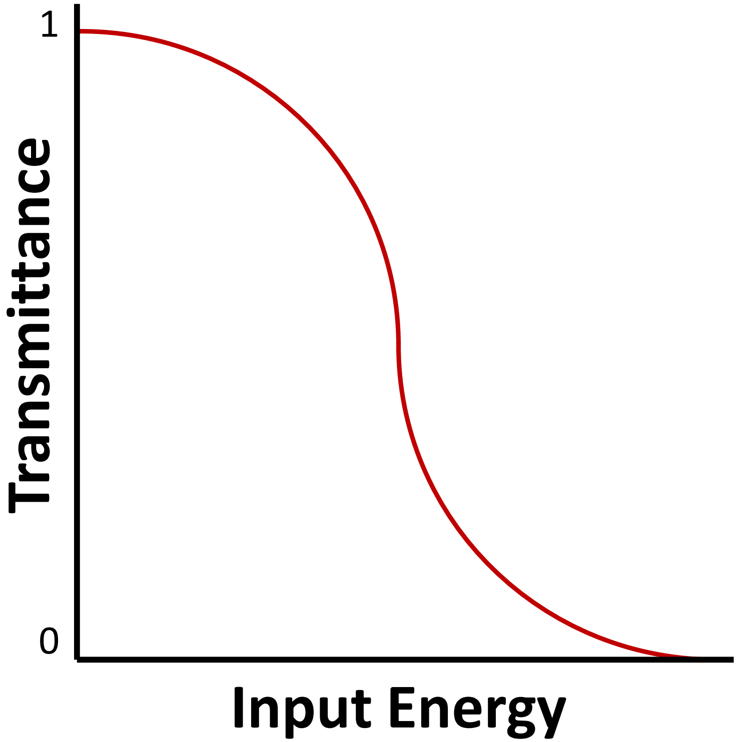

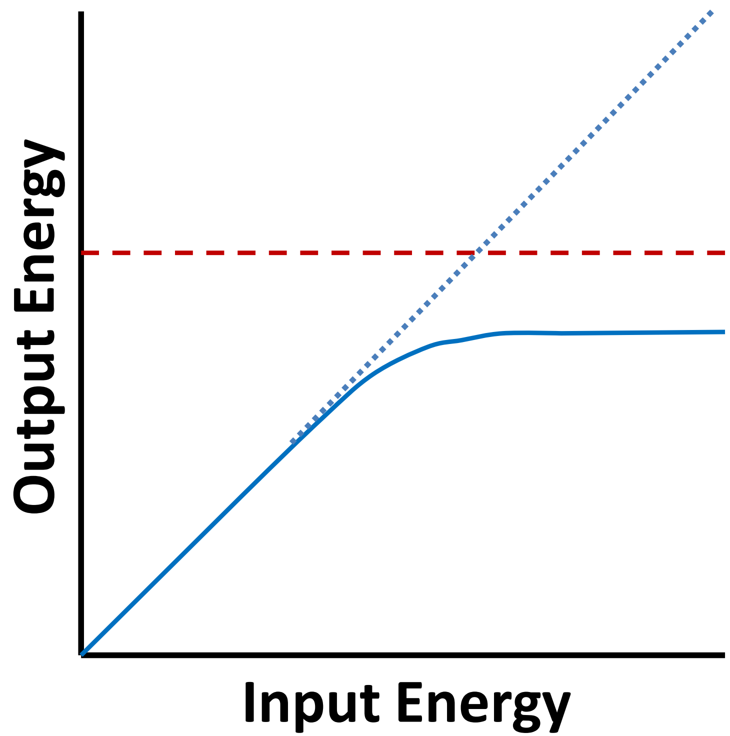

Potential Applications:

- All-optical switching
- Optical limiting
- Etc.

NLO Response of Real Materials

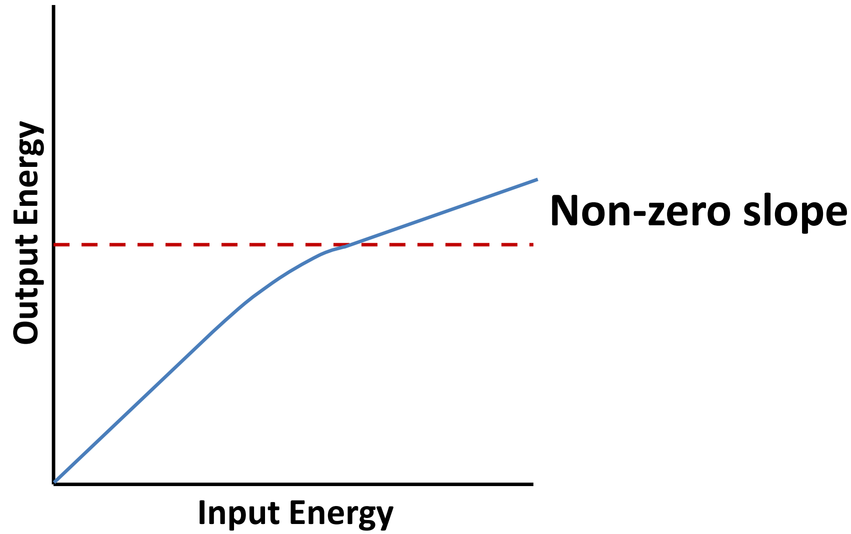

Desired Improvements:

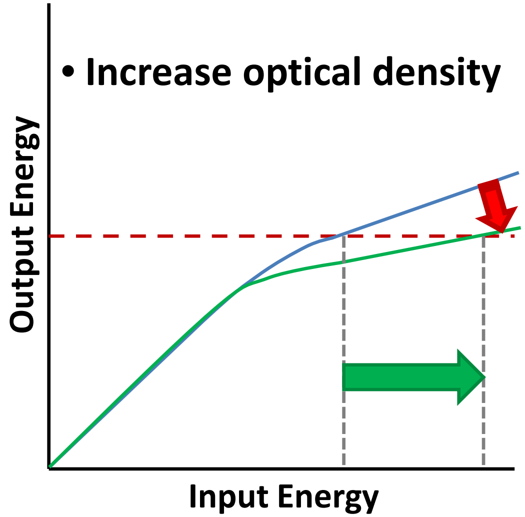

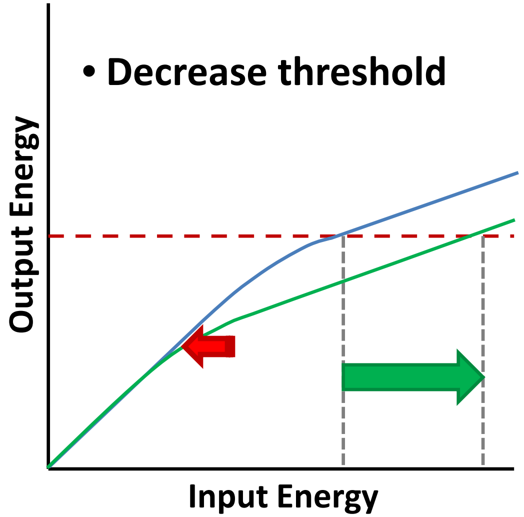

General Classes of Optical Limiting/Switching Materials

- Two Photon Absorbers
  - Instantaneous $\chi^{(3)}$ nonlinearity.
  - Irradiance dependent, so most effective at very short pulse lengths. Less effective at nanosecond or longer pulse lengths.
  - Relatively high activation threshold.
  - Highly transmissive in the visible spectrum.
- Excited State Absorbers
  - Effective at attenuating picosecond pulses if the excited singlet absorption cross-section is greater than the ground state cross-section.
  - Effective at attenuating nanosecond pulses if the excited triplet absorption cross-section is greater than the ground state cross-section.
  - Often highly colored.
  - Excited state absorption spectra are often narrow.
  - Highly concentration dependent.
  - Can have very low activation thresholds.
- Nonlinear Scatterers
  - Response due to phase change caused by heating of particles by absorbed light. Scattering centers take time to nucleate, so less effective below 1 ns.
  - Color neutral.
  - Broadband NLO response.
- Other
  - Nonlinear refraction (self-focusing and self-defocusing)
  - Photorefractives (slow response)
  - Liquid crystals (slow response)
  - Free carrier absorption (semiconductors)
  - Metal nanoparticles

<u>Bottom line</u>:
No one NLO material is best for all temporal and spectral regimes.
All have some room for improvement.

The primary mechanisms considered in this dissertation are nonlinear scattering and excited state absorption.

Nonlinear Scattering

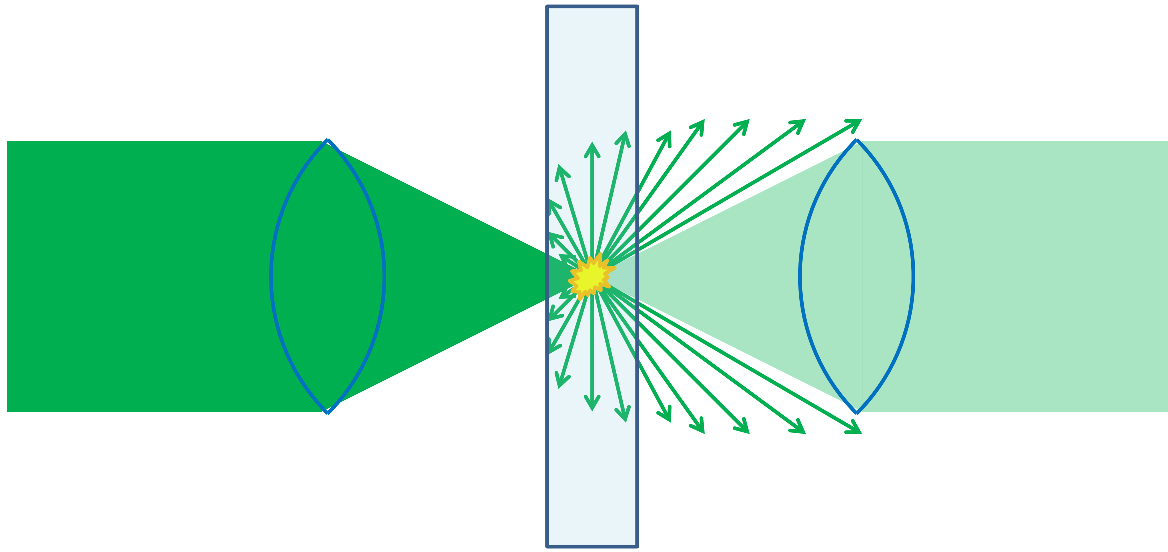

$I=I_0e^{-\alpha L}$

$\alpha=\sigma_{ext}N$

$\sigma_{ext}=\sigma_{abs} + \sigma_{scat}$

- Carbon black particles have strong linear absorption
- Absorbed energy rapidly heats the particles.
- Scattering centers form as a result of phase change (bubble formation from boiling of the liquid or vaporization of the particle). Light scatters out of the propagation path.
- Enhanced absorption from nanoplasmas.

Nonlinear Absorption

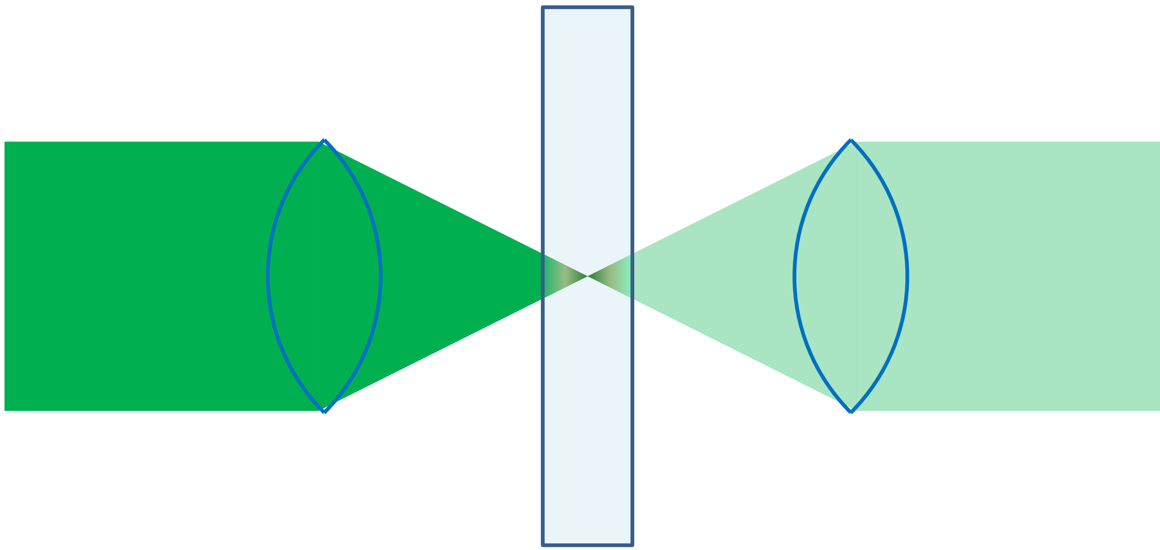

$I = I_0 e^{-\alpha L}$
$\alpha = \sigma_{ext} N$
$\sigma_{ext} = \sigma_{abs}$

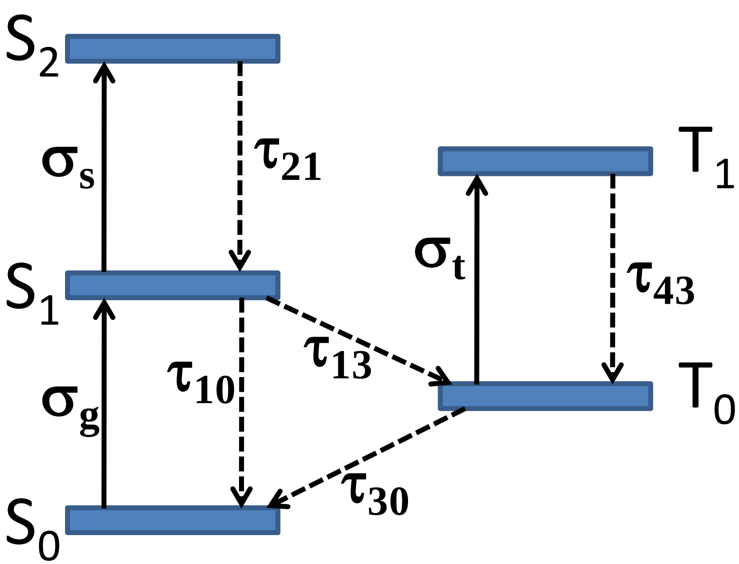

C_{60} has strong RSA.

Reverse Saturable Absorption

- Excited singlet and/or excited triplet state has a larger absorption cross-section than the ground state cross-section
- Long-lived excited state(s)
- Efficient inter-system crossing (ISC) to the triplet manifold

Previous Scholarship / Context

- K. Mansour, M. J. Soileau and E. W. Vanstryland, J. Opt. Soc. Am. B-Opt. Phys. 9 (7), 1100-1109 (1992).
  - Pioneering work in carbon black suspensions
- D. Riehl and F. Fougeanet, Molecular Crystals and Liquid Crystals Science and Technology Section B: Nonlinear Optics 21 (1-4), 391-398 and 435-446 (1999).
  - Thermodynamic model of bubble creation in CBS
    - My modeling drew from this work
- K. J. McEwan, P. K. Milsom and D. B. James, presented at the Nonlinear Optical Liquids for Power Limiting and Imaging. San Diego, CA, 1998.
  - Beer-Lambert law with a digital extinction coefficient to model beam propagation in CBS
    - My modeling drew from this work
- H. W. Kroto, J. R. Heath, S. C. Obrien, R. F. Curl and R. E. Smalley, Nature 318 (6042), 162-163 (1985).
  - Discovery & naming of C_{60} (Buckminsterfullerene)
- L. W. Tutt and A. Kost, Nature 356, 225-226 (1992).
  A. Kost, L. W. Tutt, M. B. Klein, T. K. Dougherty and W. E. Elias, Opt. Lett. 18 (5), 334-336 (1993).
  - Pioneering work with C_{60} as an optical limiter
- K. M. Nashold and D. P. Walter, Journal of the Optical Society of America B (Optical Physics) 12 (7), 1228-1237 (1995).
  - Examined transmitted, scattered, and absorbed energy in CBS and C_{60}
    - Fore-runner of the total scattering experiment that I extended to C_{60} colloids
- D. M. Guldi, R. E. Huie, P. Neta, H. Hungerbühler and K.-D. Asmus, Chemical Physics Letters **223** (5-6), 511-516 (1994). & M. Fujitsuka, H. Kasai, A. Masuhara, S. Okada, H. Oikawa, H. Nakanishi, A. Watanabe and O. Ito, Chem. Lett. (12), 1211-1212 (1997).
  - Nanosecond laser flash photolysis of C_{60} colloids

Thesis Question

- Can the combination of nonlinear absorption and nonlinear scattering processes in C_{60} colloids result in a stronger NLO response (more attenuation) than benchmark materials such as CBS and molecular C_{60} solutions?
- How can the C_{60} colloid material system be optimized for nonlinear transmission based on an understanding of the processes involved?

Dissertation Research Overview

• Transmission Electron Microscopy	Particle size & morphology
• Dynamic Light Scattering • Nanoparticle Tracking Analysis	Particle size distribution
• UV-Vis Spectrometry	Linear absorption spectrum
• Femtosecond Transient Absorption Spectroscopy • Nanosecond Laser Flash Photolysis	Nonlinear absorption spectra and kinetics
• Z-Scan	Nonlinear absorption coefficient, triplet-triplet absorption cross-section
• Total Scattering	Total accounting for transmitted, scattered, and absorbed energy
• Computer modeling	Analysis of results with respect to theory

Samples

- CBS-1 (Monarch-1000® carbon black in water)
- CBS-2 (Sterling-1120® carbon black in water)
- C_{60}-Tol (C_{60} in Toluene molecular solution)
- C_{60}-1 (C_{60} colloids in water with 15% Triton X-100)
- C_{60}-2 (C_{60} colloids in water with 11% Triton X-100)
- C_{60}-3 (C_{60} colloids in water with 10% Triton X-100)

Why 3 colloid samples? To investigate if the photophysics are dependent upon particle size.

[Note: Each of the colloidal C_{60} samples were made by different synthesis techniques. The goal of C_{60}-3 was to synthesize a much smaller particle size than C_{60}-1 and C_{60}-2.]
[Note: C_{60} has an extremely low solubility in water. C_{60} is highly soluble in toluene and there is much published data on C_{60} in toluene, so this was chosen for the solution.]

Dissertation Research Outline

• Transmission Electron Microscopy	Particle size & morphology
• Dynamic Light Scattering • Nanoparticle Tracking Analysis	Particle size distribution
• UV-Vis Spectrometry	Linear absorption spectrum
• Femtosecond Transient Absorption Spectroscopy • Nanosecond Laser Flash Photolysis	Nonlinear absorption spectra and kinetics
• Z-Scan	Nonlinear absorption coefficient, triplet-triplet absorption cross-section
• Total Scattering	Total accounting for transmitted, scattered, and absorbed energy
• Computer modeling	Analysis of results with respect to theory

Transmission Electron Microscopy: Colloid C_{60}-1

Broad size distribution of colloidal particles. Most < 100 nm. Several near 5 nm.

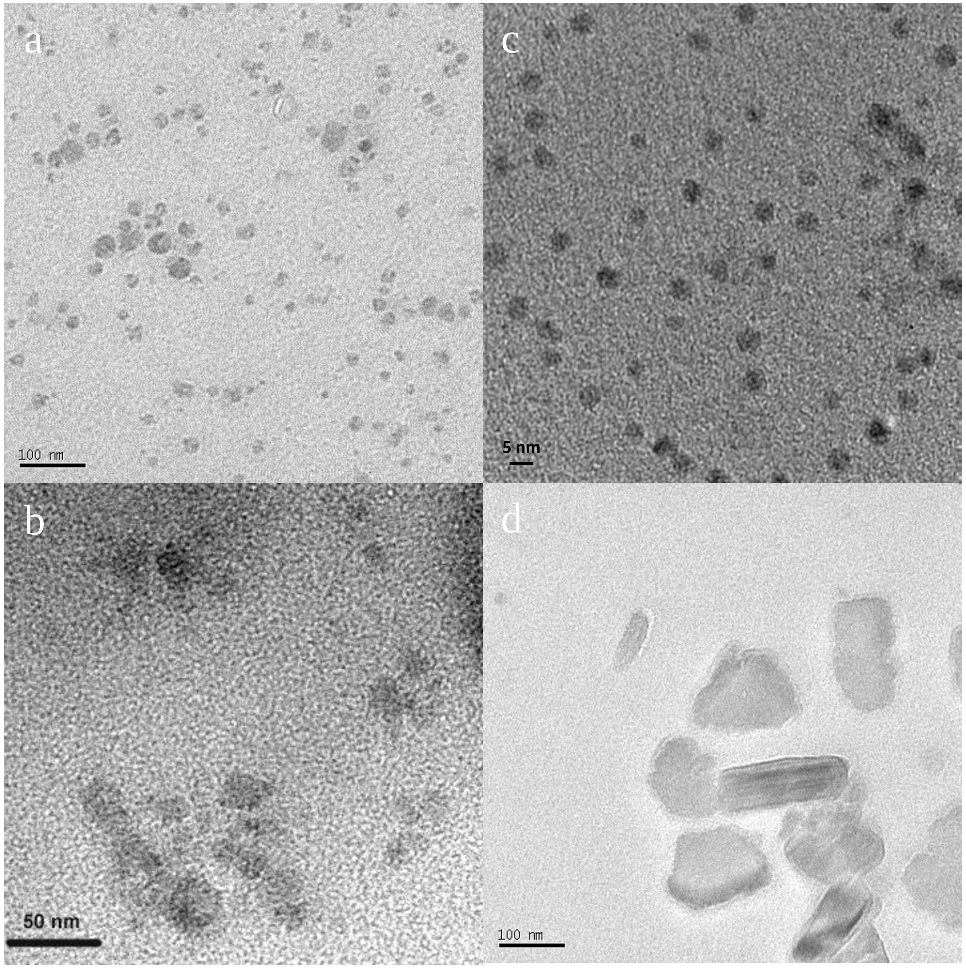

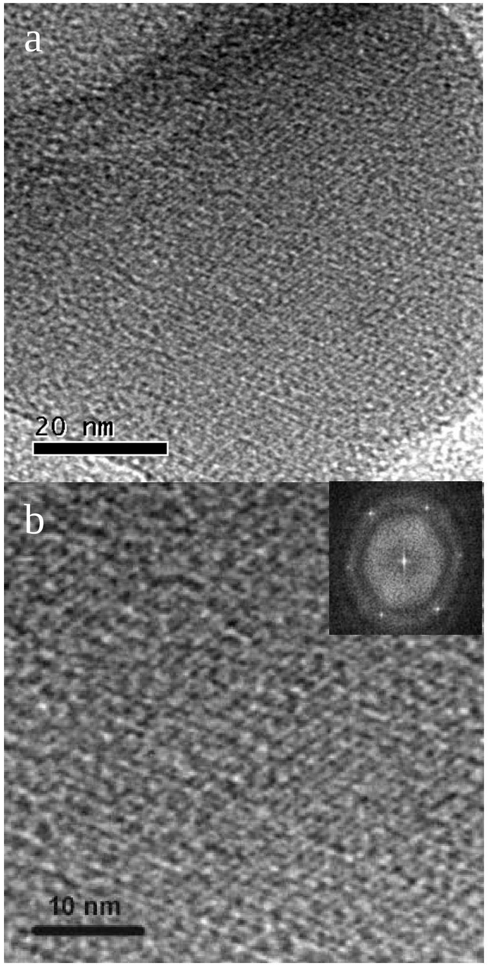

Particles > 30 nm showed sharp edges and lattice fringes: signs of crystallinity.
Fourier transform of HR-TEM shows
FCC or hexagonal close packed pattern.

Transmission Electron Microscopy: Colloid C_{60}-2

Broad size distribution of colloidal particles. Most < 100 nm. Several near 5 nm.

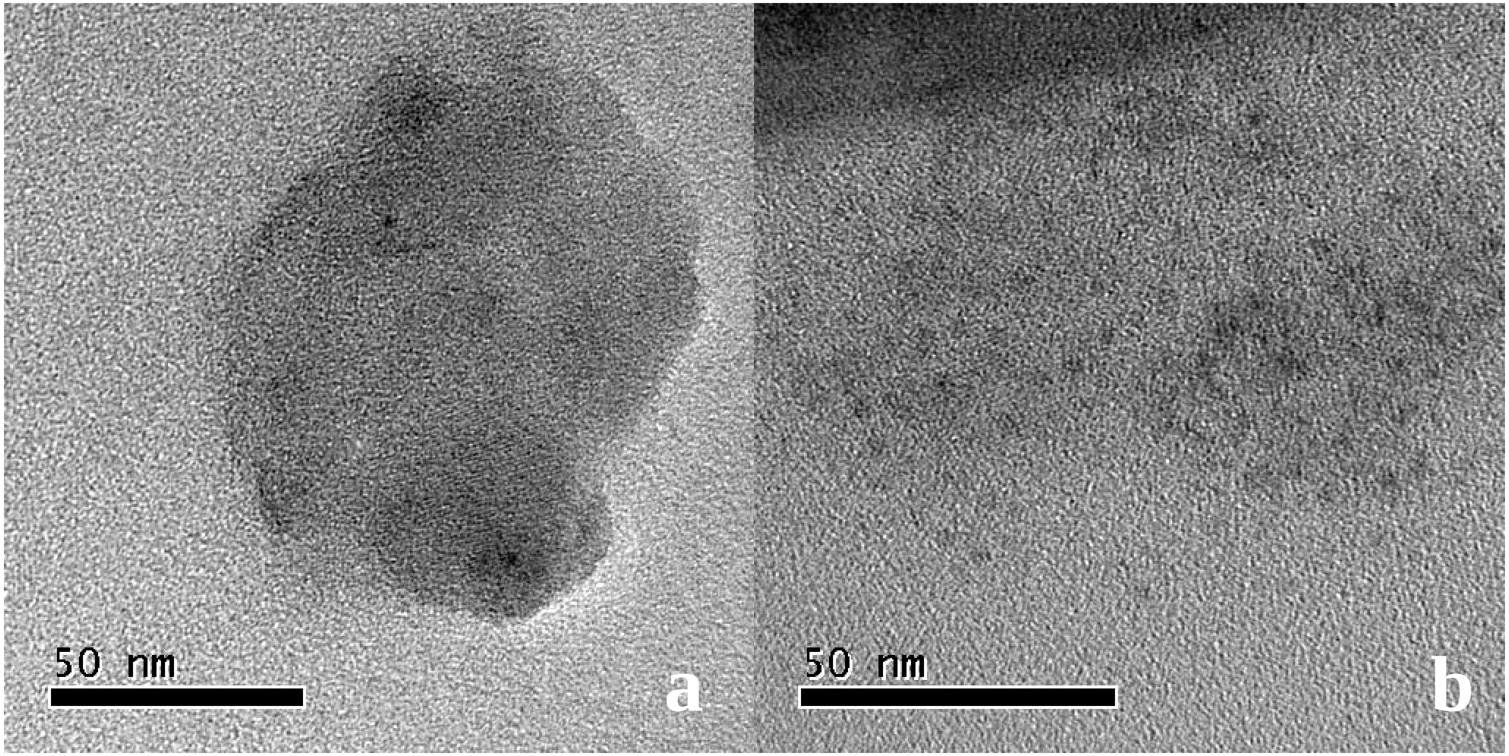

Particles appear more amorphous than C_{60}-1. Little or no evidence of lattice fringes.

Transmission Electron Microscopy: Colloid C_{60}-3

Mixture of small particles (5-10 nm) and agglomerates (50-80 nm).
Agglomerates seem to be made of round primary particles ~ 5-10 nm.

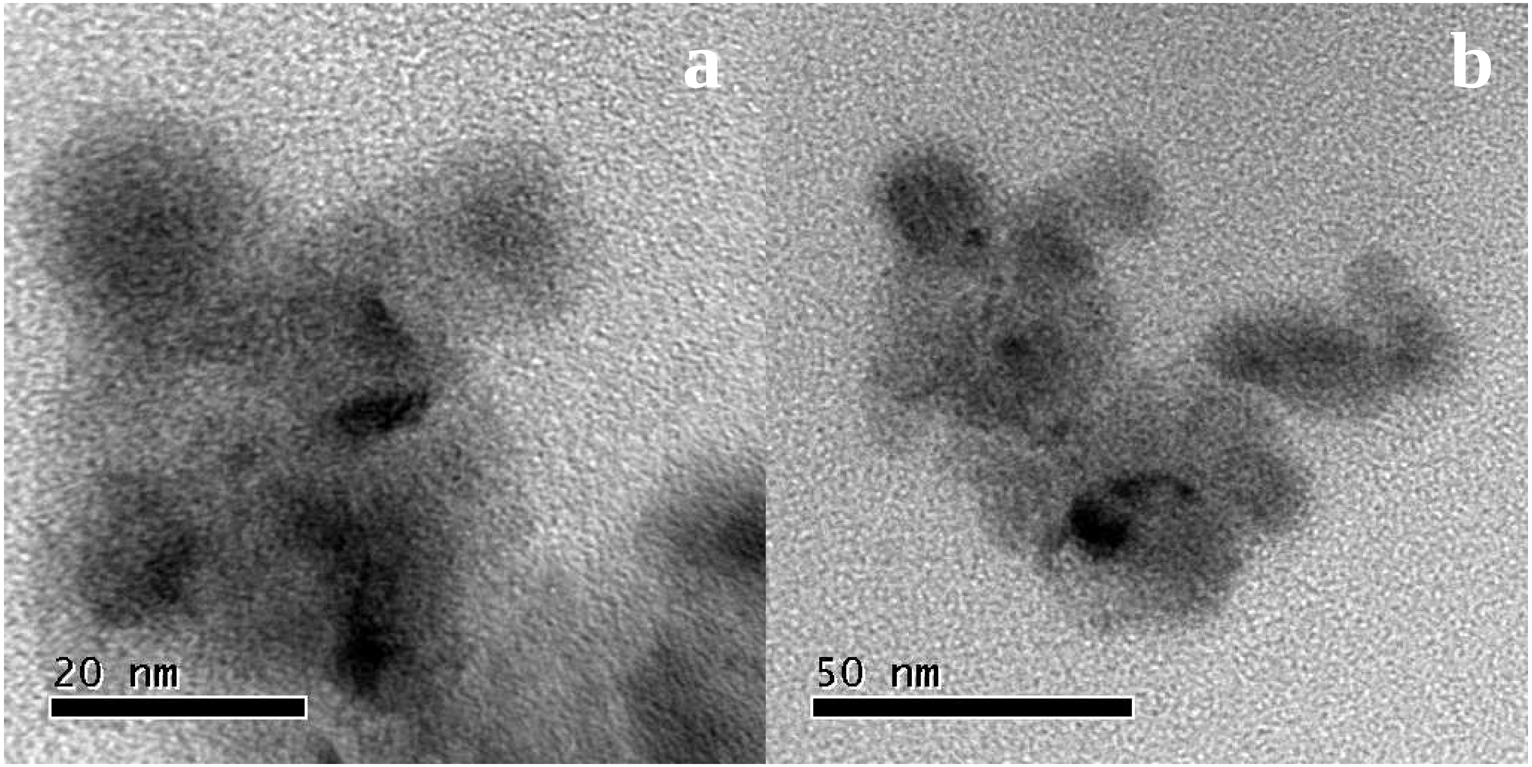

Particles appear more amorphous than C_{60}-1. Little or no evidence of lattice fringes.

TEM Conclusions

- **TEMs showed that C_{60}-1 was highly crystalline, but C_{60}-2 and C_{60}-3 were amorphous.**

Dissertation Research Outline

Technique	Information
✓ Transmission Electron Microscopy	Particle size & morphology
• Dynamic Light Scattering • Nanoparticle Tracking Analysis	Particle size distribution
• UV-Vis Spectrometry	Linear absorption spectrum
• Femtosecond Transient Absorption Spectroscopy • Nanosecond Laser Flash Photolysis	Nonlinear absorption spectra and kinetics
• Z-Scan	Nonlinear absorption coefficient, triplet-triplet absorption cross-section
• Total Scattering	Total accounting for transmitted, scattered, and absorbed energy
• Computer modeling	Analysis of results with respect to theory

Dynamic Light Scattering Results

Sample Description	Z-average (nm)		Intensity (nm)		Volume (nm)		Number (nm)	
	APS	PDI	APS	PW	APS	PW	APS	PW
CBS-1 (transient abs.)	79.9	0.197	102	51.8	67.1	48.6	37.5	13.6
C_{60}-1 (0.2 µm filtered, transient absorption)	105	0.25	117	39.7	94.9	37.4	70.3	19.9
C_{60}-1 (unfiltered, transient absorption)	106	0.219	131	55.2	101	53.3	64.5	21.1
CBS-1 (total scattering)	81.11	0.246	113.6 (99) 4041 (1)	70.35 1066	53.14 (85.4) 253 (9.2) 4552 (5.4)	29.93 81.07 1070	33.63	12.55
CBS-2 (total scattering)	1086	0.6	2102 (90.5) 135.9 (9.5)	921.2 40.24	2815 (99) 135.4 (1)	1140 49.92	1600 (1.9) 102.3 (98.1)	765.8 36.05
C_{60}-1 (total scattering)	112.1	0.207	141.9	60.38	115.6	63.85	69.39	25.7
C_{60}-2 (total scattering)	102.2	0.181	124.7	51.73	95.16	50.63	61.97	21.14
C_{60}-3 (total scattering)	11.71	0.409	9.129 (75.3) 220.4 (21.4) 4543 (3.3)	2.655 92.29 944.9	7.308 (99.9) 217.3 (0.0) 4934 (0.1)	2.123 89.53 928.7	6.221	1.495

Example Plots: C_{60}-2

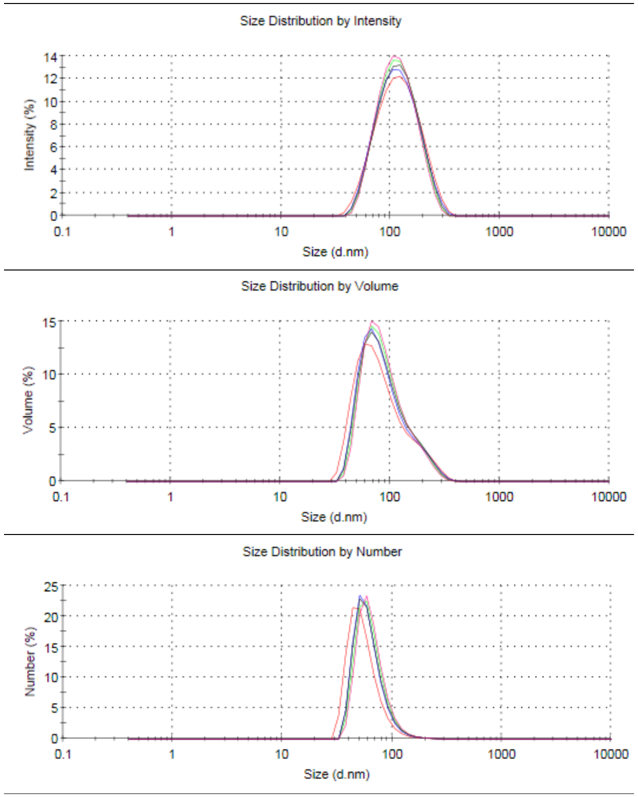

Nanoparticle Tracking Analysis Results

Sample Description	Mean (nm)	Mode (nm)	Standard Deviation (nm)	Cumulative Under Size D10 (nm)	D50 (nm)	D90 (nm)	Estimated Concentration (particles/mL)
CBS-1	143	89	78	62	123	256	1.3×10^8
CBS-2	151	127	80	71	133	256	0.93×10^8
C_{60}-1	100	67	66	44	81	173	2.7×10^8
C_{60}-2	106	74	65	52	88	175	1.92×10^8
C_{60}-3	157	80	96	66	133	274	1.67×10^8

Example Plot: C_{60}-2

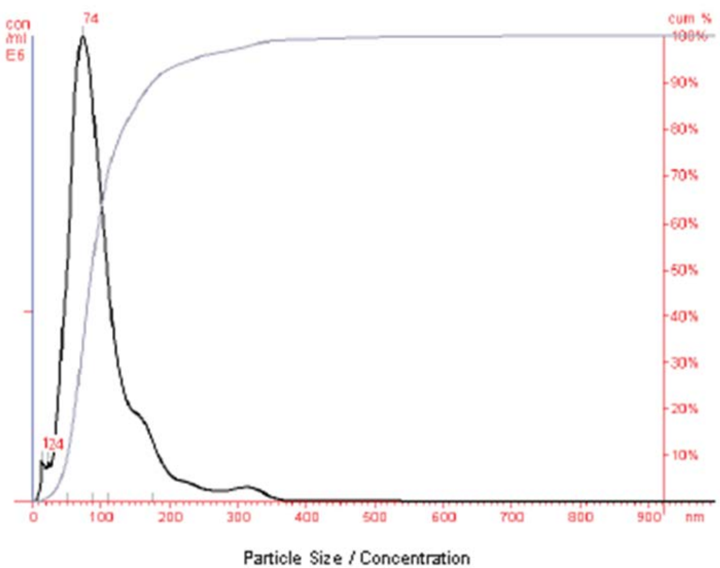

Results

Mean:	106 nm
Mode:	74 nm
SD:	65 nm
D10:	52 nm
D50:	88 nm
D90:	175 nm
User Lines:	0 nm, 0 nm
Concentration:	1.92 E8 particles/ml
Completed Tracks:	2161

Confirmed DLS size estimates for C_{60}-1 and C_{60}-2.

Other data is suspect: likely outside of NTA optimal range.

Particle Size Conclusions

- **Particle size measurements showed broad size distributions with average particle size diameters of (on a number density basis):**

35 nm for CBS-1,

100 nm, 1600 nm (bimodal) for CBS-2,

Very similar sizes, different morphology

69 nm for colloid C_{60}-1,

62 nm for colloid C_{60}-2,

and 6 nm for colloid C_{60}-3.

Same morphology, 10x size difference

[Note: Even though TEM showed some 5 nm particles in C_{60}-1 and C_{60}-2, DLS did not indicate a significant number of particles in this size regime. DLS looks at many more particles than TEM.]

Dissertation Research Outline

- ✓ Transmission Electron Microscopy — Particle size & morphology
- ✓ Dynamic Light Scattering
- ✓ Nanoparticle Tracking Analysis — Particle size distribution
- **UV-Vis Spectrometry — Linear absorption spectrum**
- Femtosecond Transient Absorption Spectroscopy
- Nanosecond Laser Flash Photolysis — Nonlinear absorption spectra and kinetics
- Z-Scan — Nonlinear absorption coefficient, triplet-triplet absorption cross-section
- Total Scattering — Total accounting for transmitted, scattered, and absorbed energy
- Computer modeling — Analysis of results with respect to theory

UV-Vis Spectrometry Results

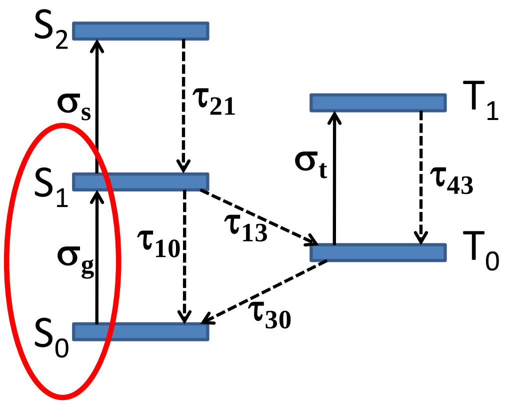

- Ground state absorption spectrum
- 350, 410, 600 nm features characteristic of C_{60}
- 450 nm feature characteristic of C_{60} colloids
- Note: C_{60}-2 has higher peaks than C_{60}-1.

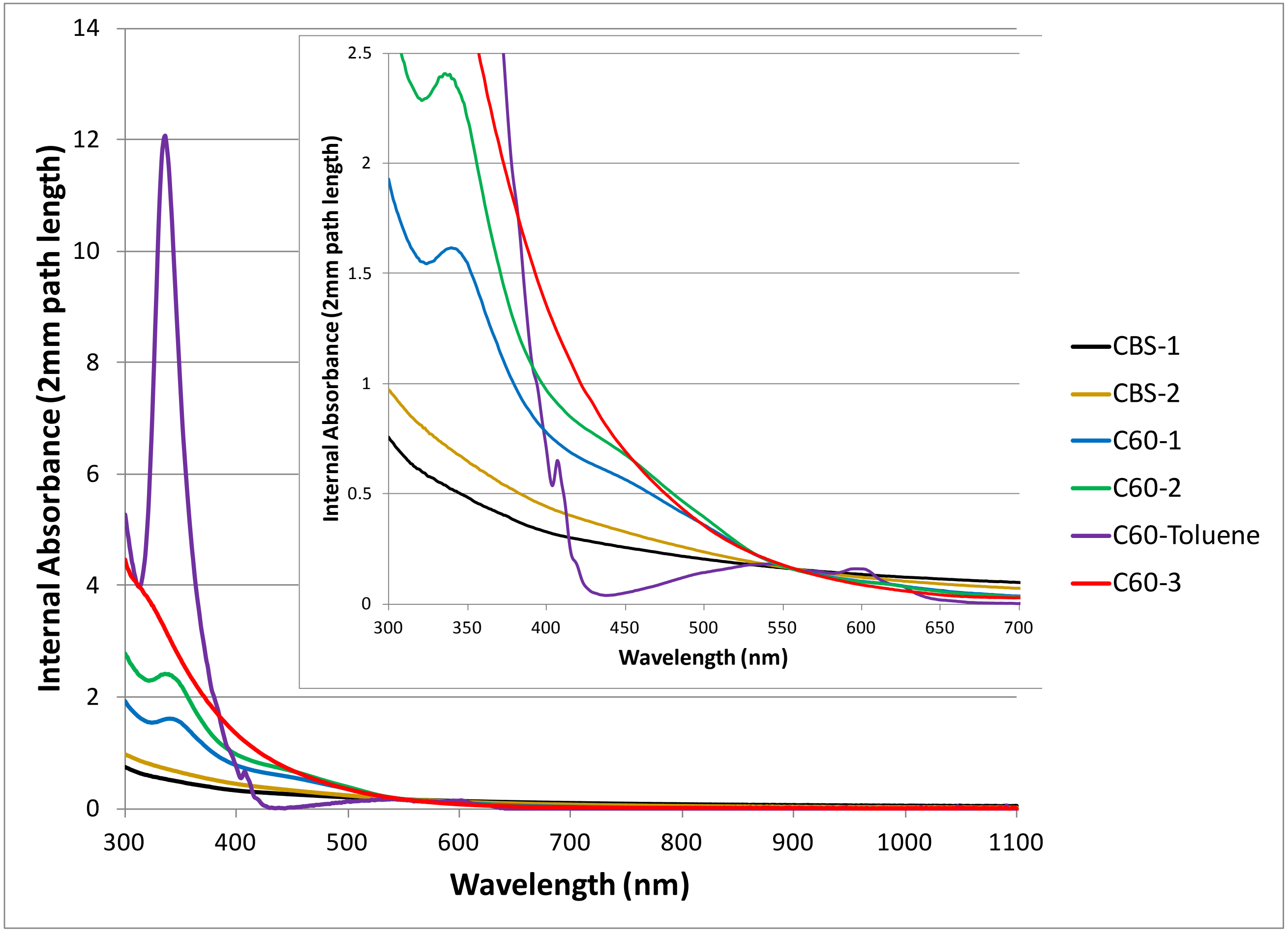

All samples have 70% internal transmittance at 560 nm.

UV-Vis Spectrometry Conclusions

- CBS-1 and CBS-2 spectra are consistent with scattering materials.
- Feature at 450 nm indicating C_{60} colloids is present in the C_{60}-1 and C_{60}-2 colloids.
- Feature at 350 nm may indicate some monomeric C_{60} in C_{60}-1 and C_{60}-2.
- C_{60}-3 spectrum consistent with C_{60} in fully colloidal state.

Bottom line: The spectra confirm the presence of C_{60} colloids and the known features of CBS and C_{60}.

Dissertation Research Outline

✓ Transmission Electron Microscopy	Particle size & morphology
✓ Dynamic Light Scattering ✓ Nanoparticle Tracking Analysis	Particle size distribution
✓ UV-Vis Spectrometry	Linear absorption spectrum
• Femtosecond Transient Absorption Spectroscopy • Nanosecond Laser Flash Photolysis	Nonlinear absorption spectra and kinetics
• Z-Scan	Nonlinear absorption coefficient, triplet-triplet absorption cross-section
• Total Scattering	Total accounting for transmitted, scattered, and absorbed energy
• Computer modeling	Analysis of results with respect to theory

Transient Absorption Spectroscopy: Femtosecond Pump-Probe

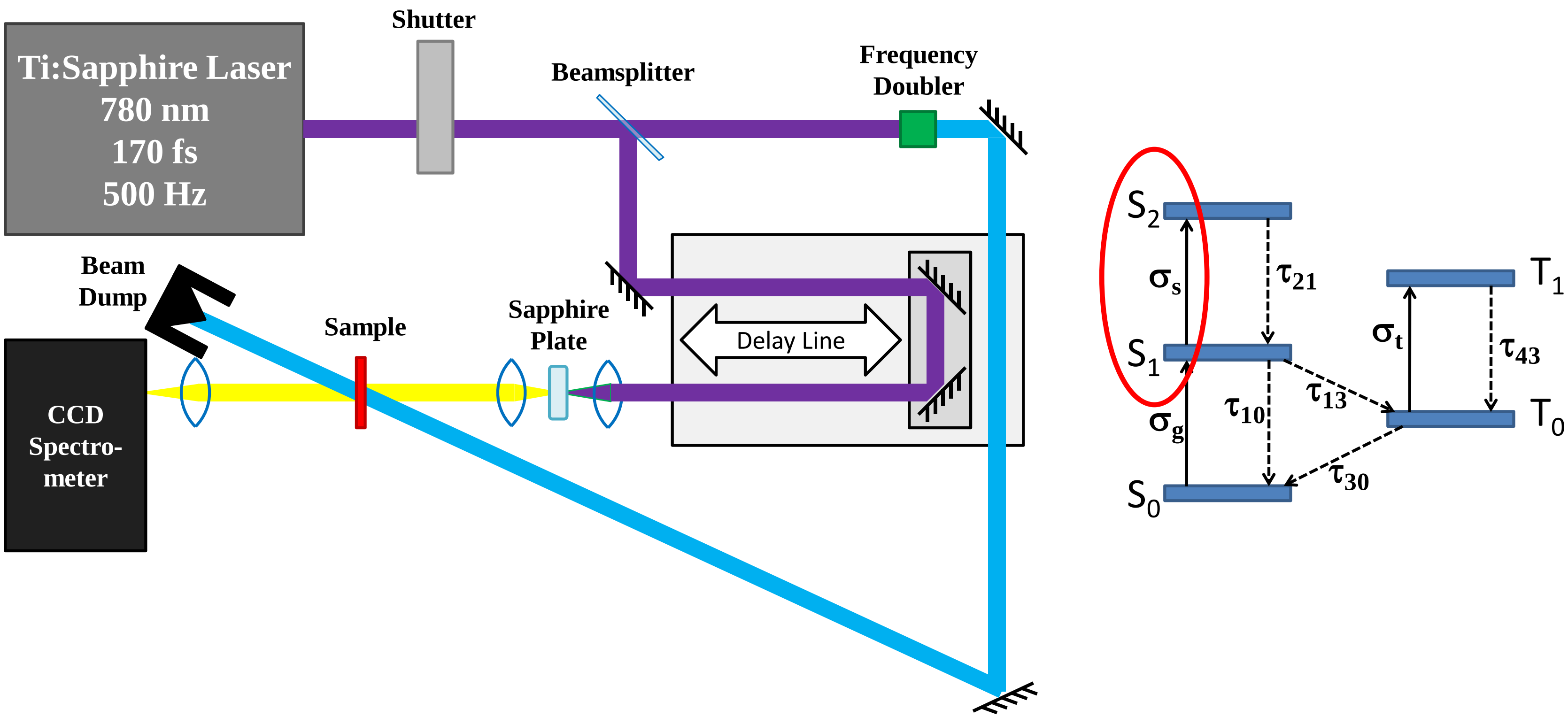

- Sample is pumped by a 390 nm femtosecond pulse.
- Sample is probed by a white light pulse at several different optical delays.
- A spectrometer records the change in the transmittance of the white light as a result of the sample's excitation.
- Measures the absorption spectrum and kinetics of the first excited singlet state.

Femtosecond Pump-Probe Results for Colloid C_{60}-1

Excitation Wavelength: 390 nm (170 fs)
Probe: white-light continuum (425-775 nm)
Max. probe delay: 6.6 ns

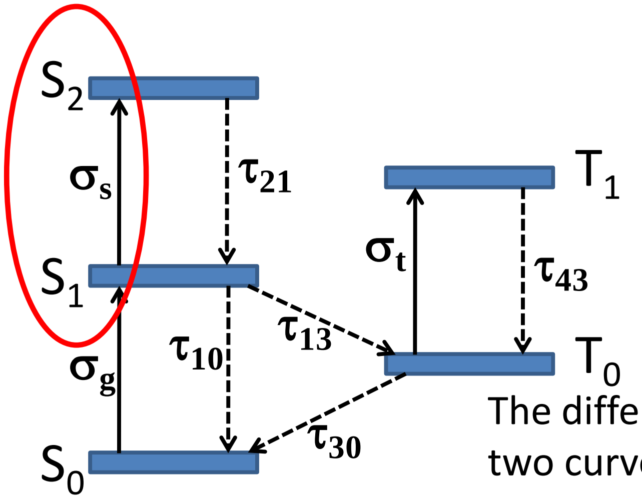

Analysis of the decay rates indicates there is significant quenching of the singlet state. Only 4.4% triplet quantum yield.

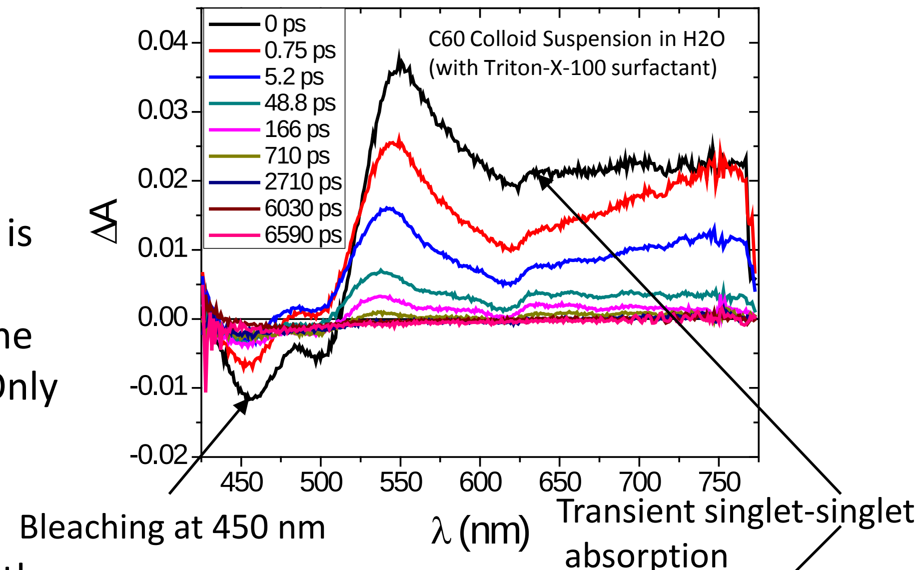

The difference between the two curves indicates that the transient singlet-singlet absorption in the C_{60} colloid sample is due to the aggregate form, not just single C_{60}. A long-lived transient absorption exhibits a peak near C_{60}'s 740 nm peak and bleaching near 450 nm.

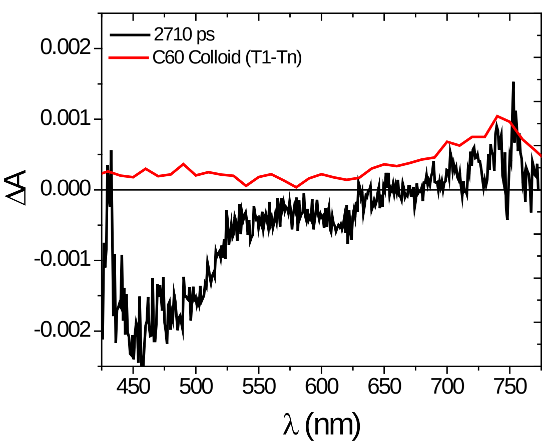

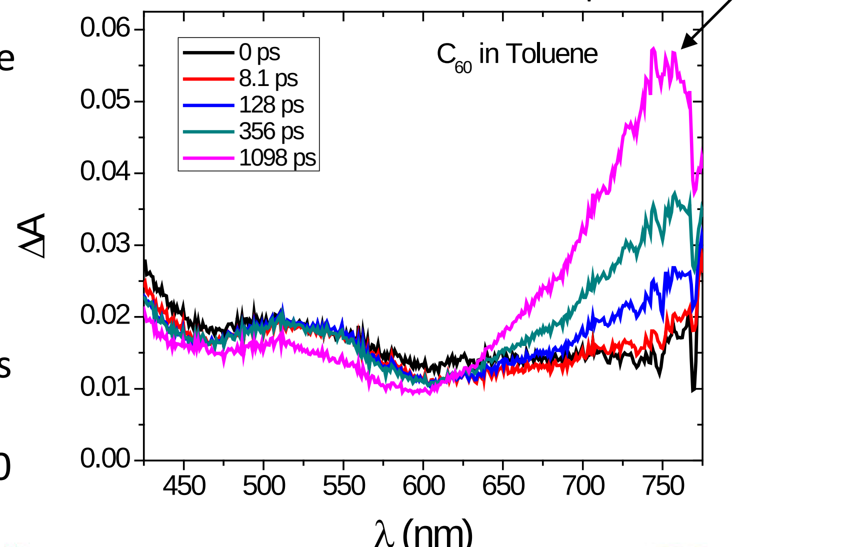

✓ I published C_{60} colloid photophysics on the femtosecond time scale in the course of this dissertation, which was previously unreported.

Transient Absorption Spectroscopy: Nanosecond Laser Flash Photolysis

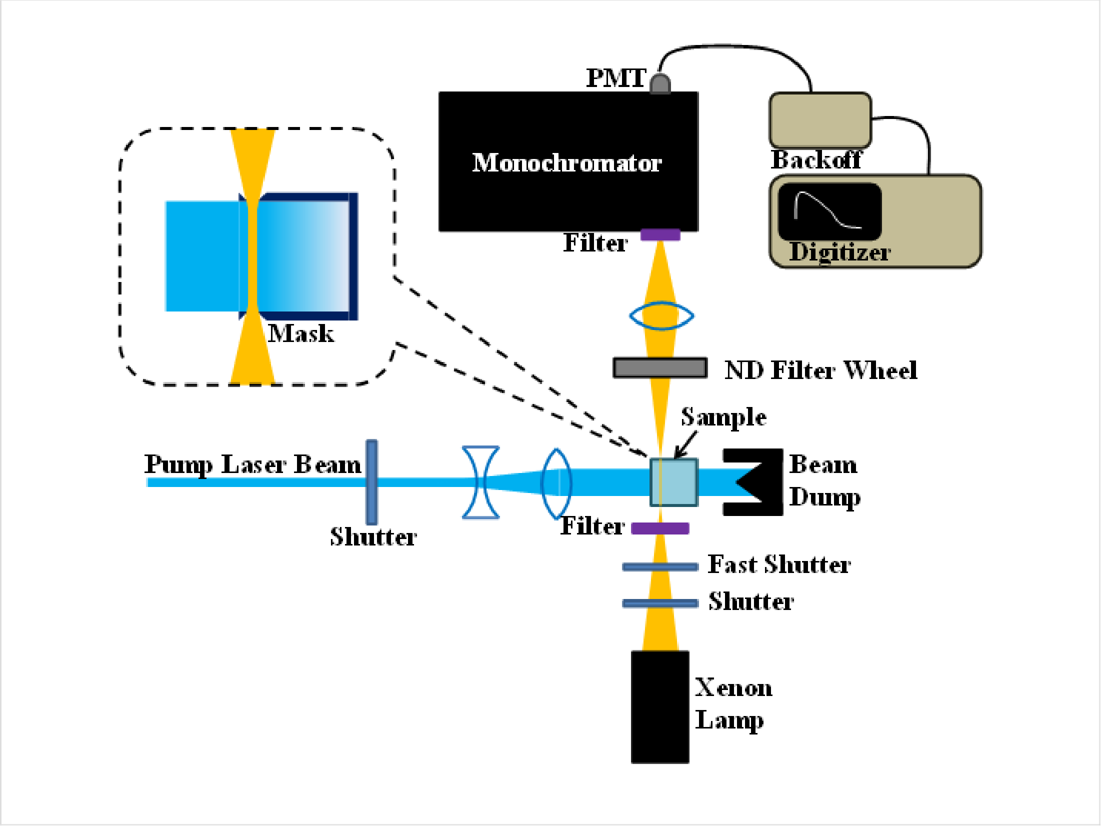

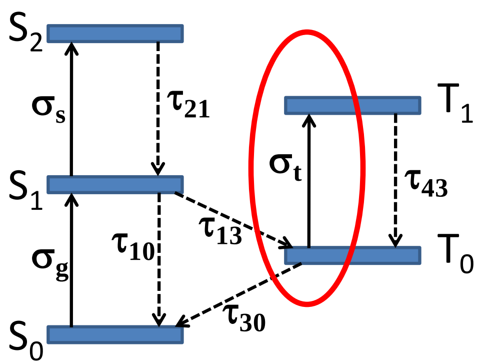

- Sample is pumped by a 355 nm nanosecond pulse.
- Sample is probed by a white light pulse from a Xenon lamp.
- A monochromator allows a single line of the white light pulse through to a photomultiplier tube, whose signal is digitized. The process is repeated over a range of wavelengths.
- Measures the absorption spectrum and kinetics of the first excited triplet state.

Nanosecond Flash Photolysis Results for Colloid C_{60}-1

Excitation Wavelength: 355 nm (4 ns)
Probe: Xenon flash lamp (white light)
Min. probe delay: 50 ns

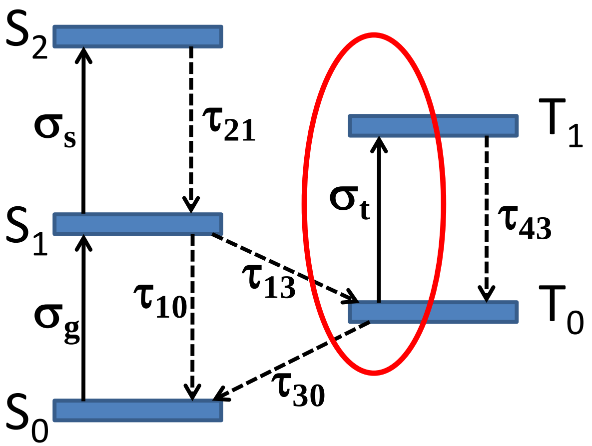

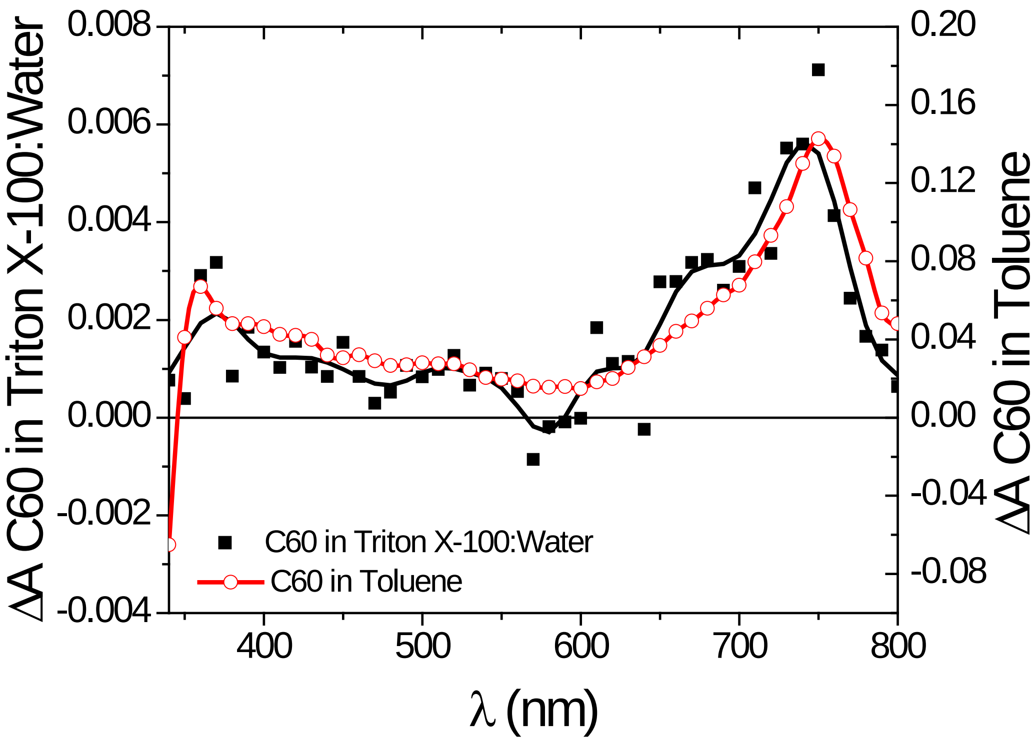

C_{60}-1 definitely exhibits triplet-triplet absorption. Its triplet-triplet absorption spectrum is nearly identical to C_{60} in solution. The magnitude of the peak near 740 nm is only 4% of C_{60} in solution. This agrees with the estimate of about 4% triplet quantum yield from the femtosecond decay rates.

Nanosecond Flash Photolysis Results for Colloid C_{60}-2

Excitation Wavelength: 355 nm (4 ns)
Probe: Xenon flash lamp (white light)
Min. probe delay: 50 ns

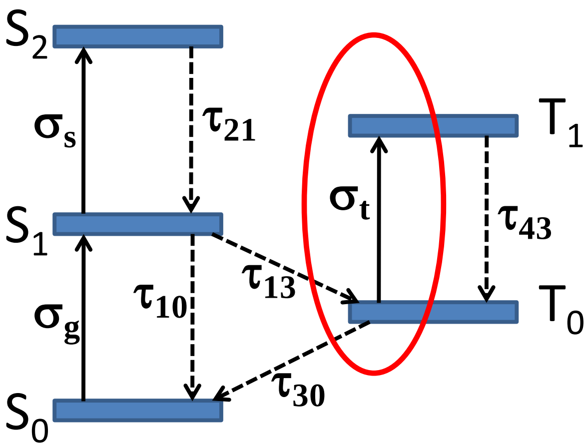

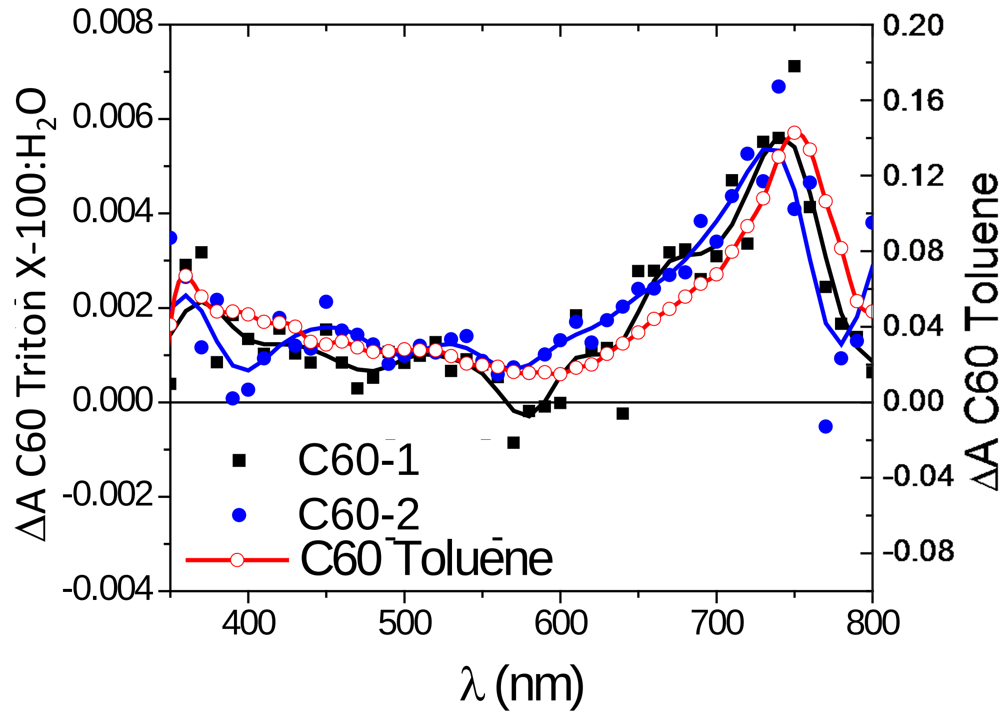

C_{60}-2 definitely exhibits triplet-triplet absorption. Its triplet-triplet absorption spectrum is nearly identical to C_{60} in solution and C_{60}-1.

Nanosecond Flash Photolysis Results for Colloid C_{60}-3

Excitation Wavelength: 355 nm (4 ns)
Probe: Xenon flash lamp (white light)
Min. probe delay: 50 ns

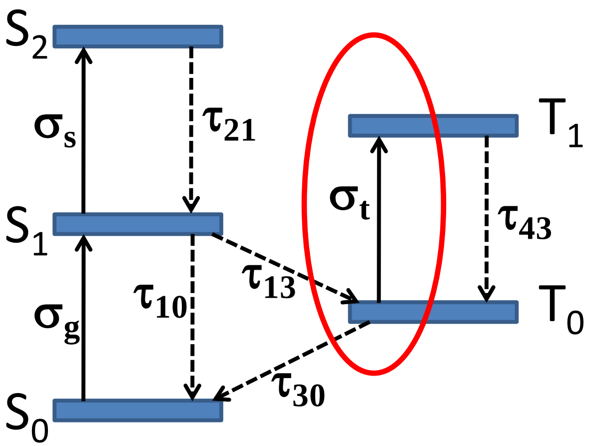

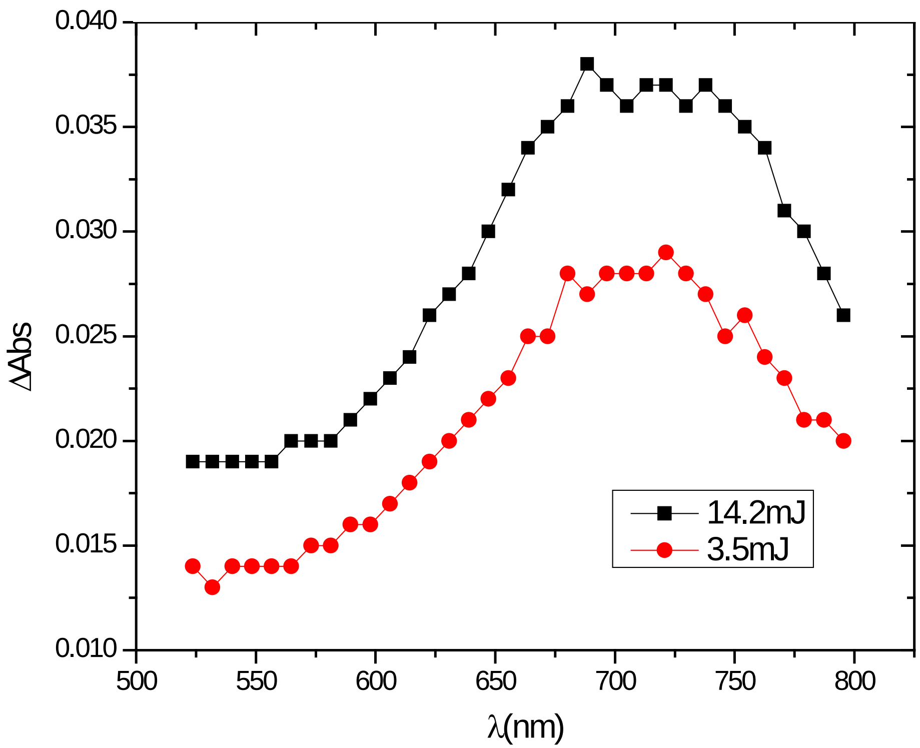

C_{60}-3 definitely exhibits triplet-triplet absorption. Its triplet-triplet absorption spectrum is very close to C_{60} in solution, C_{60}-1, and C_{60}-2, with a slightly broader and slightly blue-shifted peak.

Transient Absorption Lifetimes

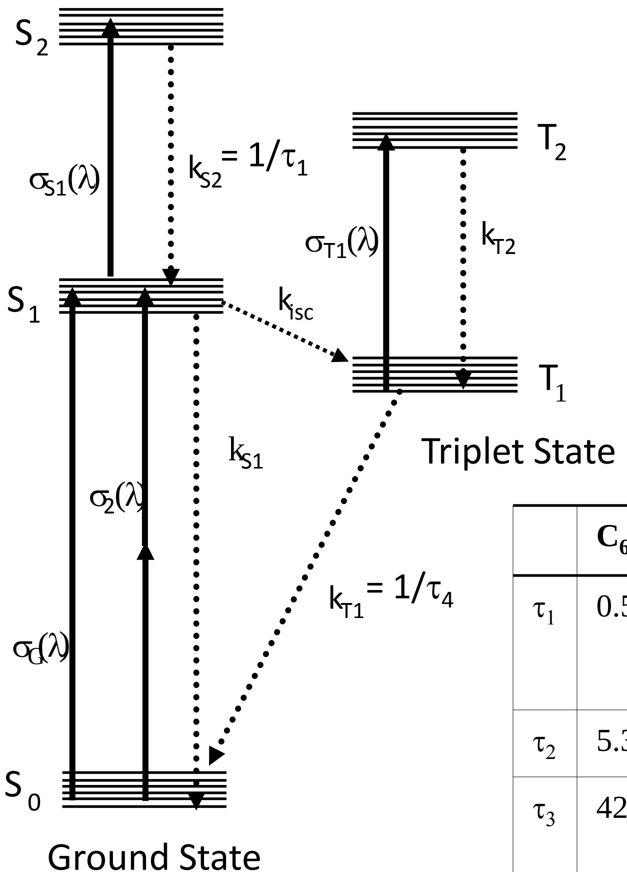

k_{s1} = fluorescence (light) and internal conversion (heat) from the singlet excited state
k_{s2} = decay from upper excited states back to S1 (~ <1 ps) it follows Kasha's rule $= \tau_1$
k_{isc} = intersystem crossing from S1 – T1
k_{T1} = decay from triplet excited state back to S0 $= \tau_4$
k_{T2} = decay from upper triplet excited states back to T1 (fast process < 1 ps)

$C_{60} \rightarrow {}^1C_{60}$
${}^1C_{60} \rightarrow C_{60}\ (\Delta, h\nu)$ $\quad k_{s1}$
${}^1C_{60} \rightarrow {}^3C_{60}$ $\quad k_{ISC}$
${}^1C_{60} + C_{60} \rightarrow$? (Products = $C_{60}^{\cdot -}$) $\quad k_{SQ}$
${}^3C_{60} \rightarrow C_{60}$ $\quad k_{T1}$

Decay from singlet state $k_s = k_{s1} + k_{ISC} + k_{SQ} \quad = \tau_3$

	C_{60} Colloid Suspension	C_{60}/Toluene	C_{60} Solid Film	Process
τ_1	0.53 ± 0.28 ps	0.58 ± 0.52 ps	0.26 ps	Intramolecular vibrational relaxation
τ_2	5.3 ± 1.8 ps	8.0 ± 4.7 ps	4.6 ps	Solvent reorganization
τ_3	42.6 ± 13.2 ps	960 ± 380 ps	64 ps	Self-quenching or singlet-singlet annihilation / Inter-system crossing
τ_4	1.1 µs (from air sat LFP) 86 µs (from deoxy LFP)	333 ns (air sat LFP) 3.7 µs (deoxy LFP)	N/A	Long-lived Triplet excited state

The k_{SQ} term controls the overall rate that was observed. In toluene there is no quenching so the lifetime is dominated by fluorescence, internal conversion, and intersystem crossing (mainly ISC). In the colloid k_{SQ} is large and dominates over other processes – inhibiting ISC to the triplet excited state.

Transient Absorption Conclusions

- The kinetics of C_{60} colloids are very similar to C_{60} solid films.

- Femtosecond pump-probe measurements show that in C_{60}-1, the first excited singlet state is strongly quenched, preventing efficient ISC, and resulting in a triplet quantum yield of only ~4% (compared to 96% for C_{60} in solution).

- Nanosecond flash photolysis measurements show that all C_{60} colloid samples do have some population of the triplet state, which has an absorption spectrum very similar to C_{60} in solution.

- Consequently, all C_{60} colloid samples should exhibit some RSA behavior, but much weaker than C_{60} in solution.

Dissertation Research Outline

✓ Transmission Electron Microscopy	Particle size & morphology
✓ Dynamic Light Scattering ✓ Nanoparticle Tracking Analysis	Particle size distribution
✓ UV-Vis Spectrometry	Linear absorption spectrum
✓ Femtosecond Transient Absorption Spectroscopy ✓ Nanosecond Laser Flash Photolysis	Nonlinear absorption spectra and kinetics
• Z-Scan	Nonlinear absorption coefficient, triplet-triplet absorption cross-section
• Total Scattering	Total accounting for transmitted, scattered, and absorbed energy
• Computer modeling	Analysis of results with respect to theory

Z-Scan

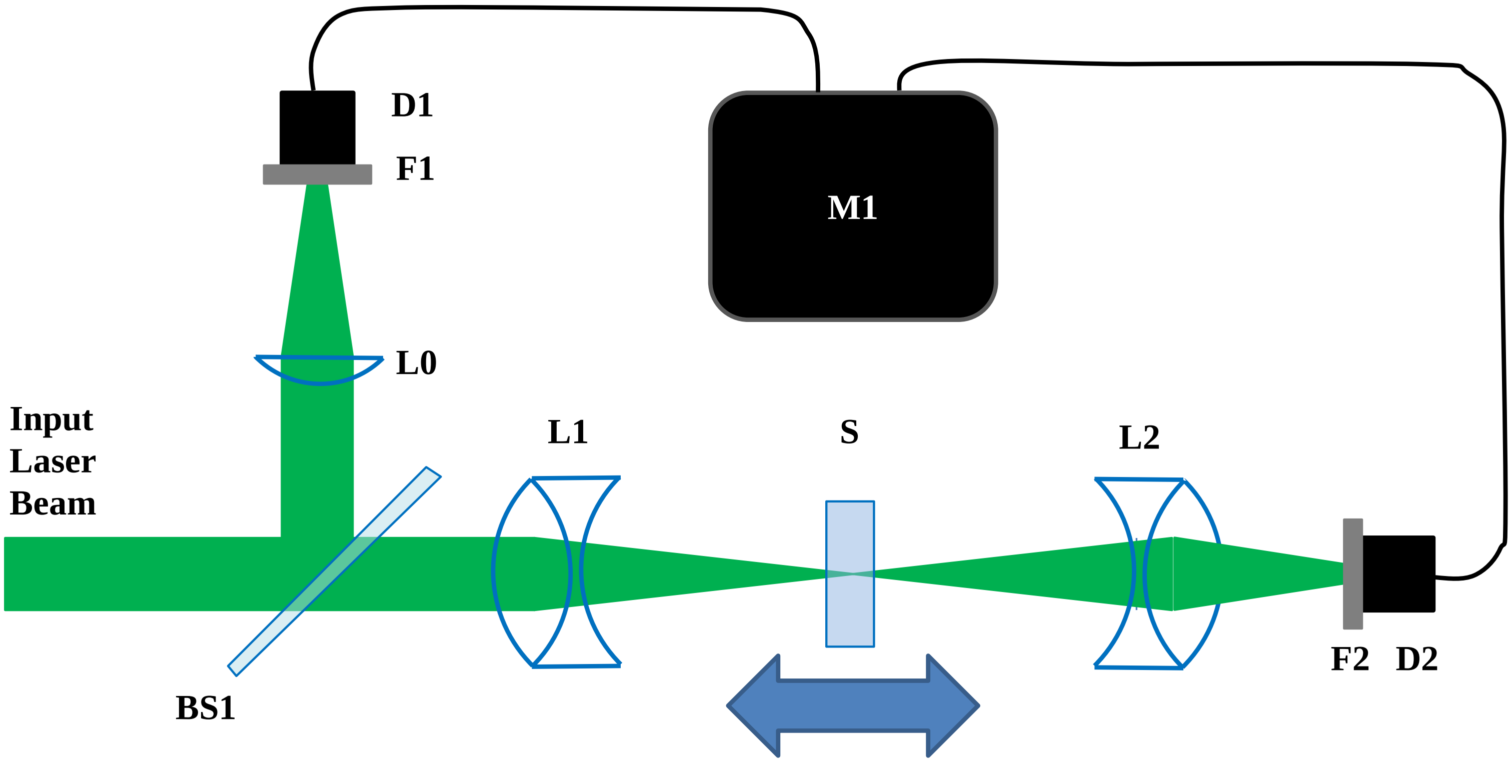

- Used to determine nonlinear refraction and nonlinear absorption coefficients. (Only nonlinear absorption here.)
- As the sample is scanned through the focal region, the beam diameter (and thus the irradiance) changes.
- The transmittance is recorded as a function of z-position.
- There are established treatments with which to examine the results with respect to RSA theory and extract the nonlinear absorption coefficient. If the concentration is known, one can determine the triplet-triplet absorption cross-section (assuming nanosecond laser irradiation).

Z-Scan Results

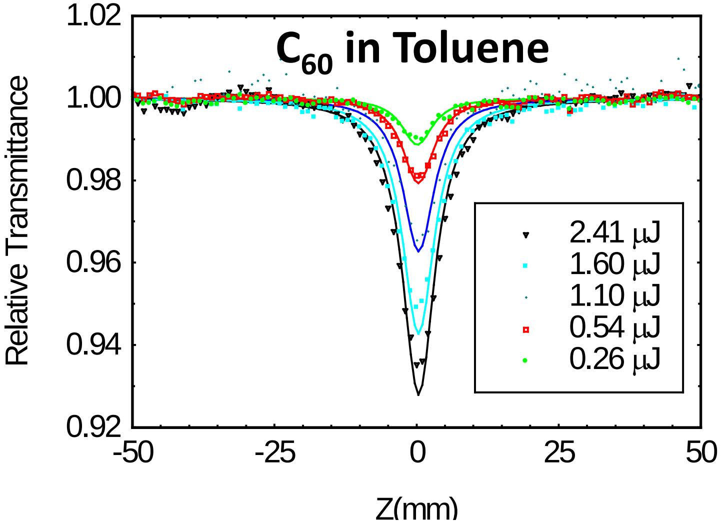

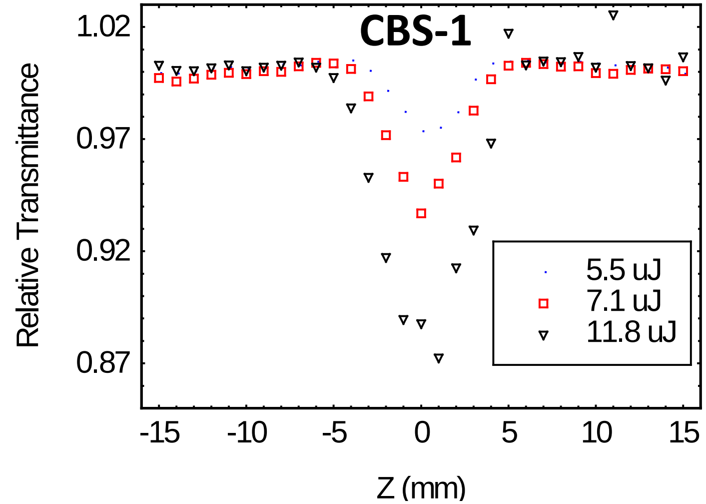

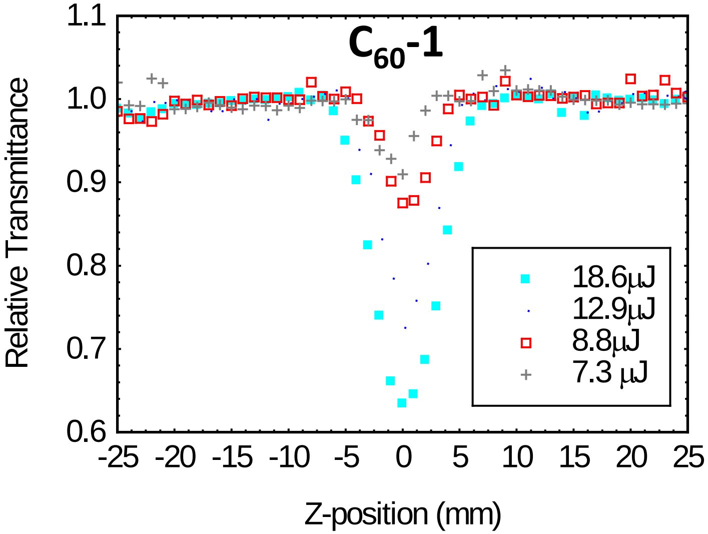

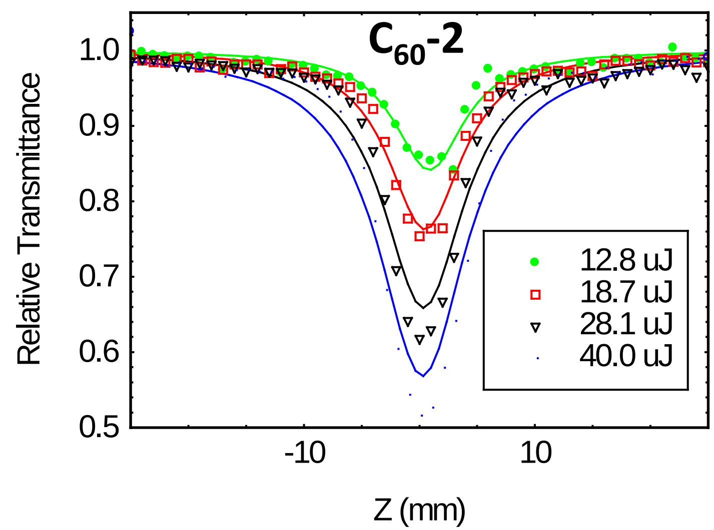

- C_{60} in Toluene and C_{60}-2 data fit to RSA analysis. CBS-1 and C_{60}-1 do not. Therefore, C_{60}-2 has stronger RSA behavior than C_{60}-1.

Z-Scan Conclusions

- The z-scan results for C_{60}-1 strongly resemble that of CBS, indicating that nonlinear scattering is dominant with little or no RSA occurring.

- C_{60}-2 has stronger RSA behavior than C_{60}-1, because it fits RSA analysis of the z-scan results.

Dissertation Research Outline

✓ Transmission Electron Microscopy	Particle size & morphology
✓ Dynamic Light Scattering ✓ Nanoparticle Tracking Analysis	Particle size distribution
✓ UV-Vis Spectrometry	Linear absorption spectrum
✓ Femtosecond Transient Absorption Spectroscopy ✓ Nanosecond Laser Flash Photolysis	Nonlinear absorption spectra and kinetics
✓ Z-Scan	Nonlinear absorption coefficient, triplet-triplet absorption cross-section
• **Total Scattering**	**Total accounting for transmitted, scattered, and absorbed energy**
• Computer modeling	Analysis of results with respect to theory

Total Scattering Experiment

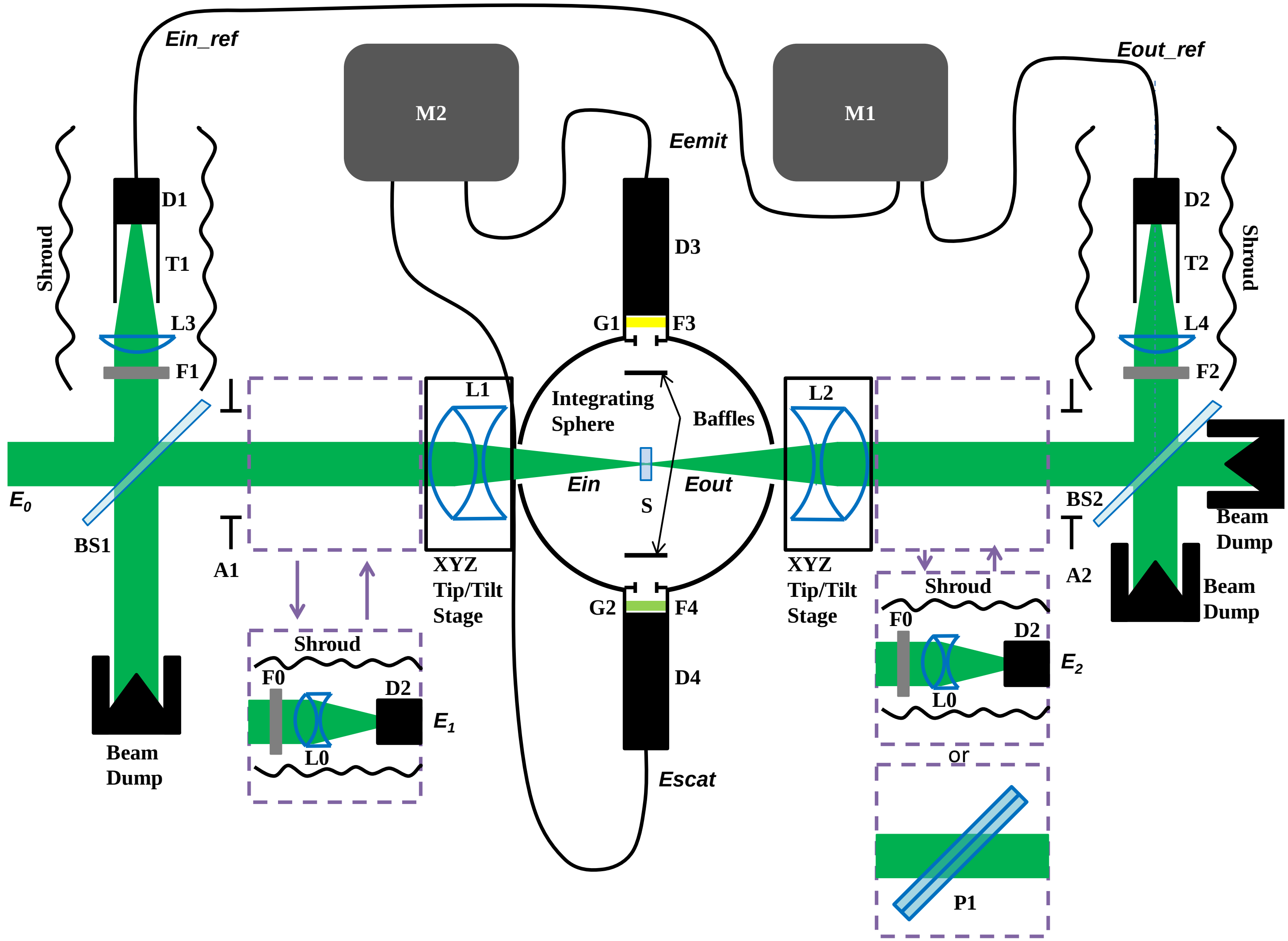

Custom Integrating Sphere

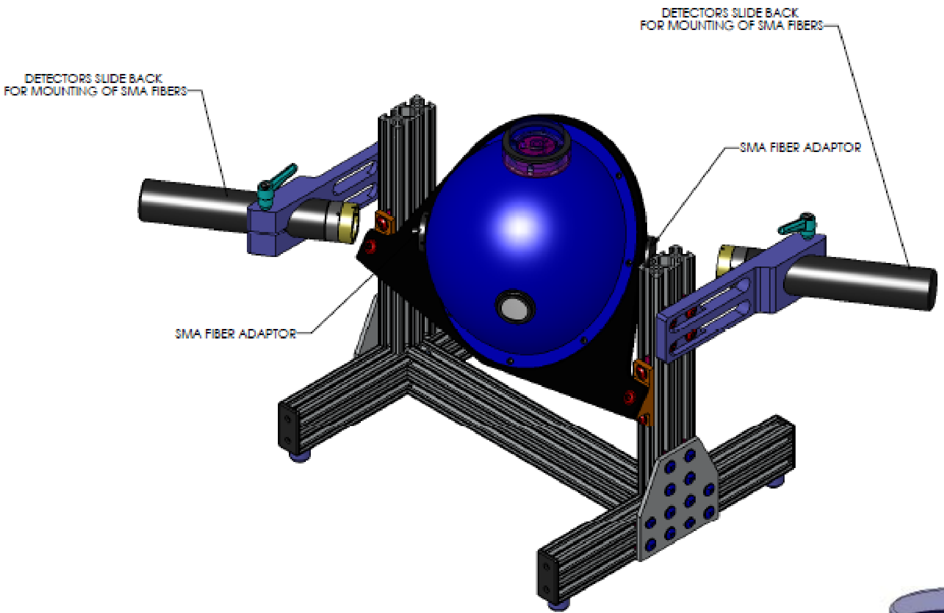

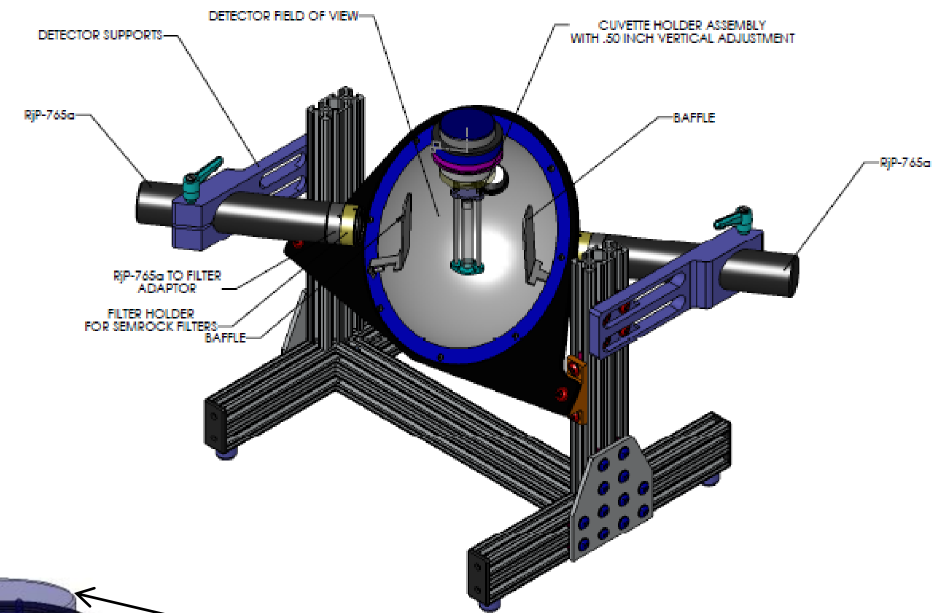

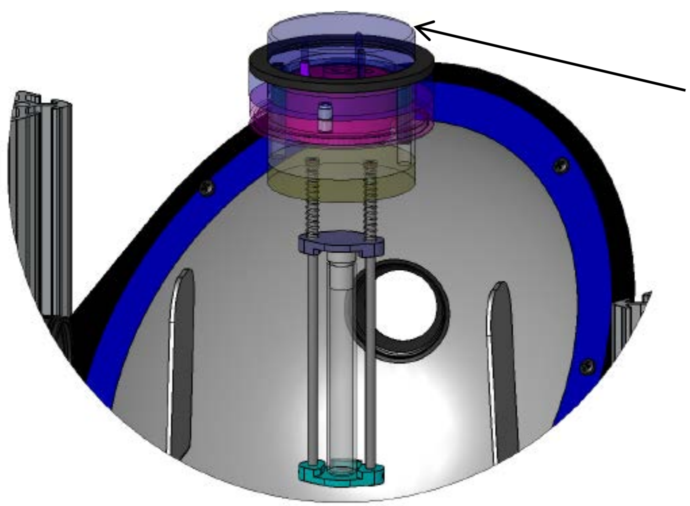

Sample translated vertically by turning top knob, so that a fresh location was exposed to each pulse.

Total Scattering Results for CBS-1

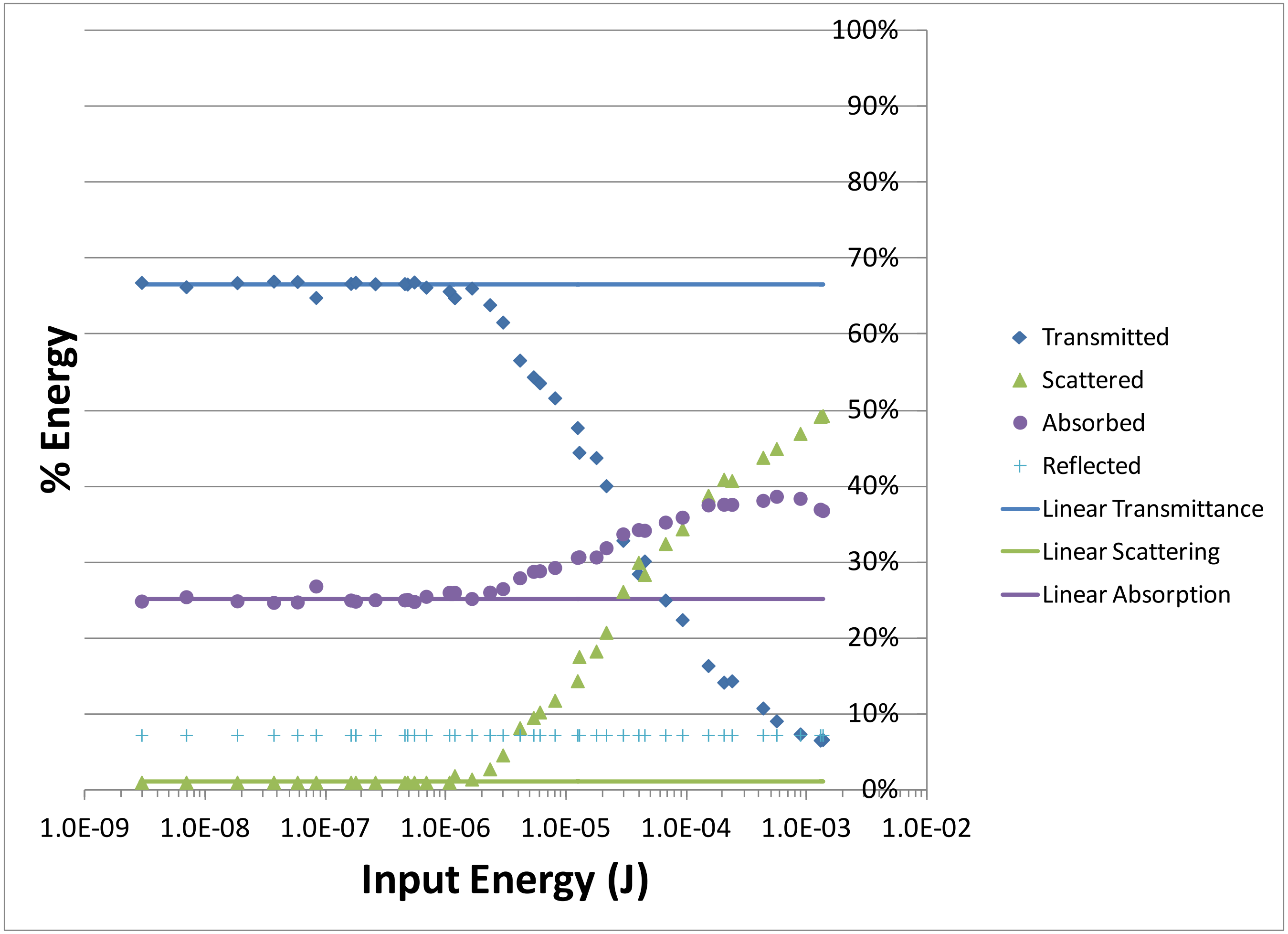

- Sharp onset of NLO behavior at threshold.
- Both nonlinear absorption and nonlinear scattering are present, but scattering dominates.

Total Scattering Results for CBS-2

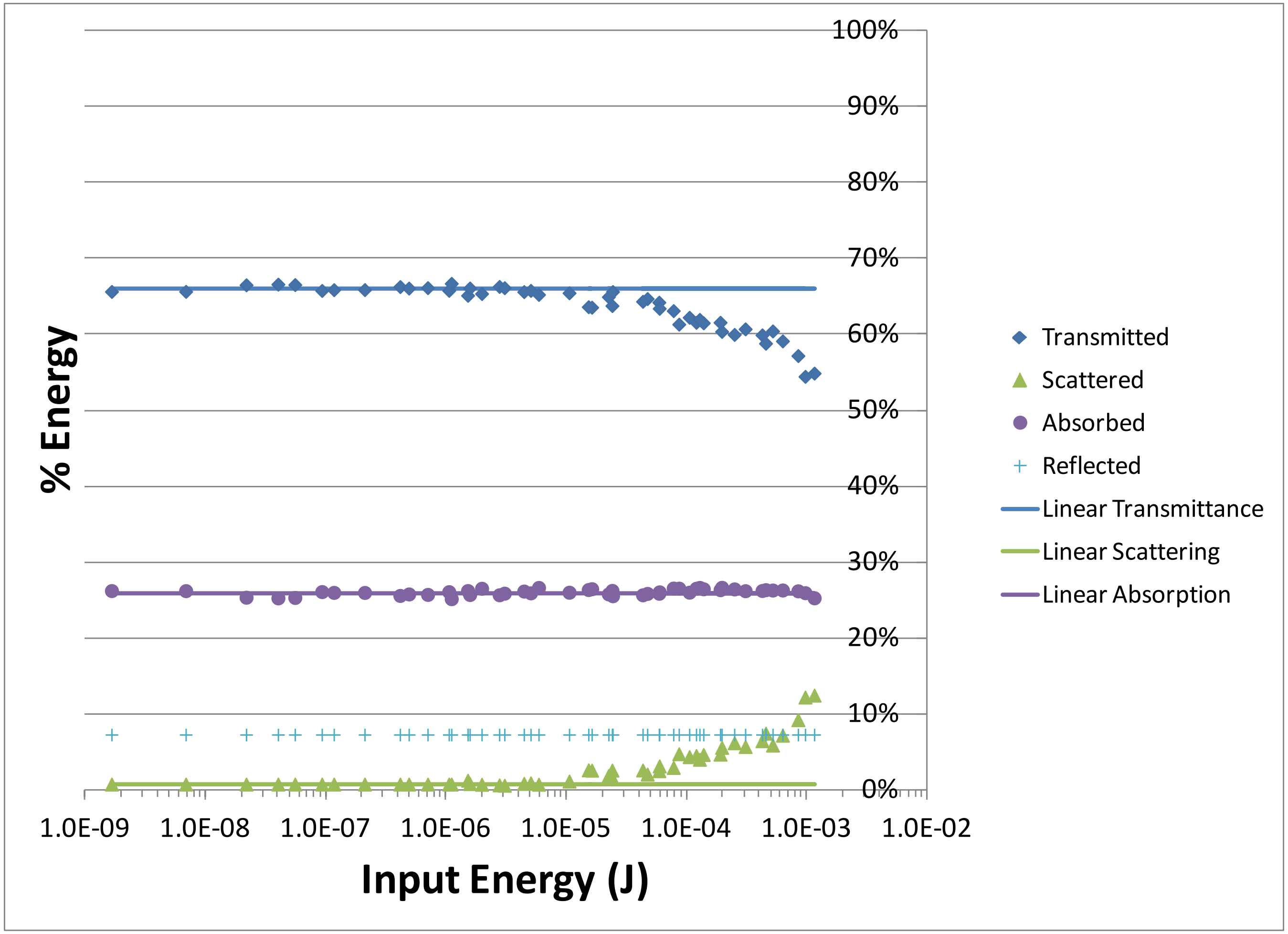

- Higher threshold than CBS-1.
- Weaker attenuation than CBS-1.
- Only nonlinear scattering. Absorptance remains linear.
- Large particles dominant, but sparse.

Total Scattering Results for C_{60} in Toluene

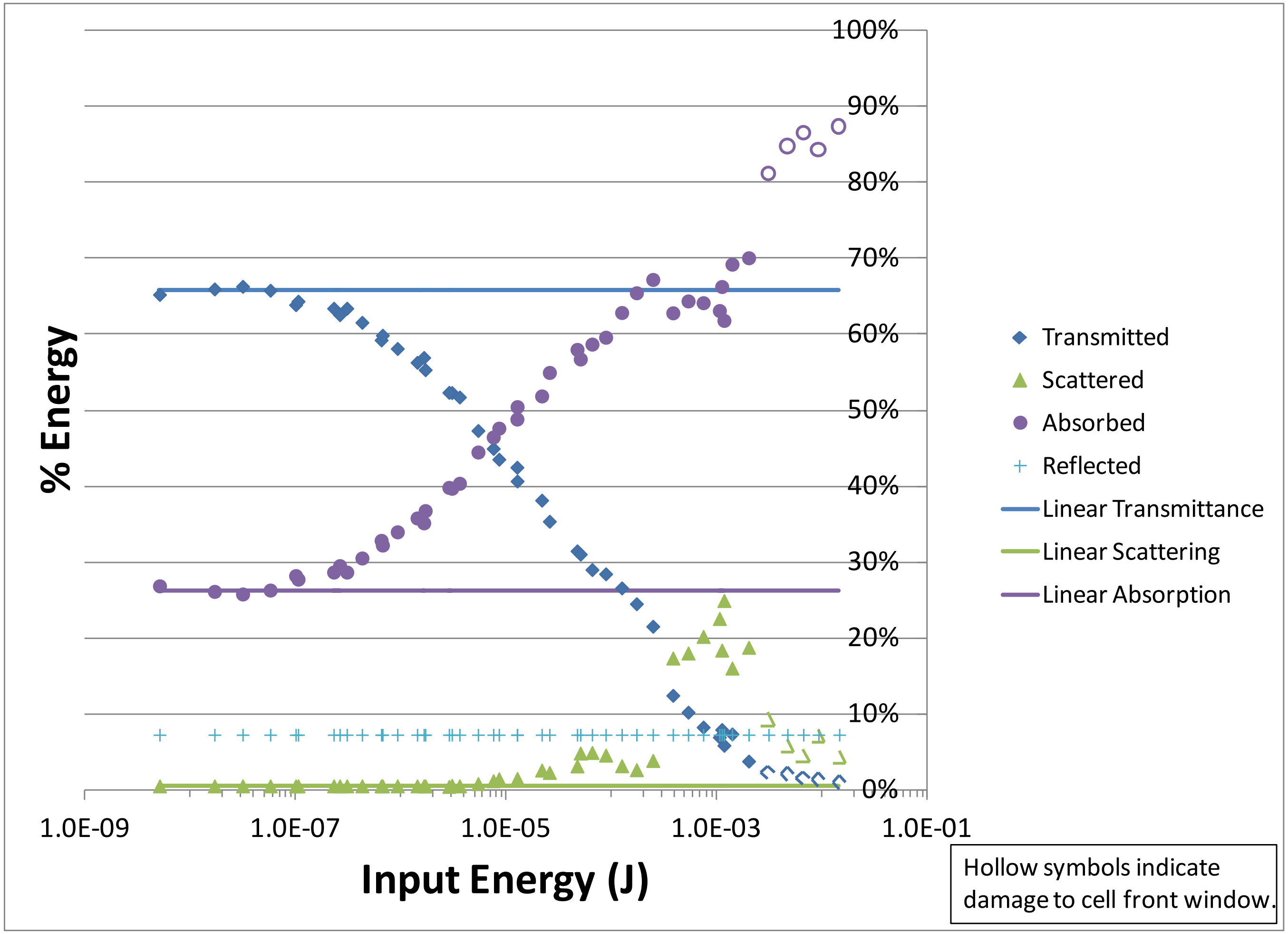

- Very low NLO threshold. Gradual attenuation.
- RSA only for 2 orders of magnitude.
- Two distinct regions of nonlinear scattering.

Total Scattering Results for Colloid C_{60}-1

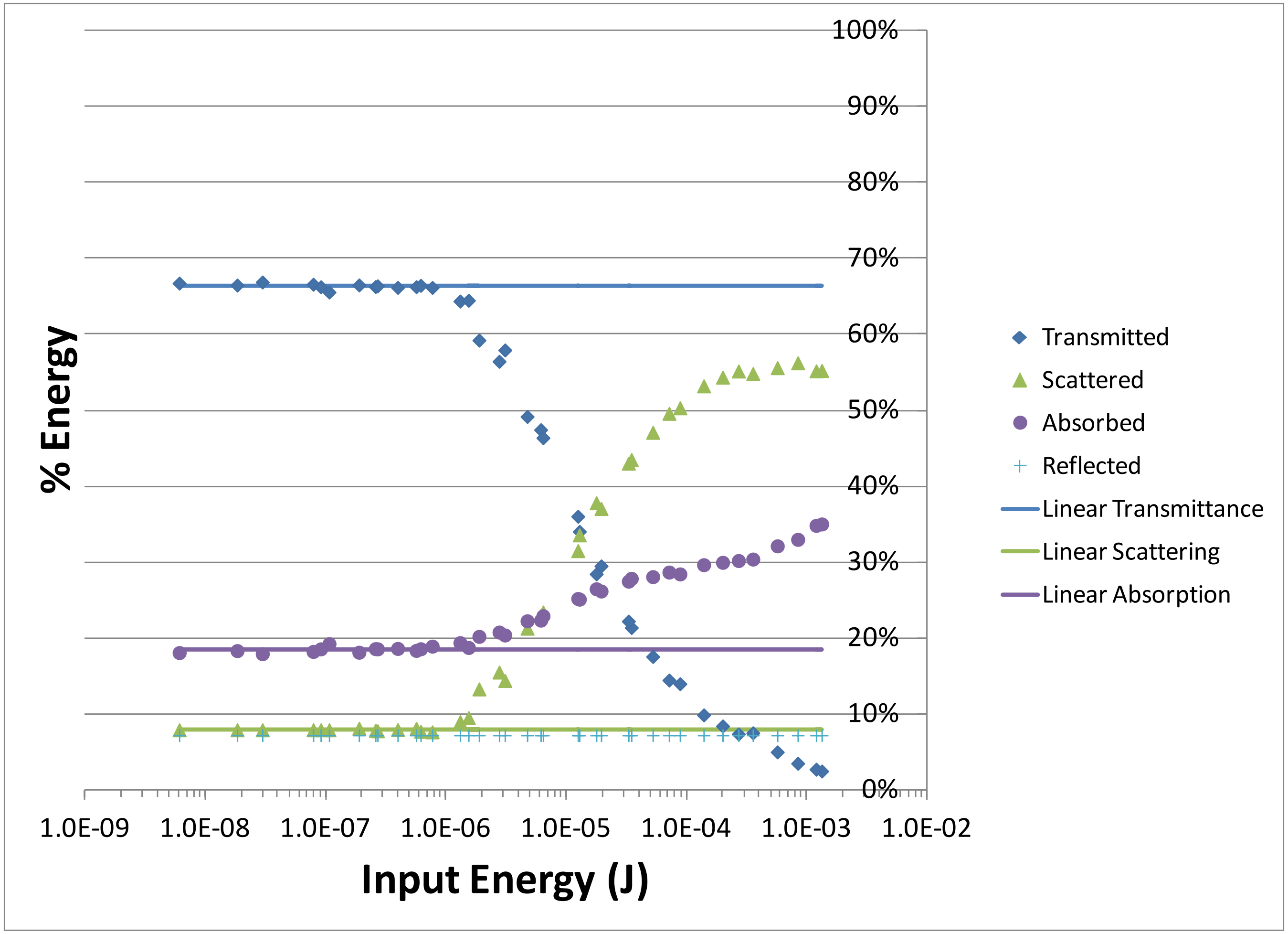

- Sharp onset of NLO behavior at threshold.
- Nonlinear absorption and nonlinear scattering both present, but scattering dominates.

Total Scattering Results for Colloid C_{60}-2

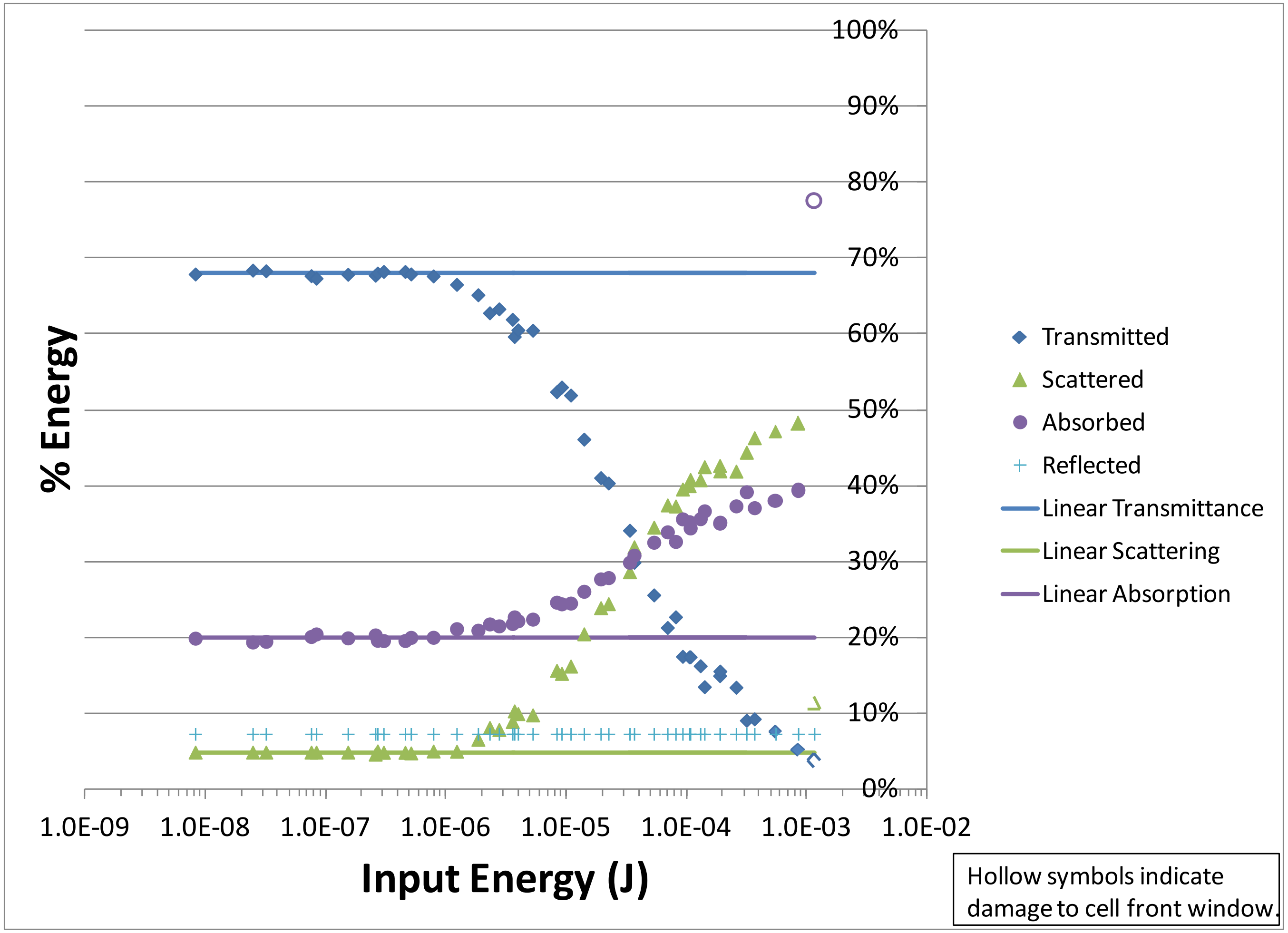

- Gradual roll at onset of NLO behavior (RSA).
- Nonlinear absorption and nonlinear scattering both present, but scattering dominates.

Total Scattering Results for Colloid C_{60}-3

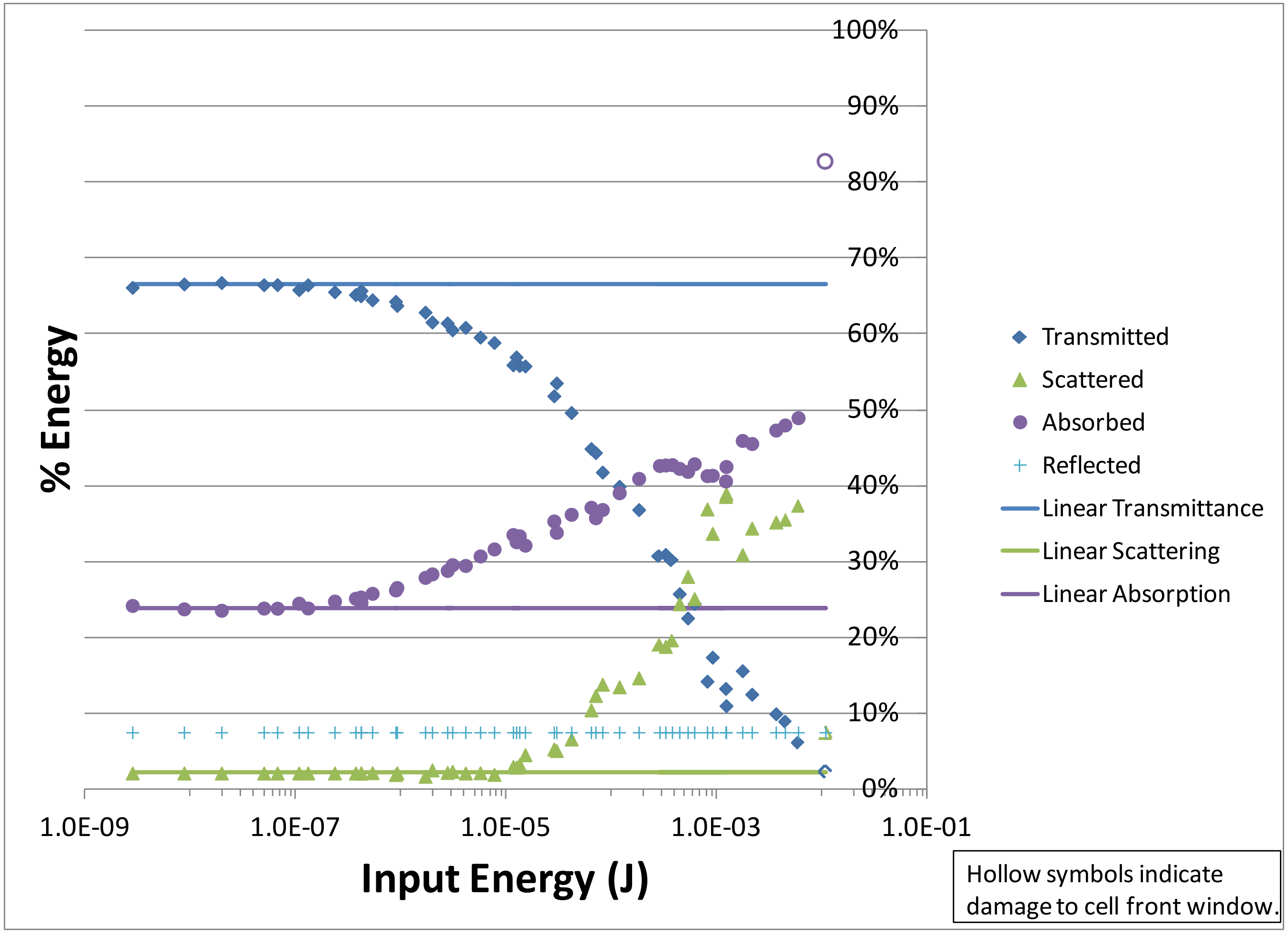

- Extended range of RSA-only behavior.
- At higher input energies, nonlinear scattering begins to dominate.

Total Scattering Results – All Samples

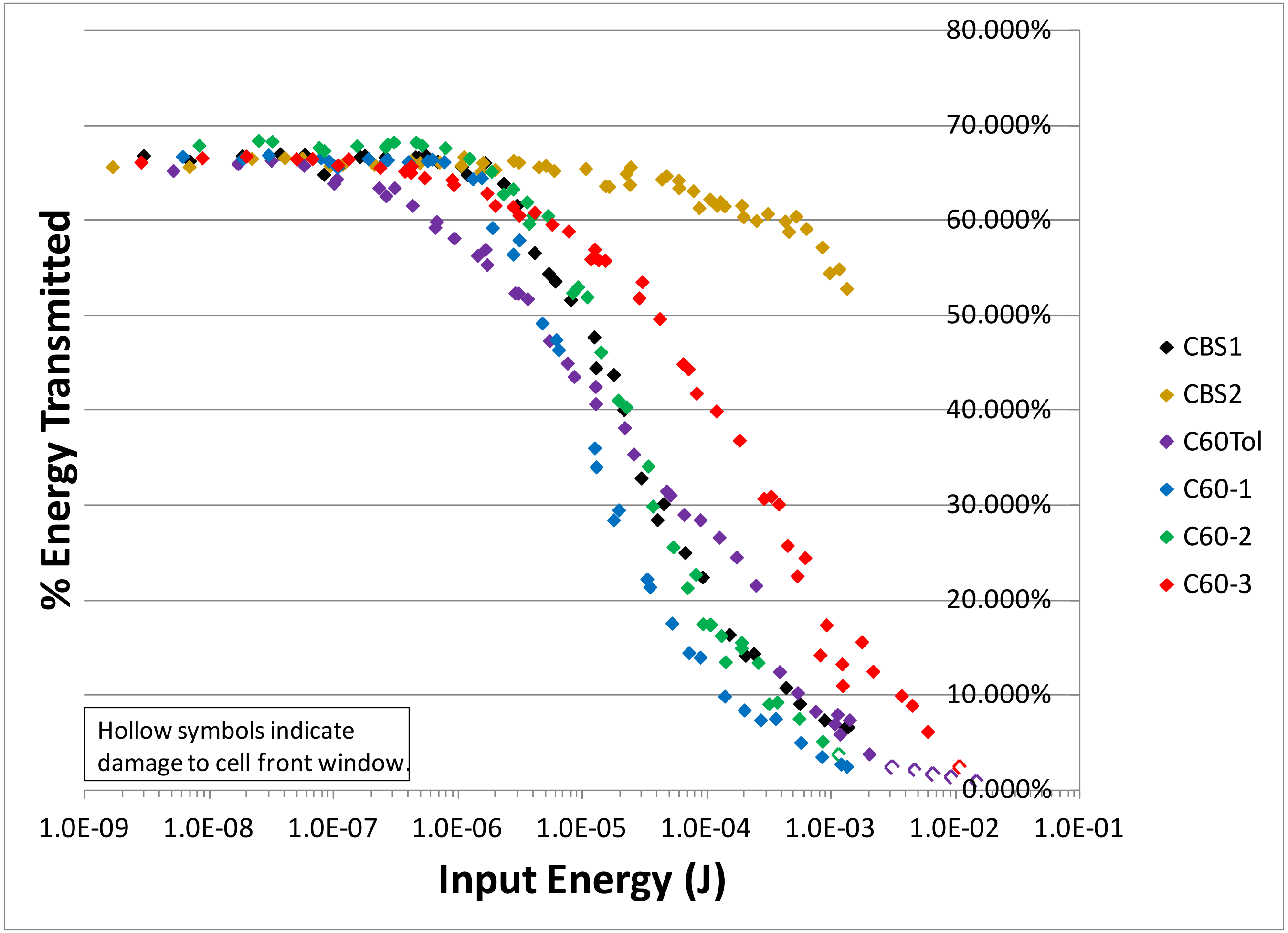

- C_{60} in toluene attenuated the most at low input energies.
- C_{60}-1 attenuated the most at medium to high input energies.

Total Scattering Results – All Samples

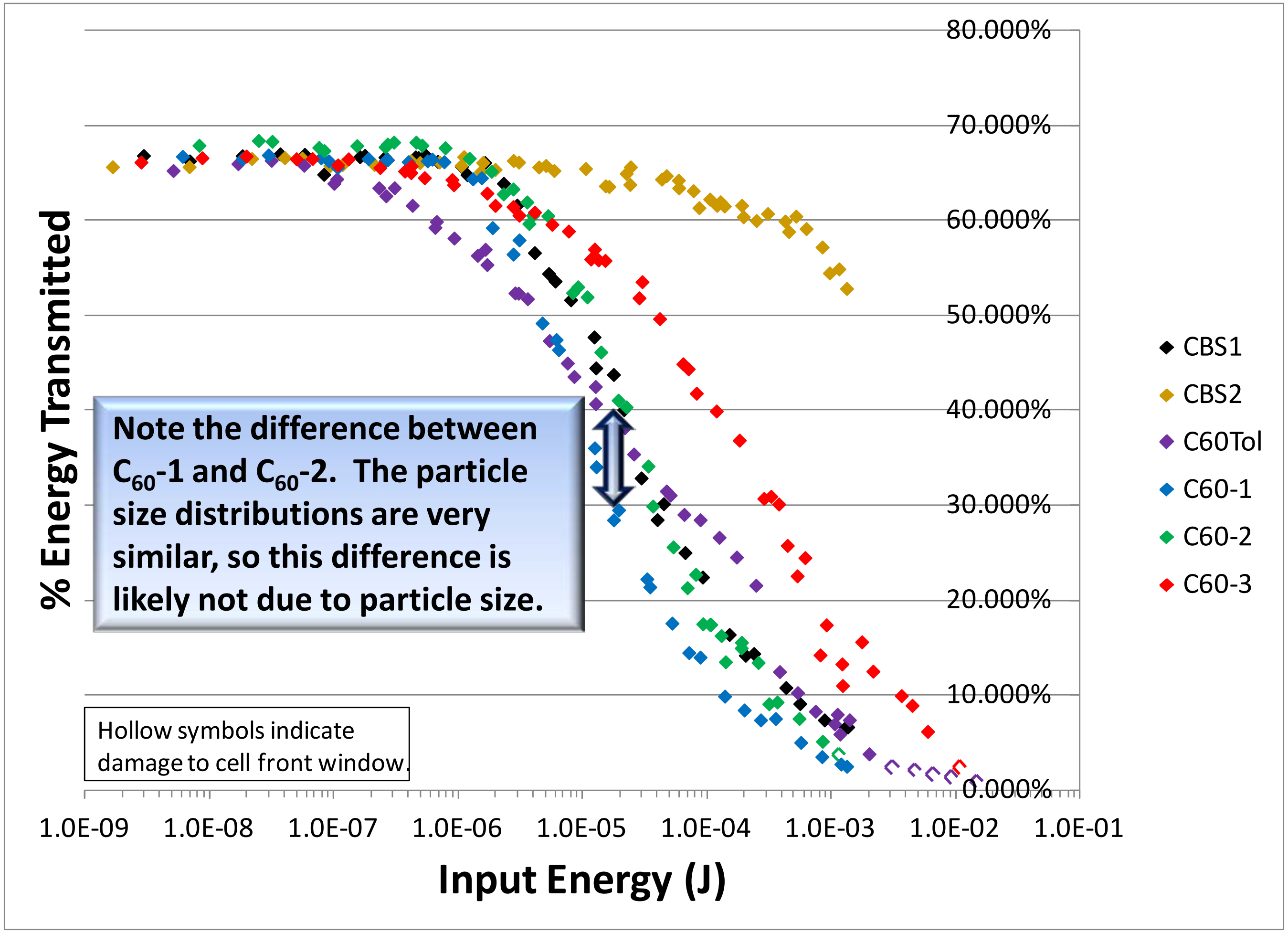

- C_{60} in toluene attenuated the most at low input energies.
- C_{60}-1 attenuated the most at medium to high input energies.

Total Scattering Conclusions

• CBS has a sharp onset of attenuation corresponding to particle sublimation. Both NLA and NLS contribute to attenuation, but NLS is dominant.

• C_{60} in toluene is dominated by pure RSA up to about 10 μJ. Above this, there are two distinctly different regions of NLS contributing to its response.

• C_{60}-1 behaves qualitatively just like CBS.

• C_{60}-2 and C_{60}-3 begin with RSA-dominated response, but transition to NLS upon particle sublimation.

• C_{60}-1 provides the most attenuation at mid to high input energies.

• There is a notable difference in attenuation between C_{60}-1 and C_{60}-2 that is correlated to something other than particle size.

Modeling analysis can yield further insight.

Dissertation Research Outline

Technique	Purpose
✓ Transmission Electron Microscopy	Particle size & morphology
✓ Dynamic Light Scattering ✓ Nanoparticle Tracking Analysis	Particle size distribution
✓ UV-Vis Spectrometry	Linear absorption spectrum
✓ Femtosecond Transient Absorption Spectroscopy ✓ Nanosecond Laser Flash Photolysis	Nonlinear absorption spectra and kinetics
✓ Z-Scan	Nonlinear absorption coefficient, triplet-triplet absorption cross-section
✓ Total Scattering	Total accounting for transmitted, scattered, and absorbed energy
• Computer modeling	Analysis of results with respect to theory

Modeling: Nonlinear Scattering

The dominant optical limiting mechanism in carbon black suspensions is nonlinear scattering. The black carbon particles have a strong linear absorption. Irradiation of such a suspension by a strong pulse of light causes rapid heating and vaporization of the particle and surrounding solvent, resulting in explosive bubble growth, creating scattering centers which scatter (and absorb) much of the incoming light, thereby attenuating the light transmitted along the original beam path.

The power per unit volume absorbed by an individual particle is given by:

$$W(t) = \frac{3\sigma_{abs} I(t)}{4\pi R^3}$$

where σ_{abs} is the absorption cross section of the particle, I(t) is the irradiance incident on the particle as a function of time, and R is the particle radius.

Modeling: Nonlinear Scattering

As a simplifying assumption, the model neglects heat transfer from the particle to the liquid. The time evolution of the particle's temperature is given by:

$$\mathbb{T}(t) = \mathbb{T}_0 + \int_0^{t(W_{max})} \frac{H\,W(t)}{\rho C_p}\,dt$$

where ρ is the density of the carbon particle, Cp is the specific heat, and H is a "heating efficiency factor" which compensates for heat dissipation.

The specific heat of carbon is strongly temperature dependent, so this value must be updated at each time slice in the computer code.

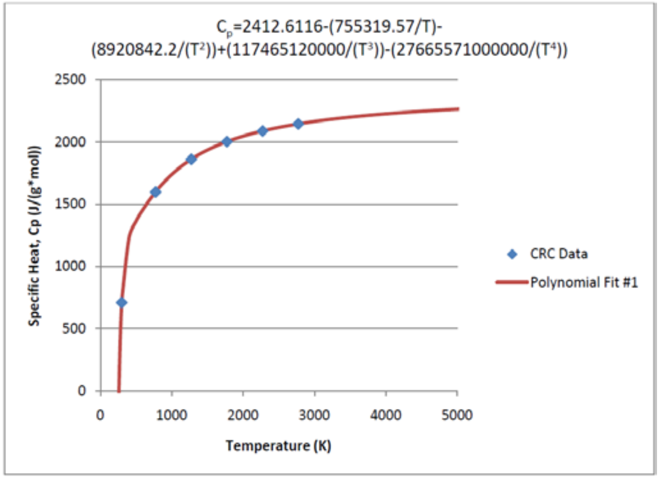

Modeling: Nonlinear Scattering

The model uses the basic framework of a model for nonlinear scattering in carbon black suspensions published by McEwan et al. A particle is assumed to be in one of two possible states, each with corresponding extinction coefficients. In the first state, the particle is considered to be in the linear region and the extinction coefficient is a combination of ground state absorption and linear scattering. When the particle has absorbed enough incident photons to be raised to carbon's sublimation temperature, a phase change is assumed and the extinction coefficient changes to account for nonlinear scattering from the bubble formed.

$$I_{out} = I_{in} 10^{-\alpha L}$$

or

$$I_{out} = I_{in} e^{-\alpha L}$$

Modeling: Nonlinear Scattering Alternate Approach

In order to develop a means to theoretically estimate what the value of the extinction coefficient should be in the nonlinear scattering state, an alternate model was developed in which the initial radius of the nonlinear scattering centers was estimated and their extinction coefficients calculated via Mie theory.

Egerev et al. present the following estimate for the size of the initial bubble radius:

$$R_0 = \left\{ \frac{3}{4\pi\rho_{cl}} \left[\frac{(F - F_c)\sigma_{abs}}{E_{cl}} \right] + R_{np}^3 \right\}^{1/3}$$

where R_0 is the initial bubble radius, ρ_{cl} is the critical density of the liquid, F is the fluence of the laser pulse, F_c is the critical fluence required to bring the liquid surrounding the nanoparticle to its boiling point, σ_{abs} is the absorption cross-section of the nanoparticle, E_{cl} is the internal energy of the liquid at the critical point, and R_{np} is the radius of the nanoparticle.

Note: This approach assumes that all of the energy of the laser pulse goes into boiling the liquid around the nanoparticle. Higher input energies will result in larger initial bubble radii.

Modeling: Nonlinear Absorption

The dominant optical limiting mechanism in molecular solutions of C_{60} is reverse saturable absorption (RSA). RSA is a special case of excited state absorption (ESA) in which the absorption cross-section of the triplet excited state is much larger than the absorption cross-section of the ground state, resulting in a decrease in transmittance with increasing input irradiance.

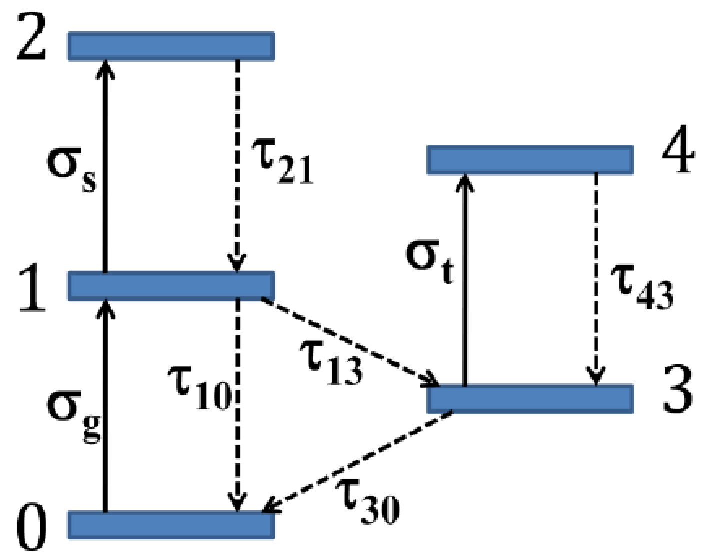

Modeling: Nonlinear Absorption

The rate equations for the 3-level approximation to the 5-level RSA model are:

$$\frac{dN_0}{dt} = -\frac{\sigma_g I(t)}{\hbar\omega} N_0 + \frac{N_1}{\tau_{10}}$$

$$\frac{dN_1}{dt} = \frac{\sigma_g I(t)}{\hbar\omega} N_0 - \frac{N_1}{\tau_1}$$

$$\frac{dN_3}{dt} = \frac{N_1}{\tau_{13}}$$

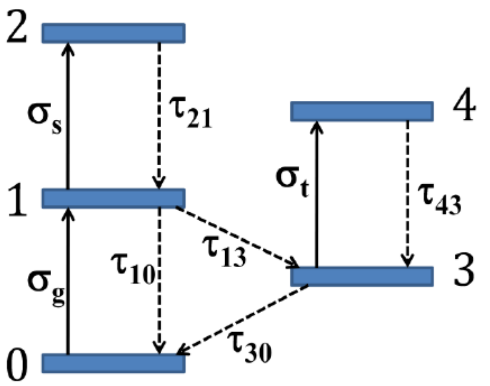

where $N_{0,1,3}$ are the population densities in the ground, first excited singlet, and first excited triplet states, $\sigma_{g,s,t}$ are the ground-state, singlet excited-state, and triplet excited-state absorption cross sections, $\tau_{10,21,43,30}$ are the respective band lifetimes, τ_{13} is the inter-system crossing lifetime, and

$$\frac{1}{\tau_1} = \frac{1}{\tau_{10}} + \frac{1}{\tau_{13}}$$

Modeling: Nonlinear Absorption

For faster computation times, I used analytical solutions to the rate equations, derived by Kobyakov et al., which apply for pulse lengths of 10 ns or longer. Using the following normalization variables,

$$T = t/t_p$$

where t_p is the temporal pulse width,

$$A = \sigma_g I_0 t_p/(\hbar\omega)$$

and

$$w = t_p/\tau_1$$

the rate equations become:

$$\frac{dn_0}{dT} = -f(T)n_0 + w(1-\phi)n_1$$

$$\frac{dn_1}{dT} = f(T)n_0 - wn_1$$

$$\frac{dn_3}{dT} = w\phi n_1$$

Where $n_j(T) = N_j(T)/N_0(T_0)$, j = 0, 1, 3, are fractional population densities, T_0 is the time when the light pulse begins to enter the material, and $\phi = \tau_1/\tau_{13}$ is the triplet quantum yield. The pulse is represented by $f(T) = A\hat{f}(T)$, where $\hat{f}(T)$ is a pulse shape with unit amplitude, given in the normalized time scale.

The total population density is conserved: $n_0(T) + n_1(T) + n_3(T) = 1$

Modeling: Nonlinear Absorption

For mathematical convenience, the hyperbolic-secant-squared function is used to approximate Gaussian temporal pulses:

$$f(T) = A \operatorname{sech}^2 T$$

The analytical solution derived for 10 ns or longer pulses is given by:

$$n_0(T) \approx \exp\left[-\phi A(\tanh T + 1)\right]$$

$$n_1(T) \approx \frac{A}{W} \operatorname{sech}^2 T \exp[-\phi A(\tanh T + 1)]$$

The total population density is conserved:

$$n_0(T) + n_1(T) + n_3(T) = 1$$

The population densities determine an effective absorption cross section:

$$\sigma_{eff} = n_0 + \bar{\sigma}_S n_1 + \bar{\sigma}_T n_3$$

where $\bar{\sigma}_S = \sigma_s/\sigma_g \quad \bar{\sigma}_T = \sigma_t/\sigma_g$ is the ground state absorption cross-section, σ_s is the first excited singlet state absorption cross-section, and σ_t is the first excited triplet state absorption cross-section at a given wavelength.

The irradiance at each point in time and space is calculated from:

$$I_{out} = I_{in} e^{-\sigma_{eff} dZ}$$

unless the sublimation temperature of C_{60} is exceeded, in which case the irradiance equation is replaced by the scattering expression: $$I_{out} = I_{in} e^{-\alpha_B dZ}$$

Modeling: Nonlinear Scattering from Nonlinearly Absorbing Particles

To estimate the response of particles composed of RSA molecules, such as colloidal C_{60}, the analytical solutions published by Kobyakov et al. are used to model the absorption dynamics prior to sublimation of the particles. After the particle temperature exceeds the sublimation temperature, attenuation of irradiance is modeled according to the nonlinear scattering method based on the published work of McEwan et al.

Hypothetical Case: CBS at Threshold

Temperature of input surface

Input surface reaches carbon sublimation temperature (3770K) shortly after the peak of the pulse.

Temperature of output surface

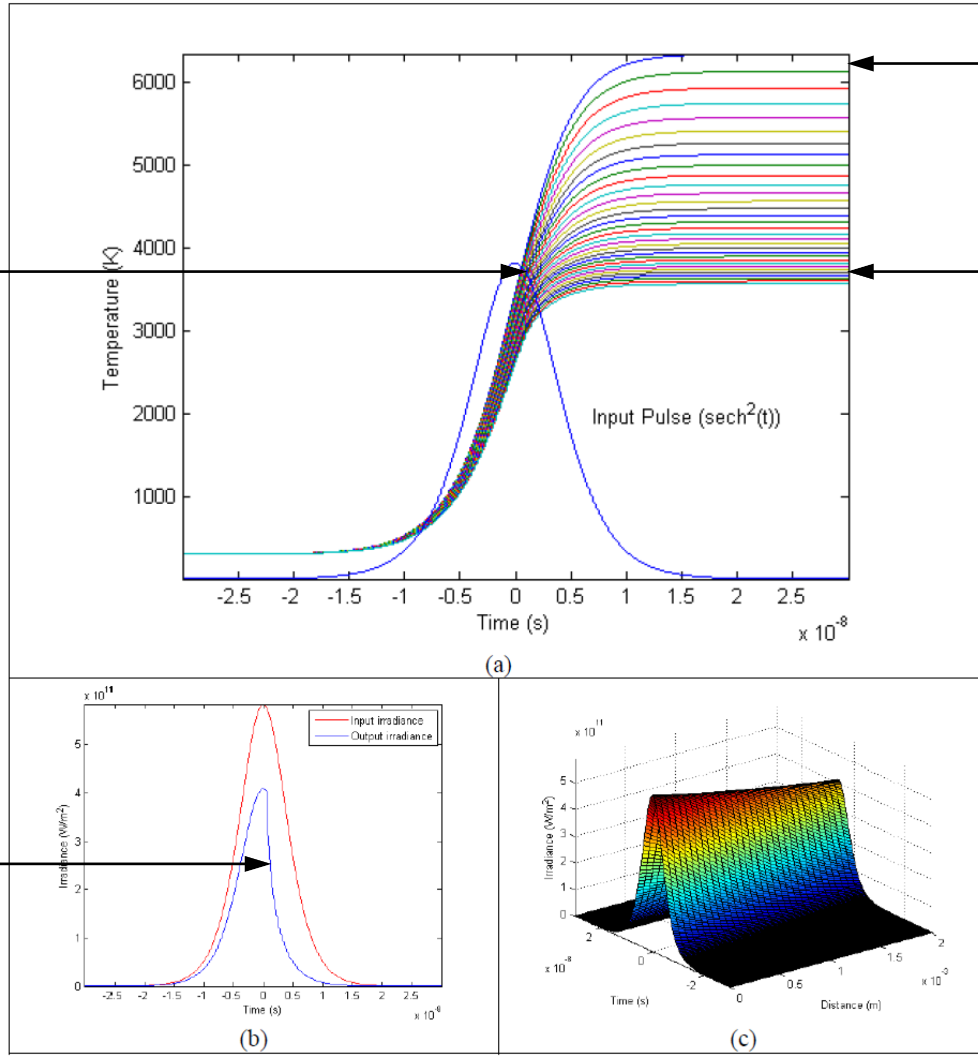

On-axis transmittance falls off sharply after threshold is reached.

(A particle radius of 85 nm was chosen for direct comparison to the published results of Riehl and Fougeanet. The results show good agreement.)

Model output for a suspension of carbon black in water with 70% linear transmittance at 532 nm through a 2 mm path length with 7.8 microJoules input energy, 20 micron spot radius, and 10 ns pulse width. (a) isolated particle temperature vs. time, (b) input and output pulse irradiance vs. time, and (c) surface plot showing the irradiance profile as the beam propagates through the material.

Collimated geometry is assumed.

Hypothetical Case: C_{60} at CBS Threshold

Ground state population density

Input surface

Output surface

Triplet state population density

Input surface

Output surface

Singlet state population density

When triplet state is strongly populated, transmittance is about 1/3 of linear. Ratio of σ_t to σ_g is about 3:1.

On-axis transmittance lower when triplet state begins to be populated.

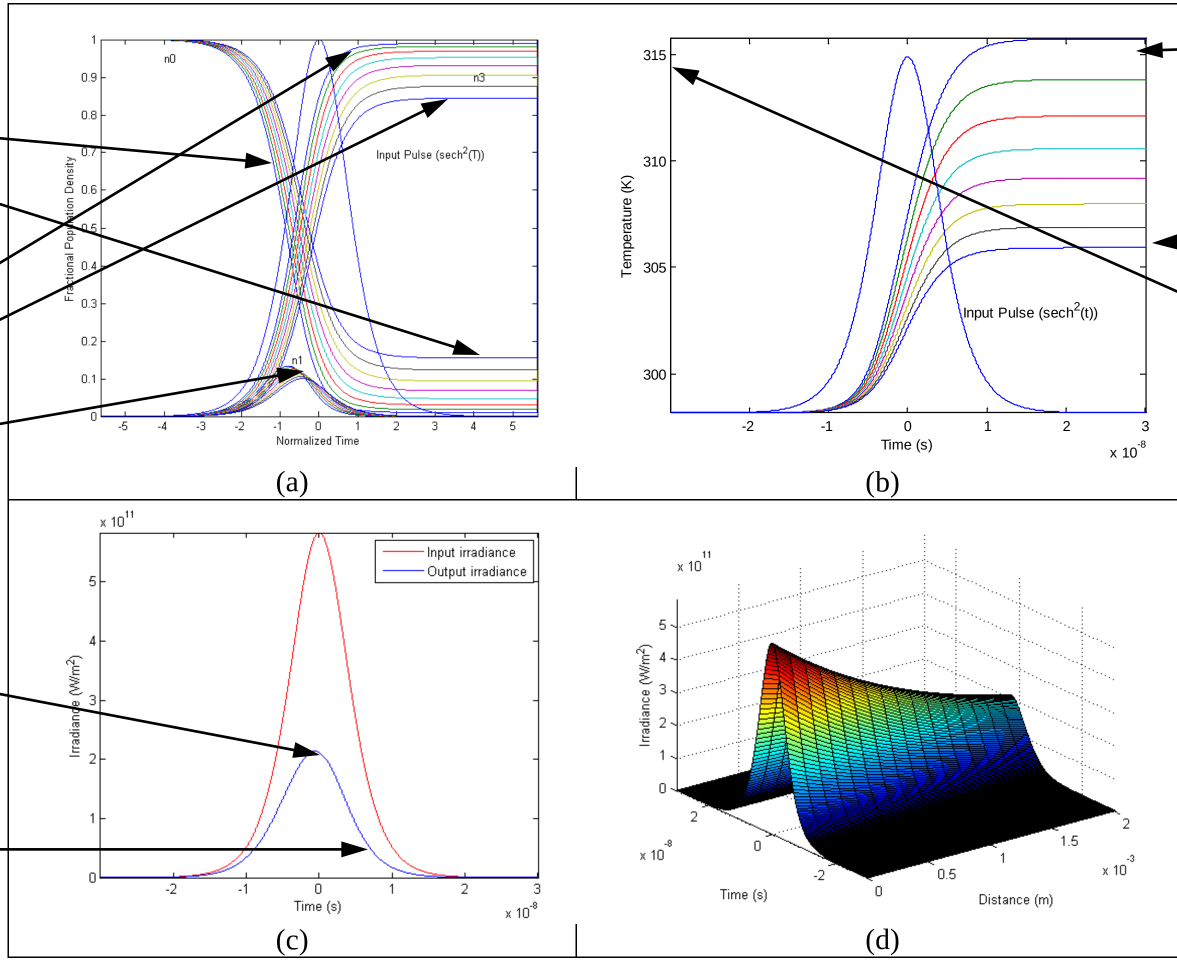

Temperature of input surface

Temperature of output surface

C_{60} molecules heat up only slightly, since their ground state absorption cross section is so small compared to carbon particles. (C_{60} molecules are much smaller than carbon black particles.)

Model output for a solution of C60 with 70% linear transmittance at 532 nm through a 2 mm path length with 7.8 microJoules input energy, 20 micron spot radius, and 10 ns pulse width. (a) Fractional population density vs. normalized time, (b) isolated molecule temperature vs. time, (c) input and output pulse irradiance vs. time, and (d) surface plot showing the irradiance profile as the beam propagates through the material.

Collimated geometry is assumed.

Hypothetical Case: Colloidal C_{60} at CBS Threshold

Ground state population density
Output surface
Input surface
Triplet state population density
Input surface
Output surface
Singlet state population density

Temperature of input surface
Temperature of output surface
C_{60} sublimation temperature (800 K)

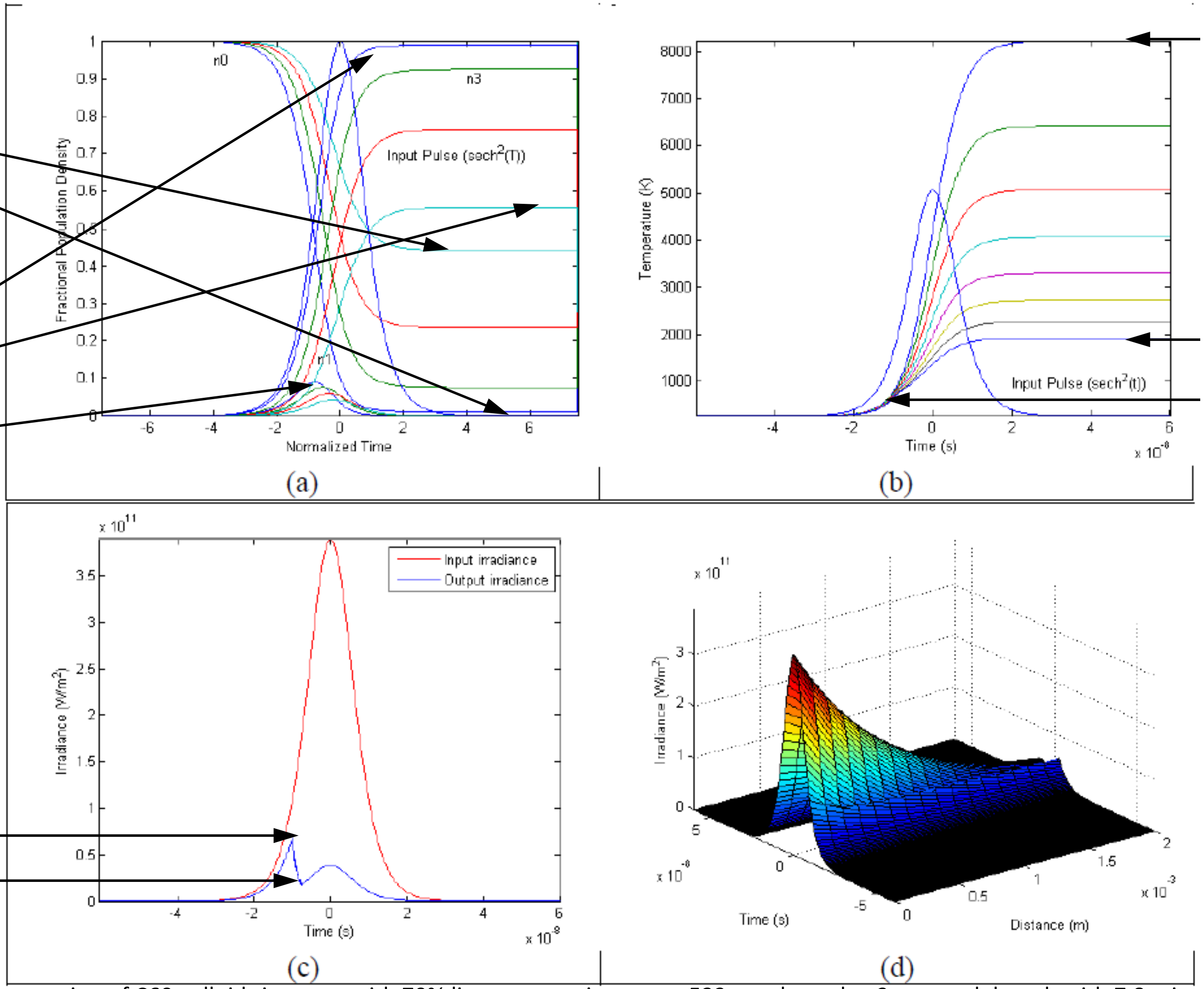

C_{60} colloids reach sublimation temperature early in the pulse (input surface).

Output surface reaches sublimation temperature.

(A particle radius of 85 nm was chosen for direct comparison to the CBS result.)

Model output for a suspension of C60 colloids in water with 70% linear transmittance at 532 nm through a 2 mm path length with 7.8 microJoules input energy, 20 micron spot radius, and 10 ns pulse width. (a) Fractional population density vs. normalized time, (b) isolated particle temperature vs. time, (c) input and output pulse irradiance vs. time, and (d) surface plot showing the irradiance profile as the beam propagates through the material.

Note: This hypothetical case assumed that all light absorbed was converted to heat and did not account for quenching. Collimated geometry is assumed.

Modeling of Total Scattering Results for CBS-1

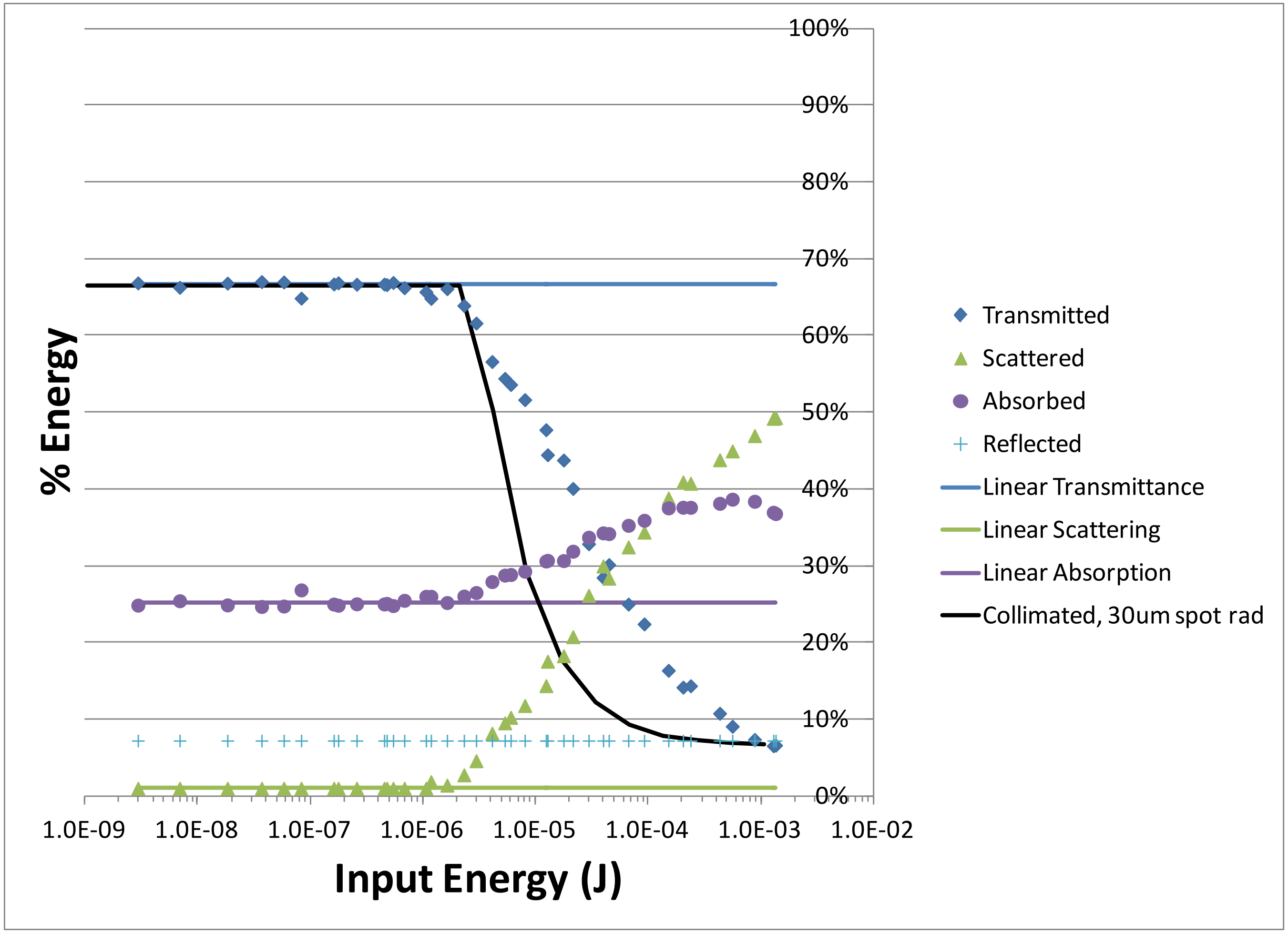

Modeling of Total Scattering Results for CBS-1

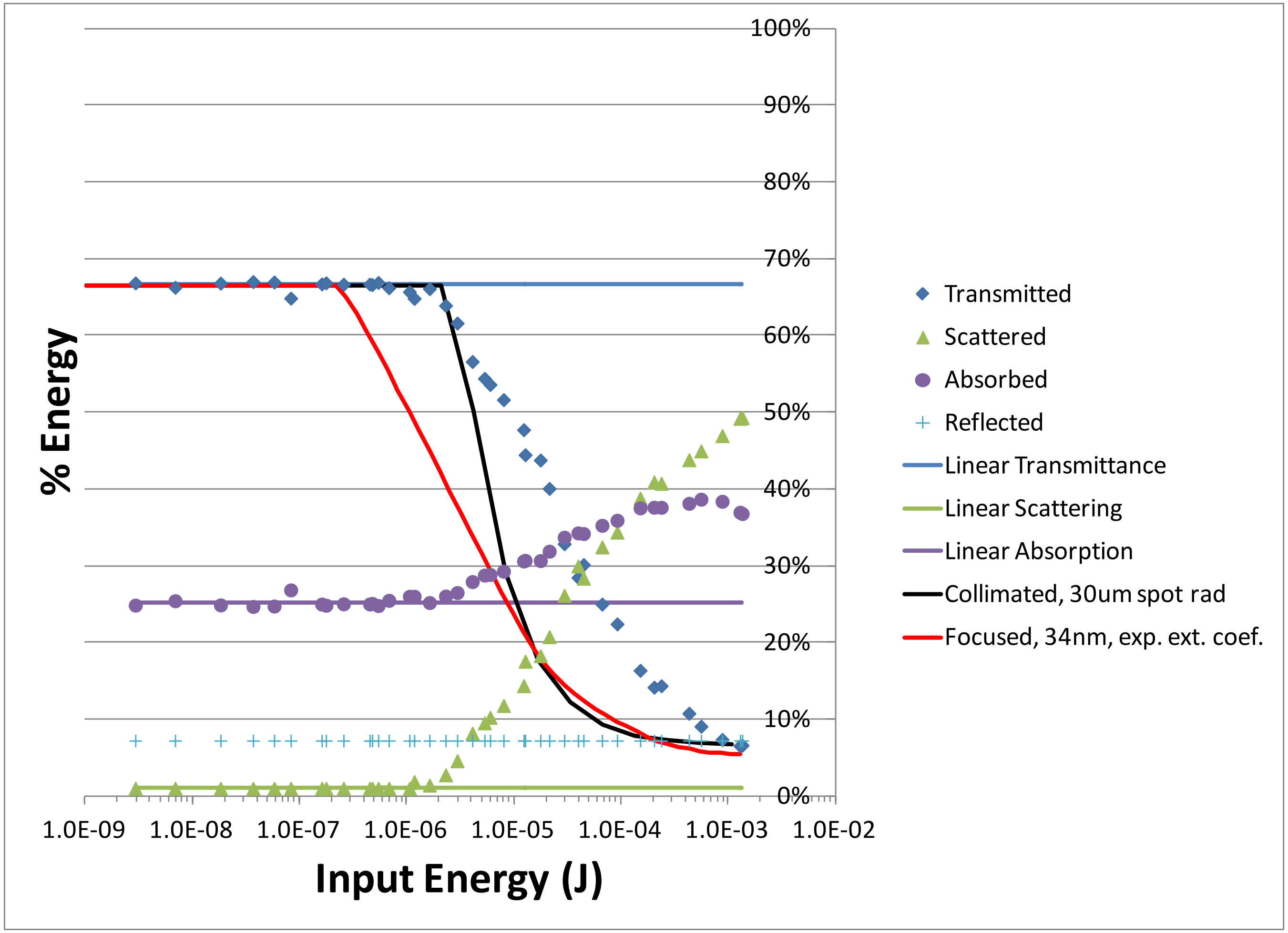

- Accounting for the focusing geometry gives the correct shape, assuming a constant extinction coefficient in the nonlinear region. The scattering centers have a characteristic size that is independent of input energy.

Modeling of Total Scattering Results for CBS-1

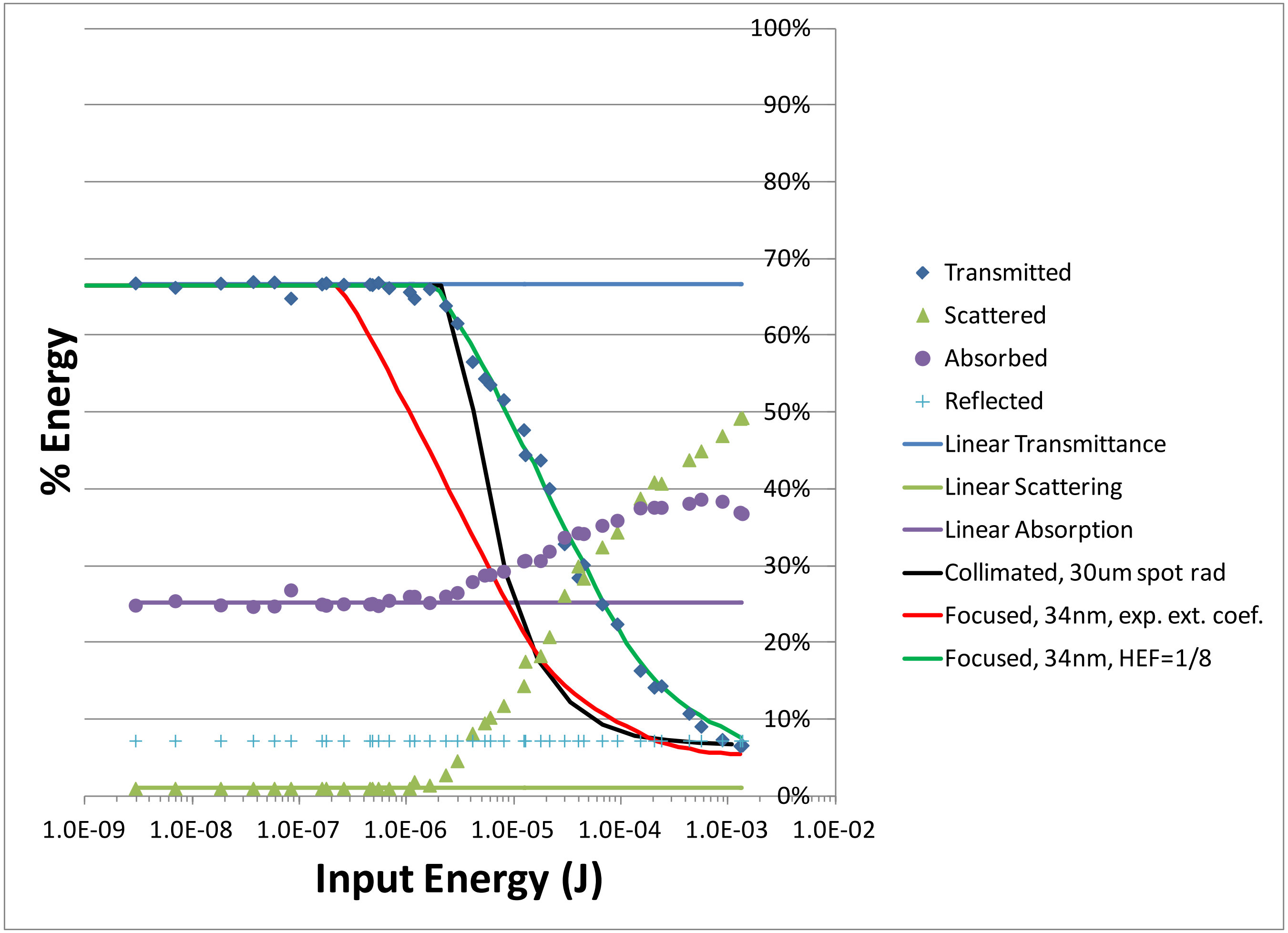

- Accounting for the focusing geometry gives the correct shape, assuming a constant extinction coefficient in the nonlinear region. The scattering centers have a characteristic size that is independent of input energy.
- A "heating efficiency factor" must be applied to match the experimental sublimation threshold.

Modeling of Total Scattering Results for CBS-1

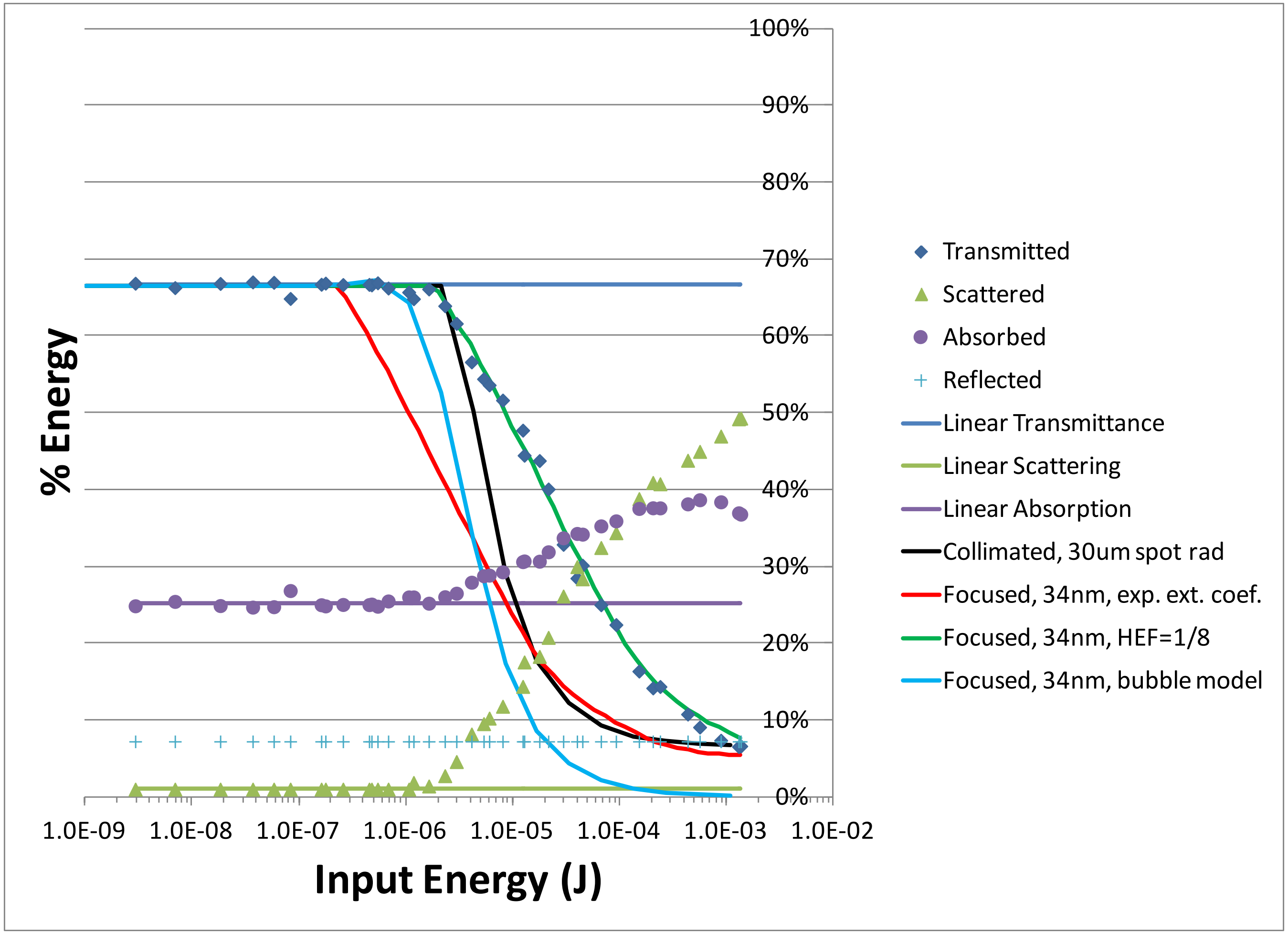

- Accounting for the focusing geometry gives the correct shape, assuming a constant extinction coefficient in the nonlinear region. The scattering centers have a characteristic size that is independent of input energy.
- A "heating efficiency factor" must be applied to match the experimental sublimation threshold.
- The bubble model predicts too much attenuation.

Modeling of Total Scattering Results for CBS-2

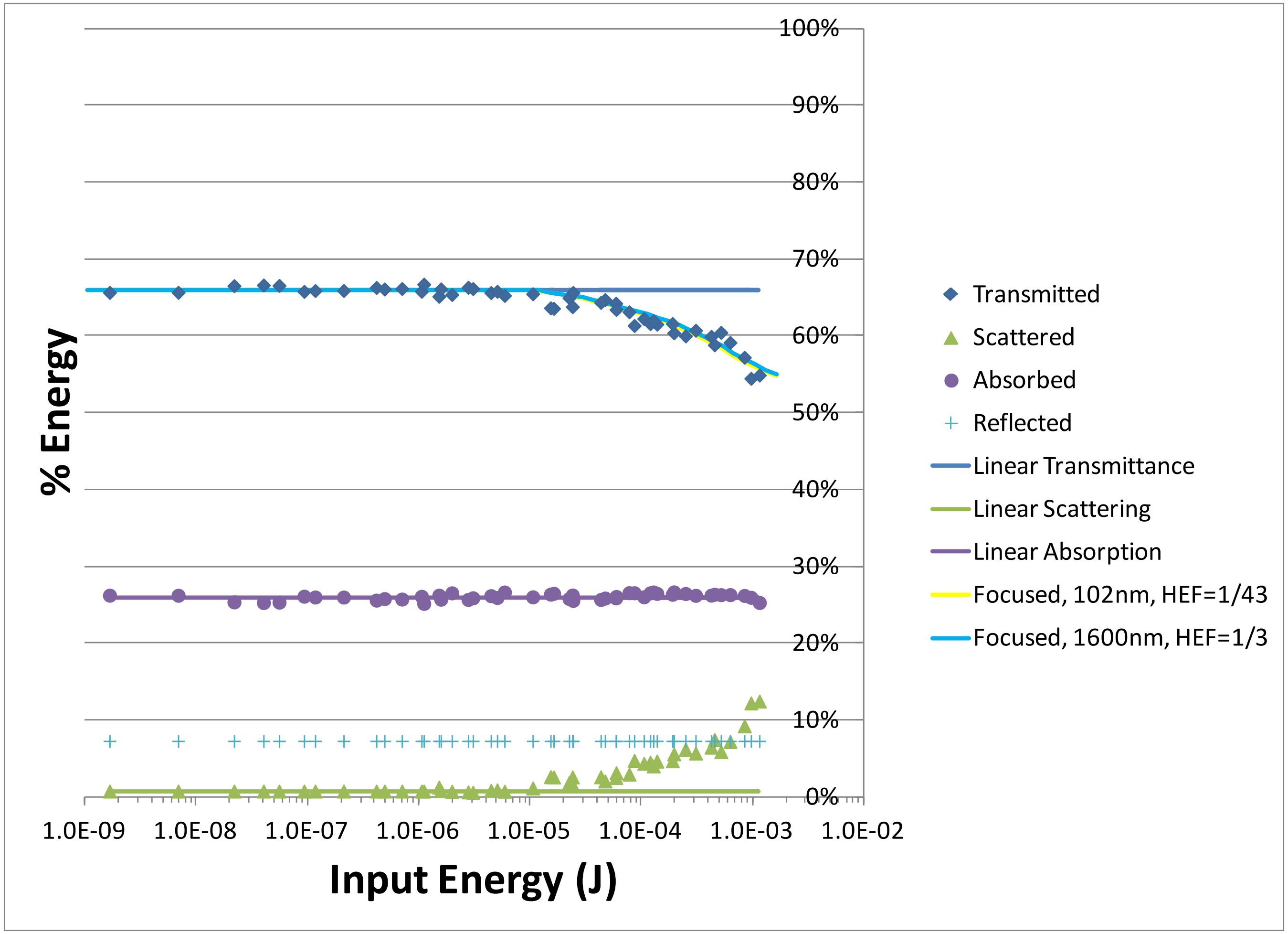

- The data can be fit to likely particle sizes, assuming a constant extinction coefficient in the nonlinear region. The scattering centers have a characteristic size that is independent of input energy.
- A “heating efficiency factor” must be applied to match the experimental sublimation threshold.

Modeling of Total Scattering Results for CBS-2

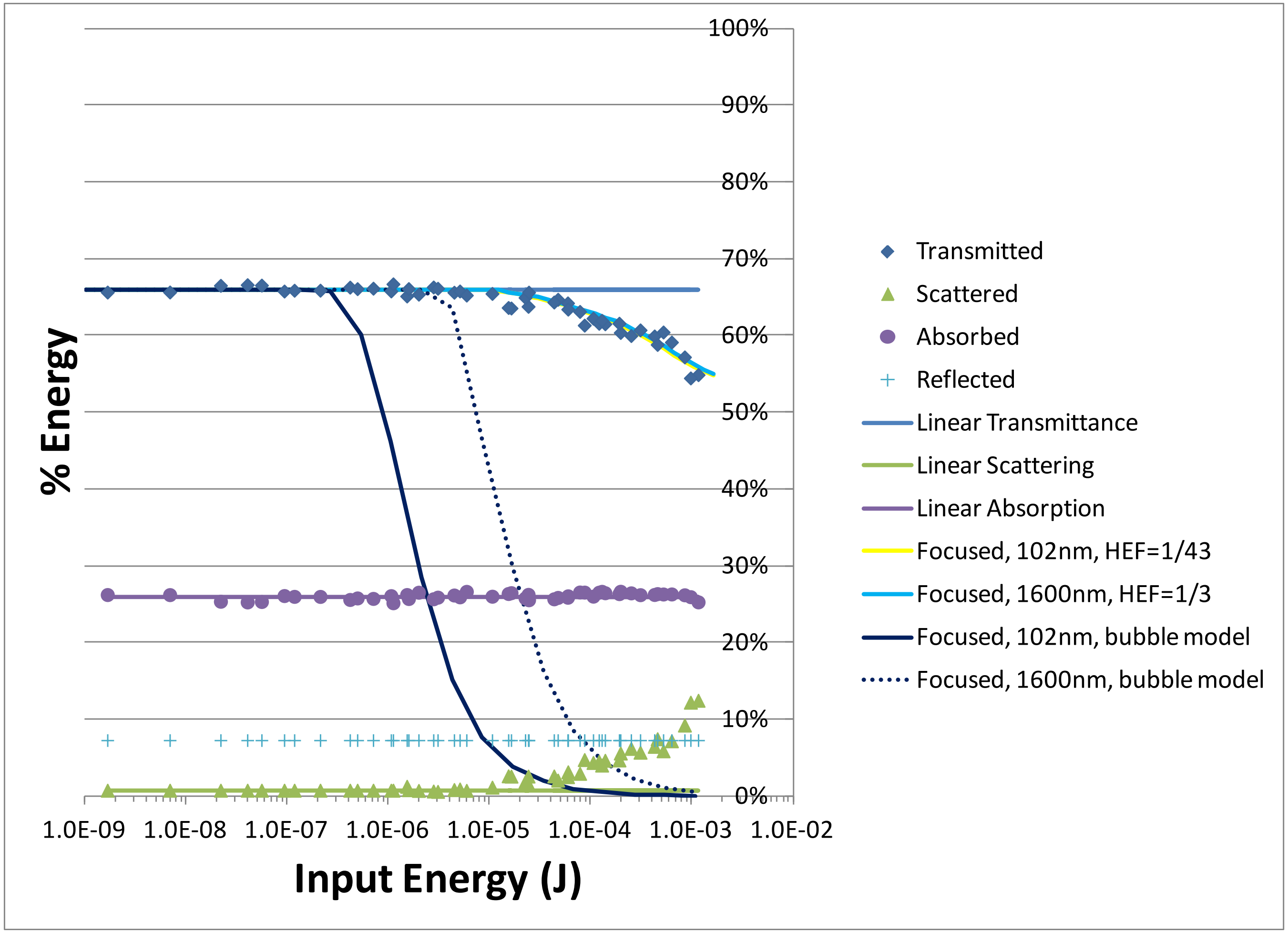

- The data can be fit to likely particle sizes, assuming a constant extinction coefficient in the nonlinear region. The scattering centers have a characteristic size that is independent of input energy.
- A “heating efficiency factor” must be applied to match the experimental sublimation threshold.
- The bubble model predicts too much attenuation.

Modeling of Total Scattering Results for C_{60} in Toluene

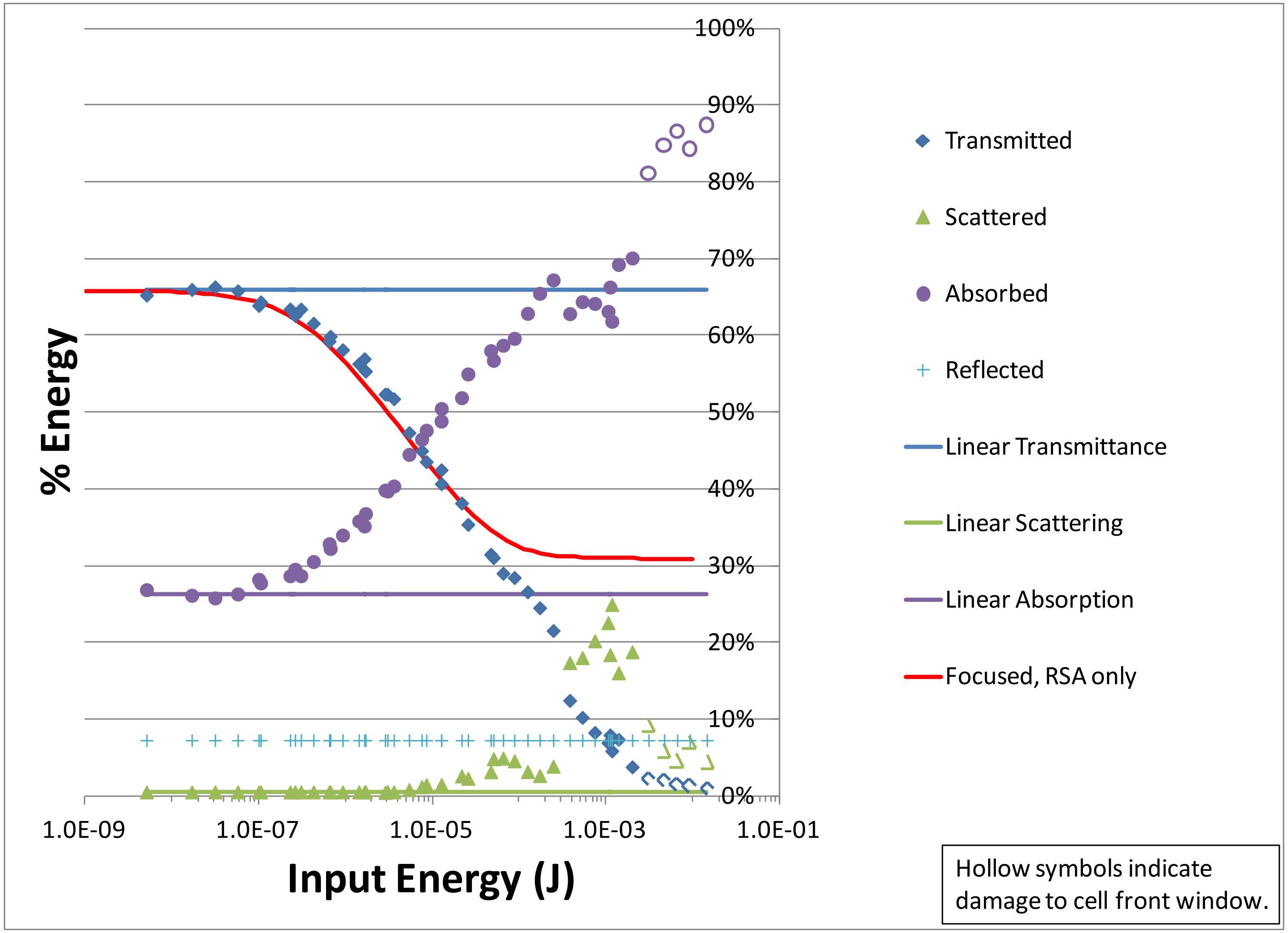

- The RSA-only region fits very well.

Modeling of Total Scattering Results for C_{60} in Toluene

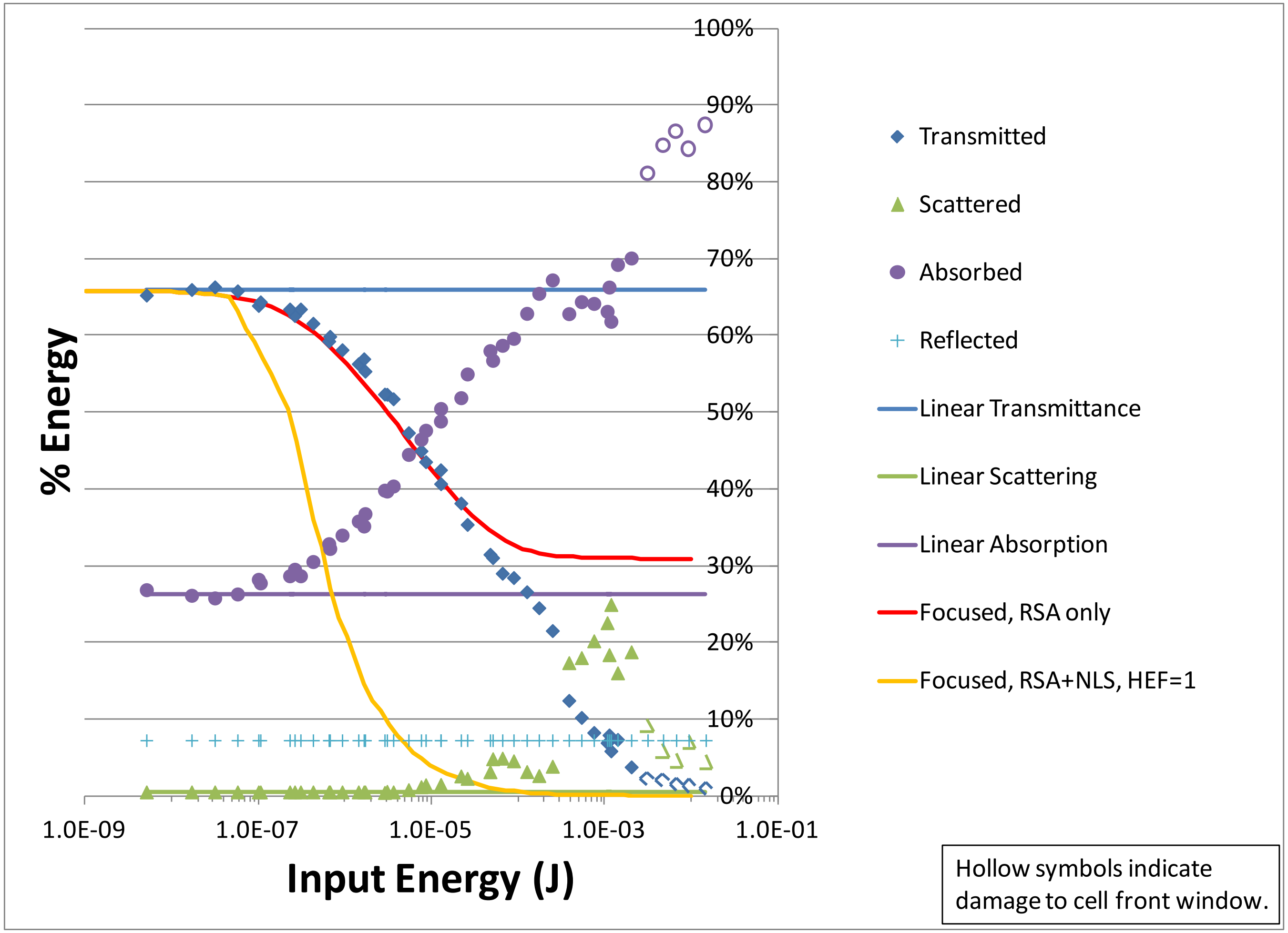

- The RSA-only region fits very well.

Modeling of Total Scattering Results for C_{60} in Toluene

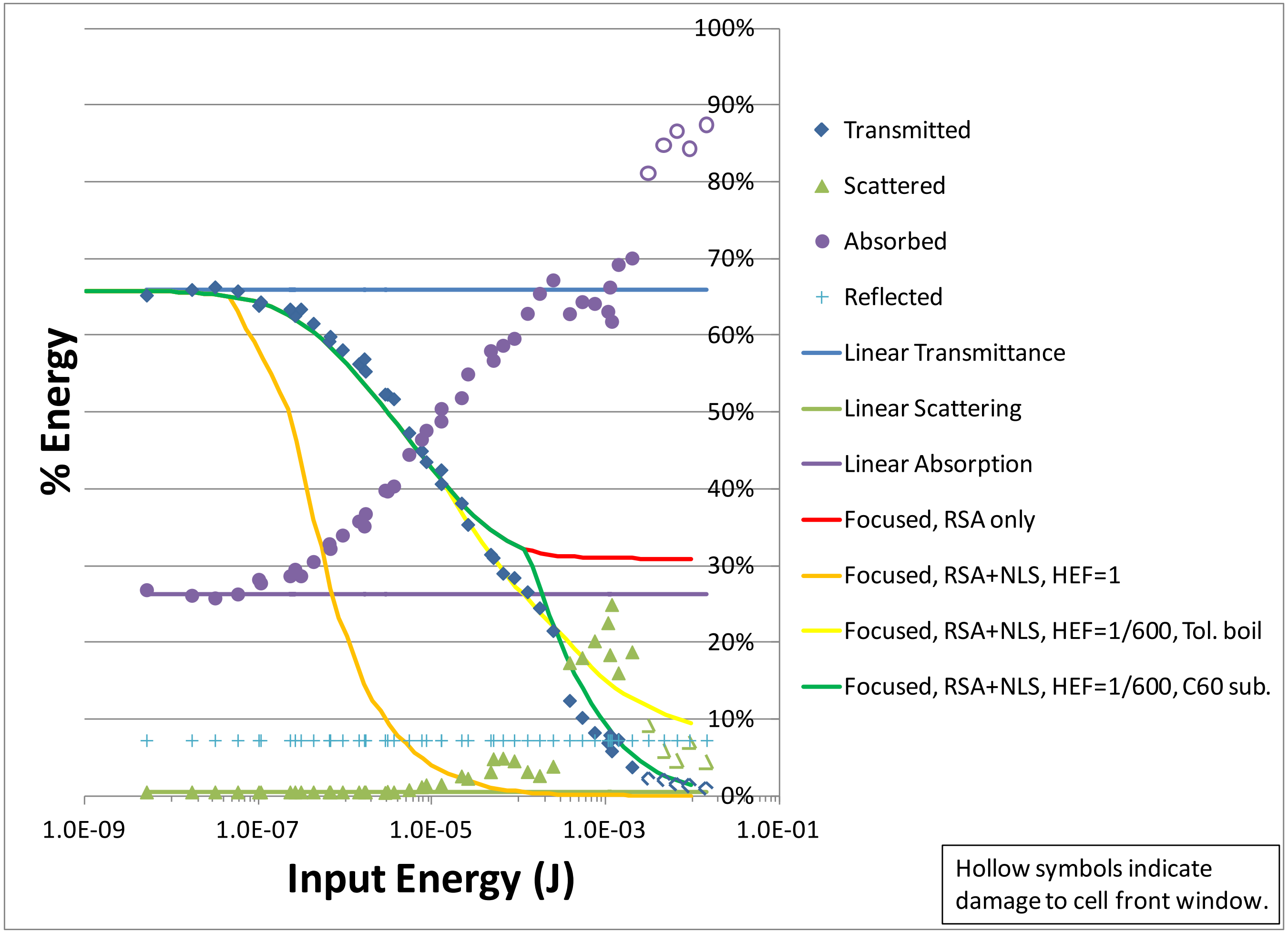

- The RSA-only region fits very well.
- With an appropriate "heating efficiency factor", the NLS data fits reasonably well assuming thresholds corresponding to the boiling point of toluene and the sublimation temperature of C_{60}.

Modeling of Total Scattering Results for C_{60} in Toluene

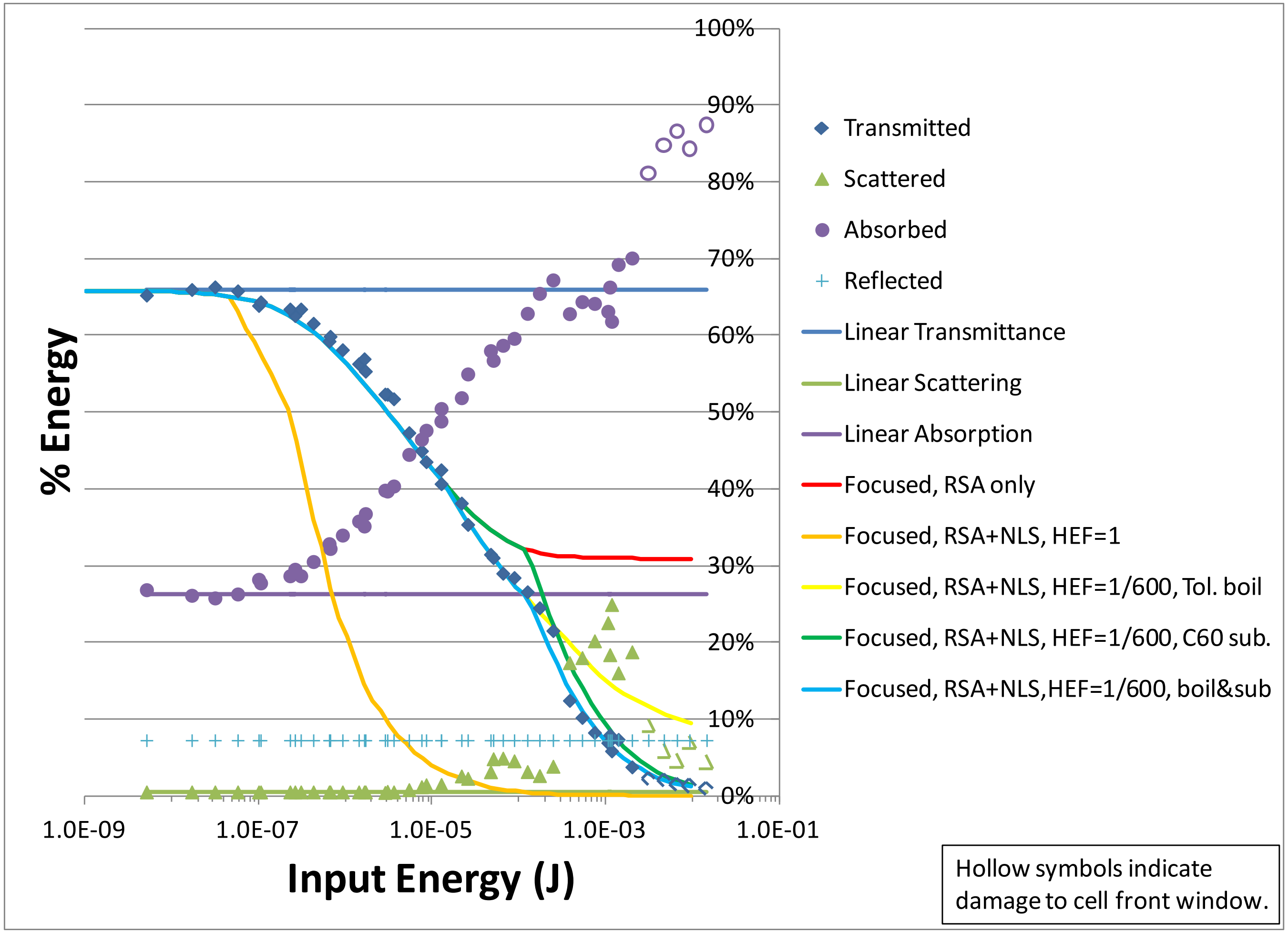

- The data in the nonlinear scattering regions fits well, assuming a constant extinction coefficient in the nonlinear region. The scattering centers have a characteristic size that is independent of input energy.
- A "heating efficiency factor" must be applied to match the experimental sublimation threshold(s).
- The RSA-only region fits very well.

Modeling of Total Scattering Results for Colloid C_{60}-1

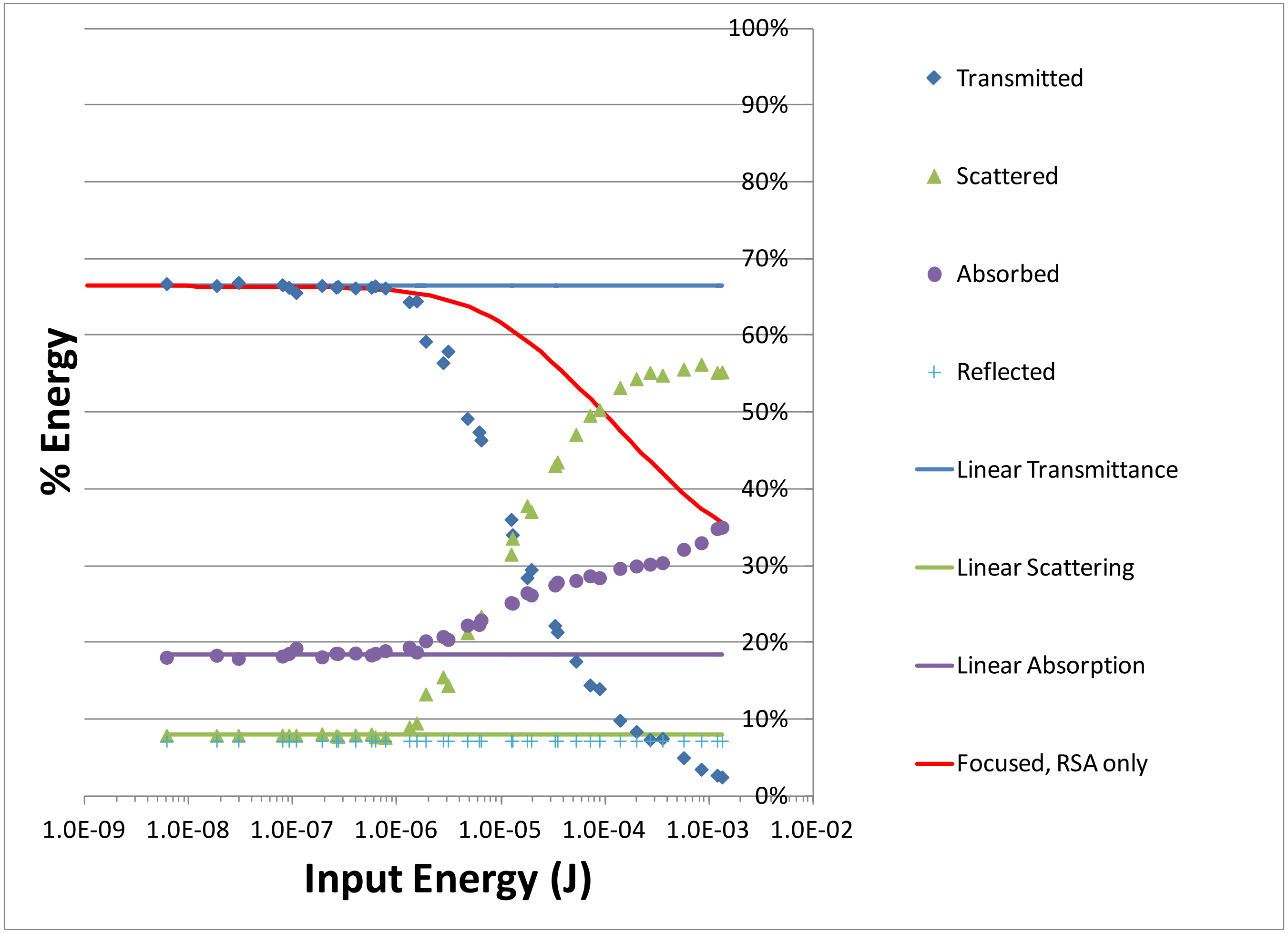

- Sublimation is reached before the triplet state is populated.

Modeling of Total Scattering Results for Colloid C_{60}-1

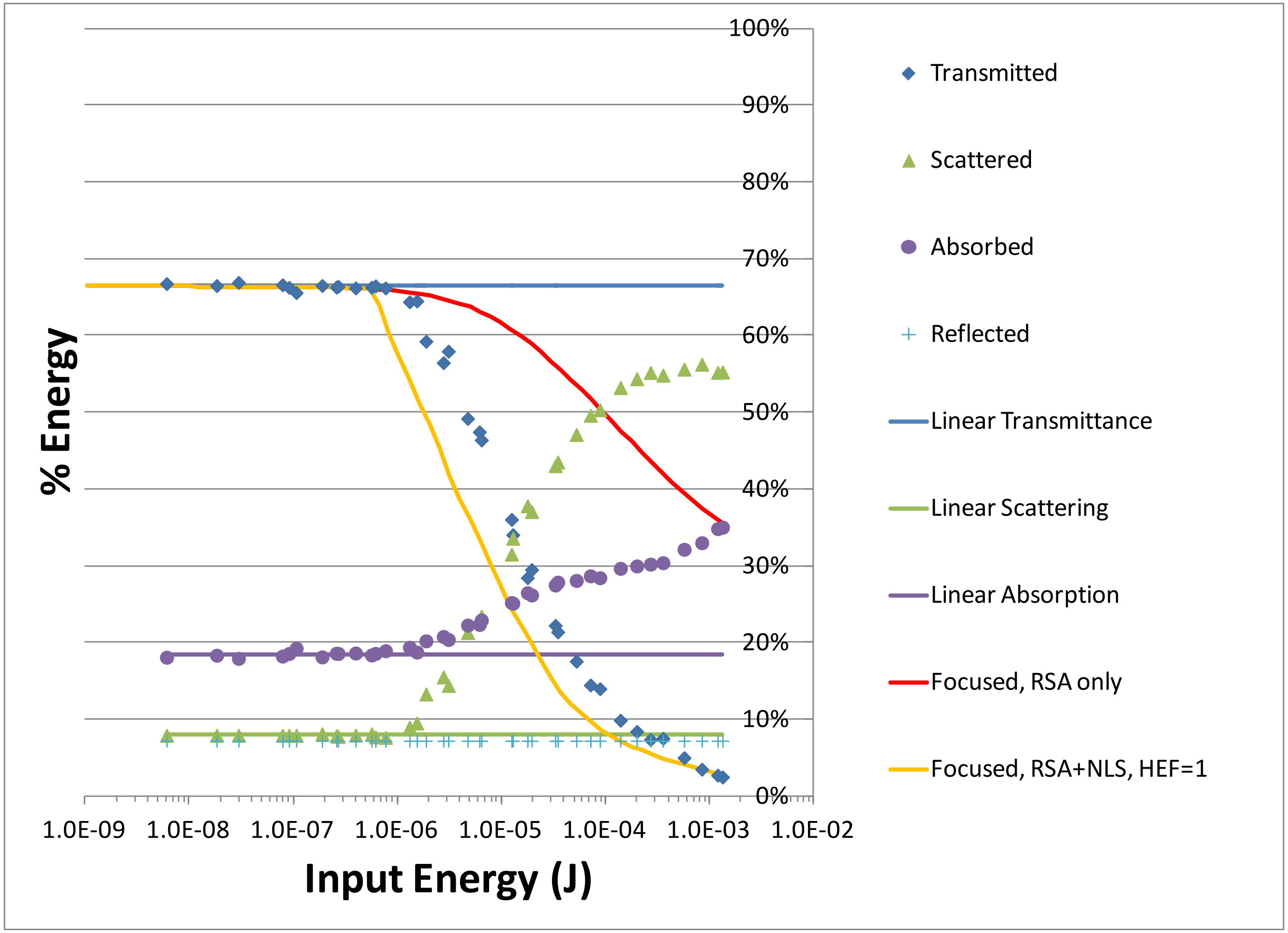

- The data in the nonlinear scattering regions fits well, assuming a constant extinction coefficient in the nonlinear region. The scattering centers have a characteristic size that is independent of input energy.
- Sublimation is reached before the triplet state is populated.

Modeling of Total Scattering Results for Colloid C_{60}-1

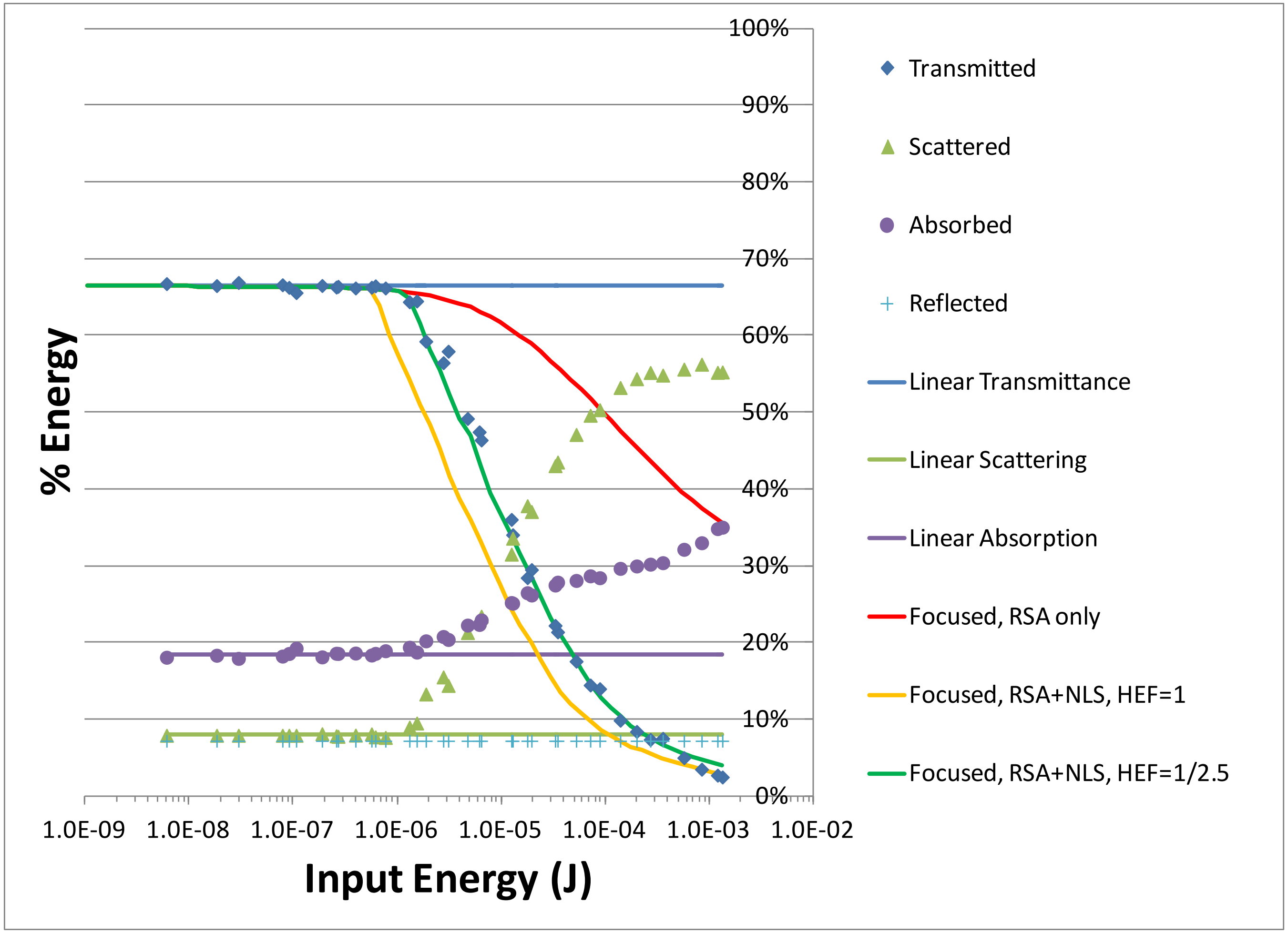

- The data in the nonlinear scattering regions fits well, assuming a constant extinction coefficient in the nonlinear region. The scattering centers have a characteristic size that is independent of input energy.
- A "heating efficiency factor" must be applied to match the experimental sublimation threshold.
- Sublimation is reached before the triplet state is populated.

Modeling of Total Scattering Results for Colloid C_{60}-2

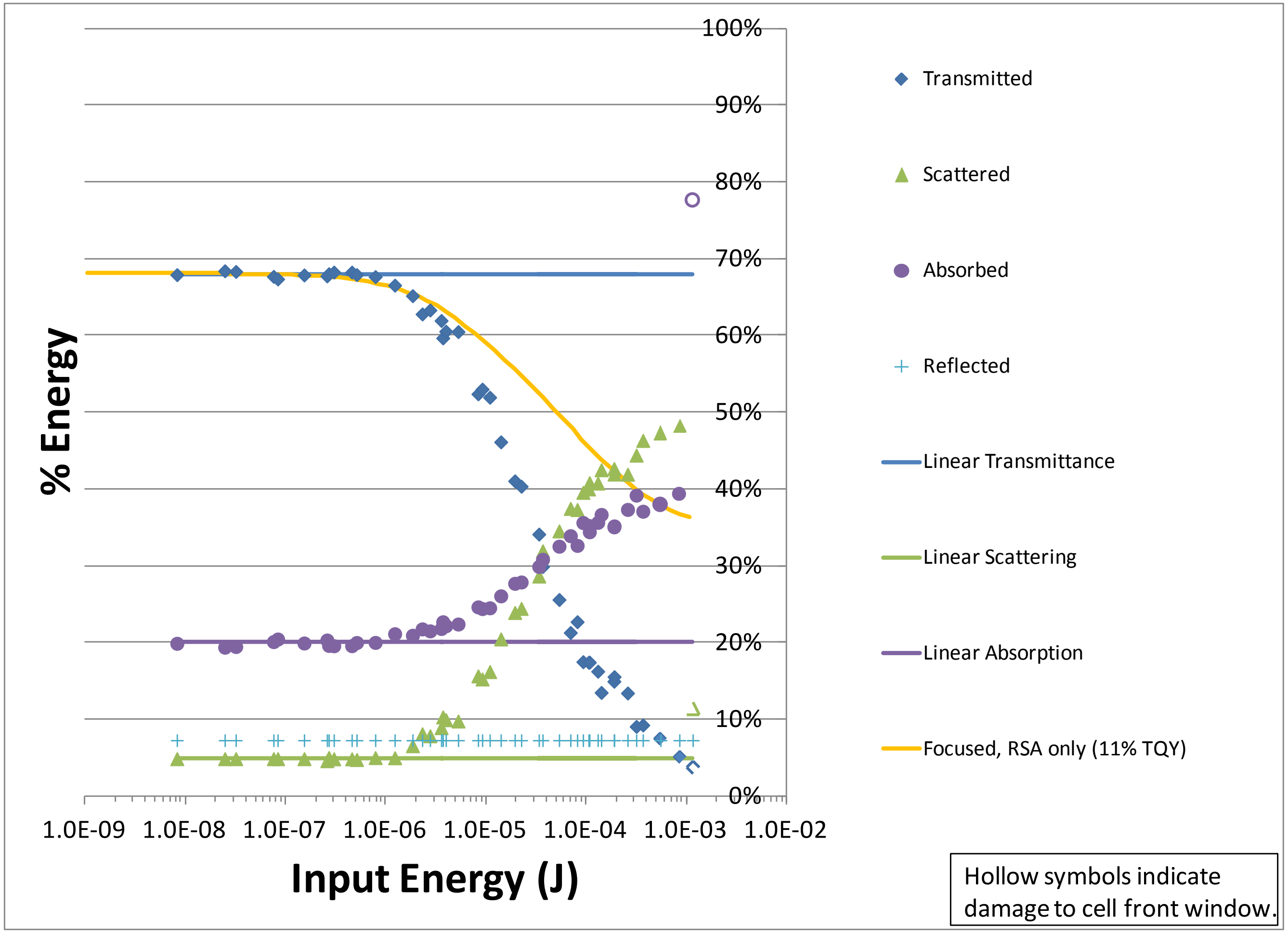

- The RSA-only region fits well assuming 11% triplet yield.

Modeling of Total Scattering Results for Colloid C_{60}-2

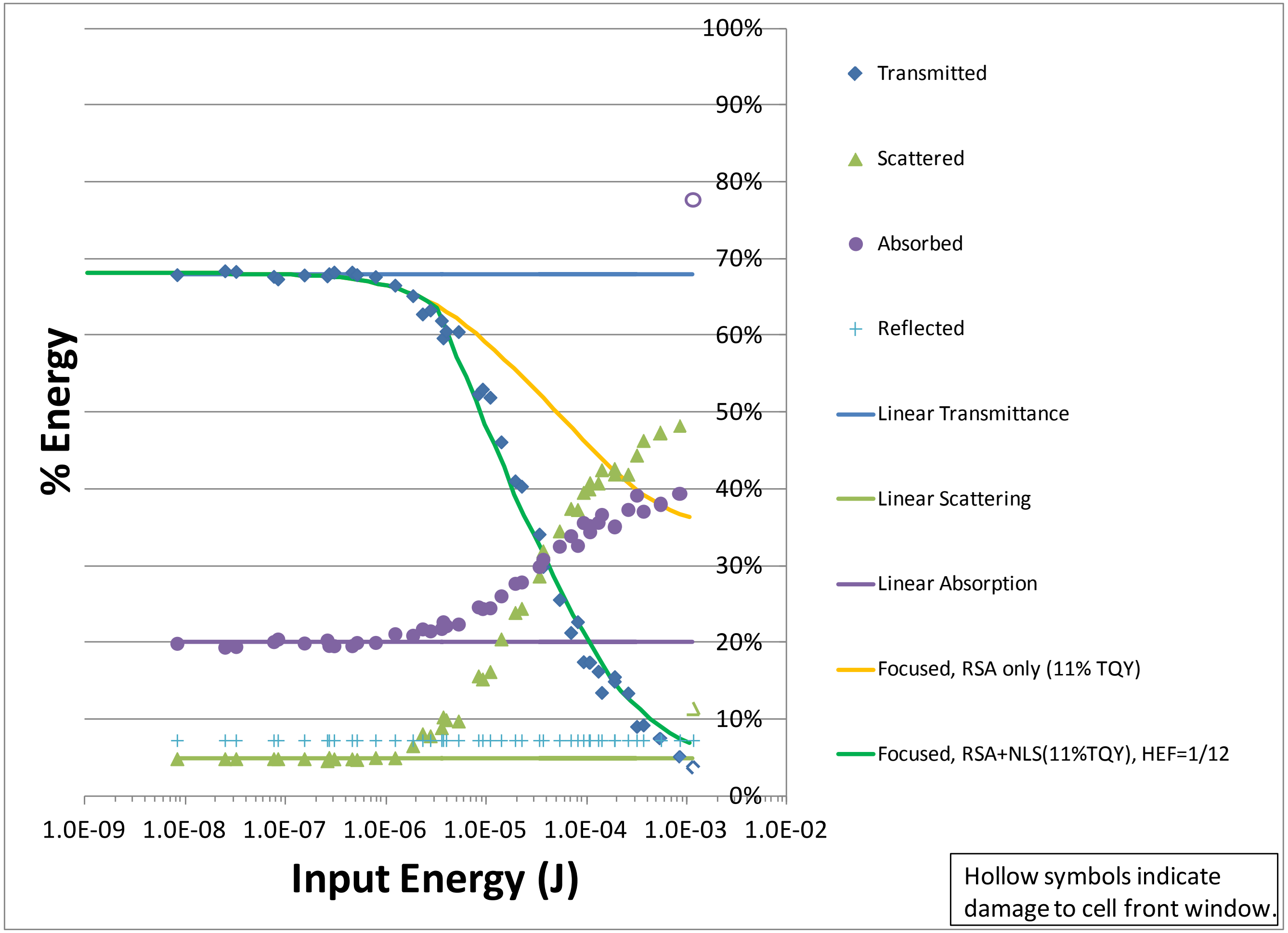

- The data in the nonlinear scattering regions fits well, assuming a constant extinction coefficient in the nonlinear region. The scattering centers have a characteristic size that is independent of input energy.
- A “heating efficiency factor” must be applied to match the experimental sublimation threshold.
- The RSA-only region fits well assuming 11% triplet yield.

Modeling of Total Scattering Results for Colloid C_{60}-2

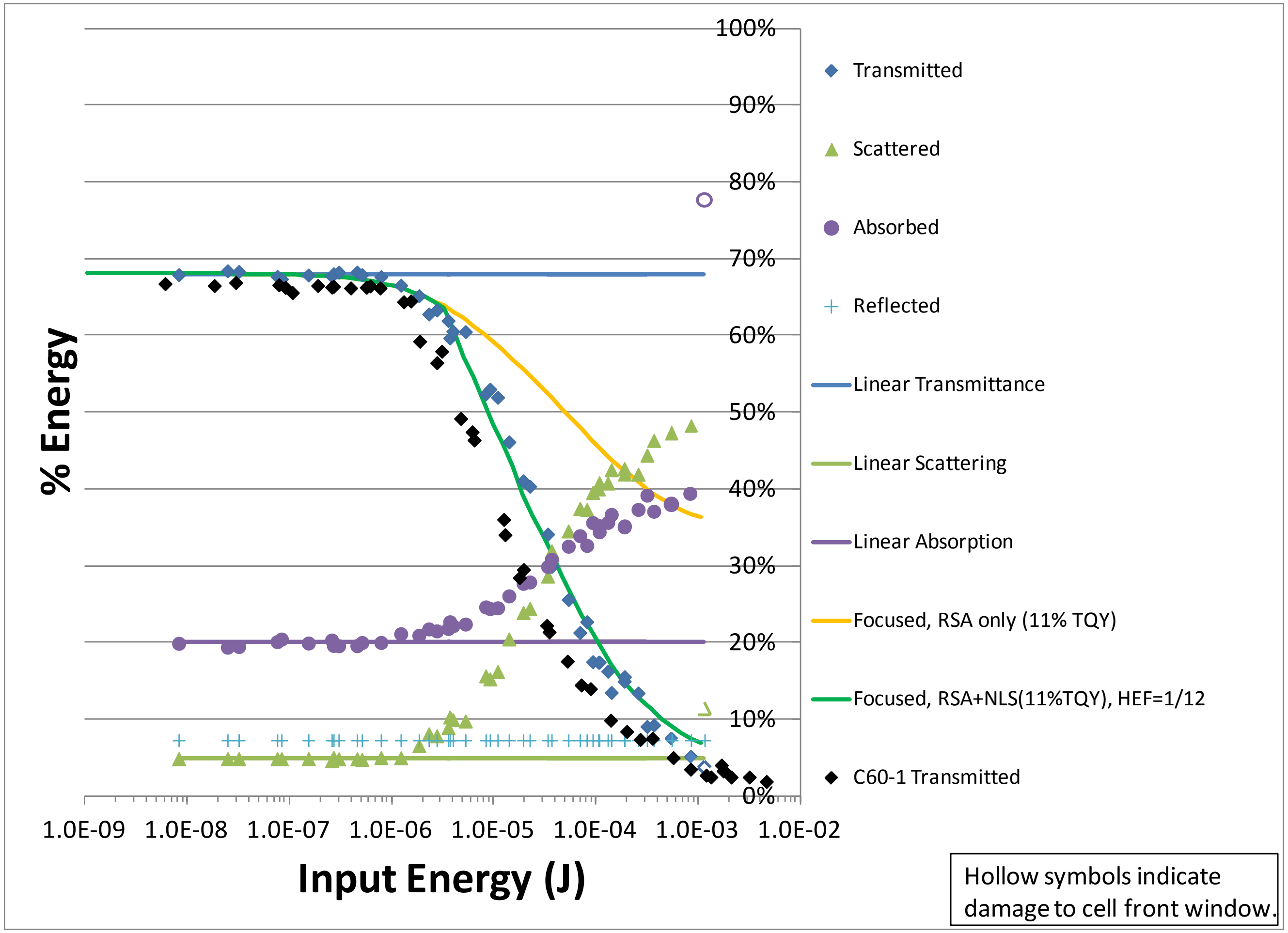

- C_{60}-2 has a higher NLS threshold than C_{60}-1. This implies that C_{60}-2 is less efficient at heating to sublimation. Since the particle size distributions are so similar, this difference in NLS threshold is not likely explained by particle size. Rather, it is more likely that the population in the triplet state contributes less to heating the particles. The triplet states are long-lived, so a portion of the energy is stored as electronic energy and cannot convert to heat until well after the input pulse.

Modeling of Total Scattering Results for Colloid C_{60}-3

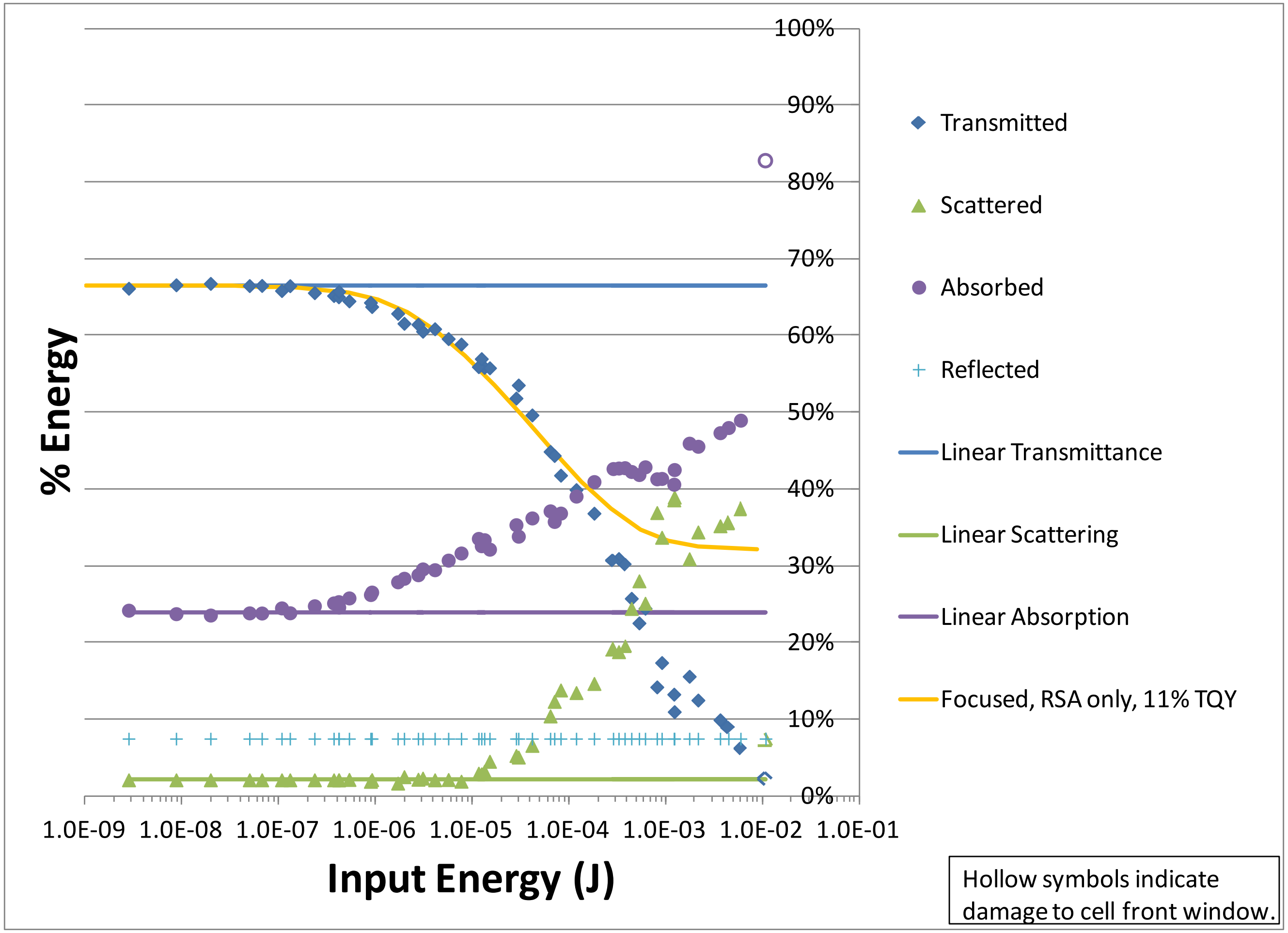

- The RSA-only region fits well assuming an 11% triplet quantum yield.
- This is the same triplet quantum yield as C_{60}-2.
- Recall that C_{60}-2 and C_{60}-3 were both amorphous, while C_{60}-1 was highly crystalline.
- Interpretation: Quenching is morphology dependent.

Modeling of Total Scattering Results for Colloid C_{60}-3

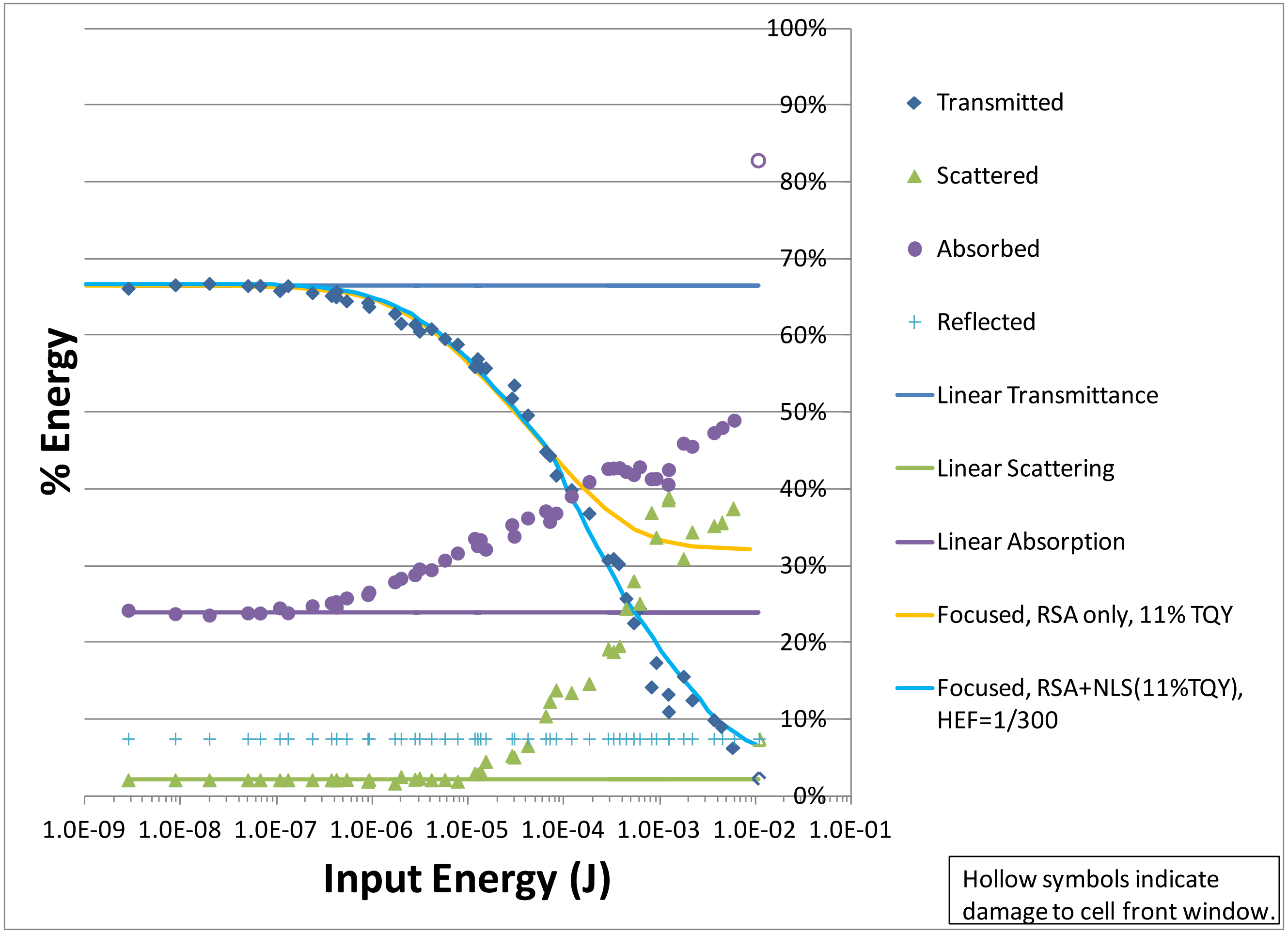

- C_{60}-3 has a much higher NLS threshold than C_{60}-1 and C_{60}-2. This is likely due to both its higher triplet quantum yield and its smaller size, resulting in faster dispersion of heat to the surrounding medium and delayed sublimation.

Modeling of Total Scattering Results for Colloid C_{60}-3

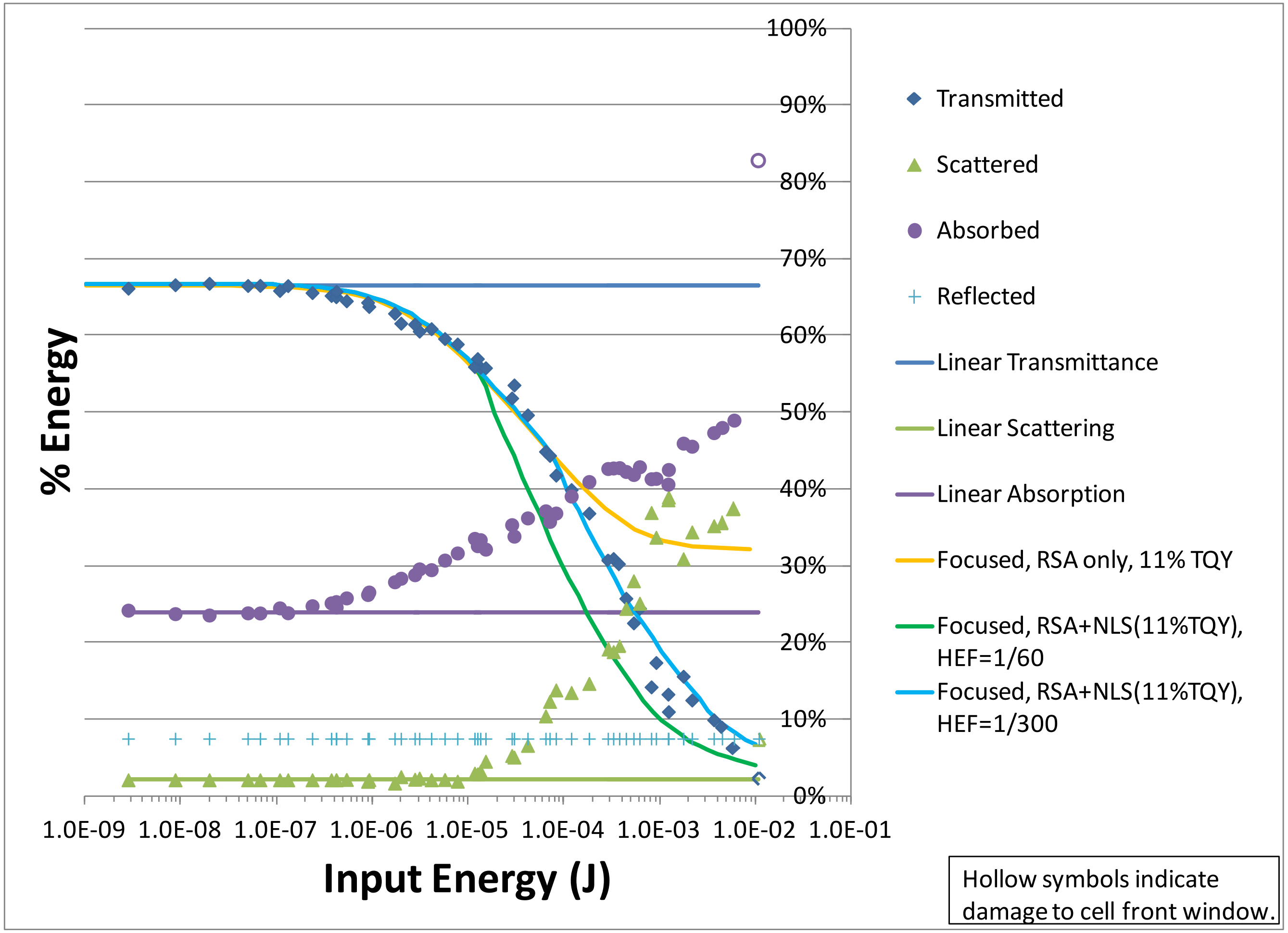

- Upon close inspection, the model that fits the transmittance curve does not correspond to the onset of nonlinear scattering.
- When fitting the onset of scattering, the hybrid model does not fit the transmittance curve well.
- This could be indicative of a two-threshold behavior: (1) generation of water vapor bubbles and (2) sublimation of the colloids.
- This would be consistent with a more rapid dissipation of heat to the medium because of the colloids' small size.

Conclusions

- All samples in this study followed an attenuation pattern in the nonlinear scattering region that is consistent with a constant extinction coefficient. This indicates that the scattering centers that are formed have a characteristic size that is independent of the input pulse energy. Once the scattering center has formed, the remaining energy in the pulse contributes only weakly to its size growth (if at all).

Conclusions

- All colloidal C_{60} samples showed evidence of some population of the triplet state, so they do exhibit RSA behavior (albeit much weaker than C_{60} molecular solutions).
- All colloidal C_{60} samples showed evidence of strong quenching of the first excited singlet state, leading to weak inter-system crossing.
- The degree of quenching is morphology dependent. The more crystalline the colloid, the stronger the quenching.

Conclusions

- The C_{60} colloids with amorphous morphology had less quenching and higher triplet quantum yield. This correlated to higher sublimation thresholds. This indicates that populating the triplet state causes a loss in efficiency of heating the particle. (A significant amount of energy is stored as electronic energy and not converted to heat until long after the pulse.) Consequently, the stronger the RSA behavior of a C_{60} colloid is, the worse its nonlinear scattering behavior will be.

Conclusions

- Overall, the most highly crystalline C_{60} colloid (C_{60}-1) provided the most attenuation out of all the samples tested. However, this was due to its lower sublimation threshold (800 K vs. 3770 K) compared to carbon black, not its RSA behavior. To optimize optical limiting/switching at high input energies, synthesize C_{60} colloids that are as highly crystalline as possible.
- C_{60} colloids do present an improvement over benchmark NLO materials such as carbon black suspensions and C_{60} solutions, but not for the reasons anticipated.

Acknowledgments

- R. David Rauh, Fei Wang, and Jane Bertone for synthesis of the C_{60} colloids
- Anthony Sutorik, Todd Stefanik, and De Gao for synthesis of the CBS samples
- David Ziegler for the TEM images
- Joy Haley, Dan McLean, Jon Slagle, Tom Cooper, and Augustine Urbas for the use of their transient absorption spectroscopy experiments, help analyzing the results, and helpful conversations
- Andy Mott and David Mackie for the Z-Scan measurements
- Dr. Kost for help designing the custom integrating sphere for the total scattering experiment

END

BACKUPS

PREVIOUS SCHOLARSHIP / CONTEXT

K. Mansour, M. J. Soileau and E. W. Vanstryland, J. Opt. Soc. Am. B-Opt. Phys. 9 (7), 1100-1109 (1992).

- Reported optical switching/limiting in carbon black suspensions (CBS)
- Proposed mechanism: strong linear absorption giving rise to thermionic emission, resulting in avalanche ionization and thus, nanoplasmas that absorb and scatter the light
- NLO behavior is fluence dependent
- Uncalibrated measurements of transmitted, absorbed, and energy scattered at one angle
- Mapped scattering patterns to Mie theory

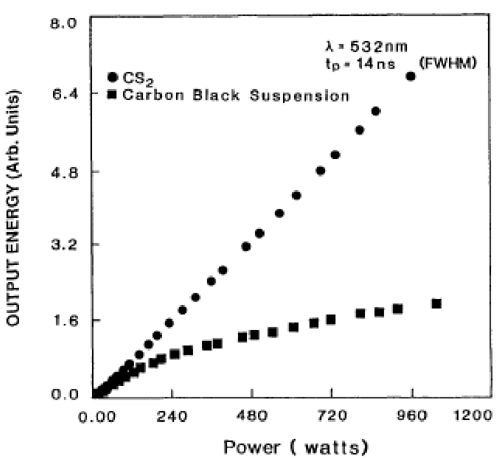

Fig. 3. Energy output for CS_2 and CBS as a function of input peak power for 14-ns (FWHM), 532-nm pulses focused to $w_0 \simeq 3.5$ μm for input powers of 1 to 1000 W.

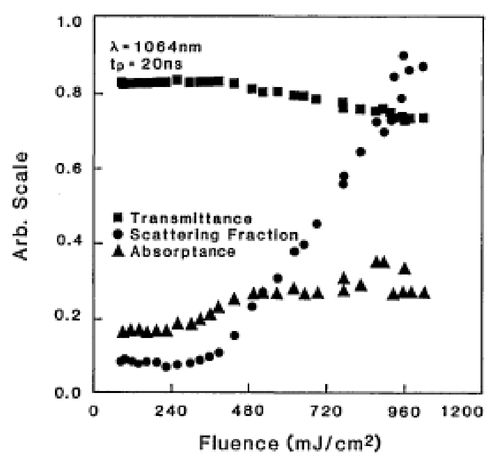

Fig. 8. Transmittance, absorptance, and scattering fraction as a function of incident fluence for 1064-nm, 20-ns (FWHM) pulses focused to $w_0 \simeq 156$ μm for incident fluences of 0.08 to 1 J/cm^2.

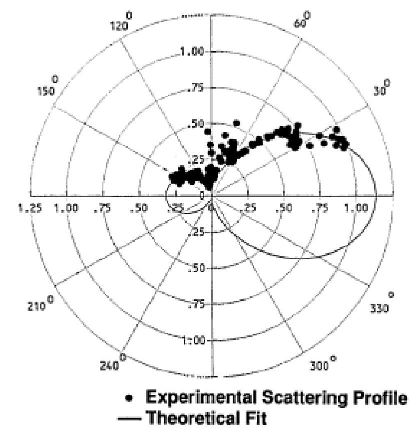

Fig. 16. Polar plot of the fraction of scattered light (arbitrarily scaled) for a CBS for an incident fluence of $\simeq$550 mJ/cm^2 for 20-ns (FWHM), 1064-nm linearly polarized light parallel to the plane of observation. The spot size was $w_0 \simeq 96$ μm. The theoretical fit is based on Mie scattering theory.

D. Riehl and F. Fougeanet, Molecular Crystals and Liquid Crystals Science and Technology Section B: Nonlinear Optics 21 (1-4), 391-398 and 435-446 (1999).

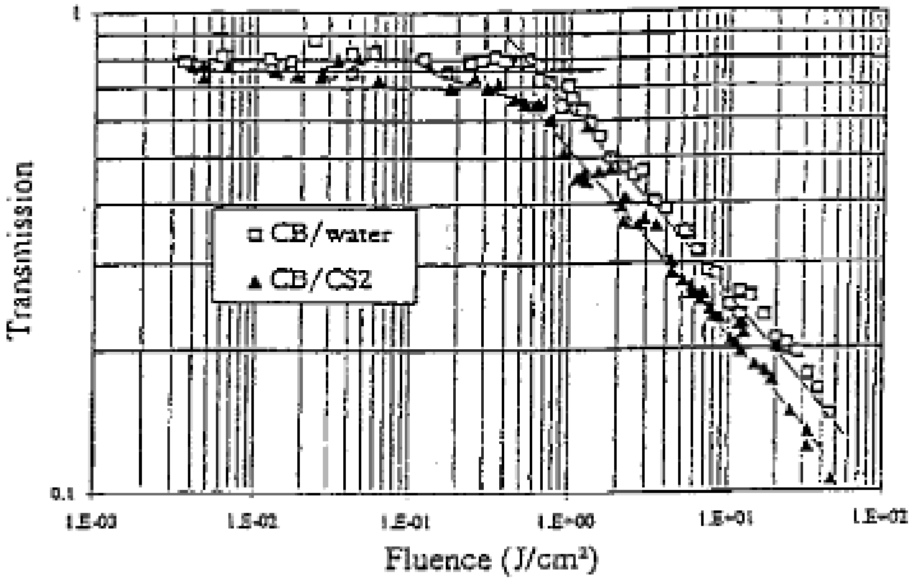

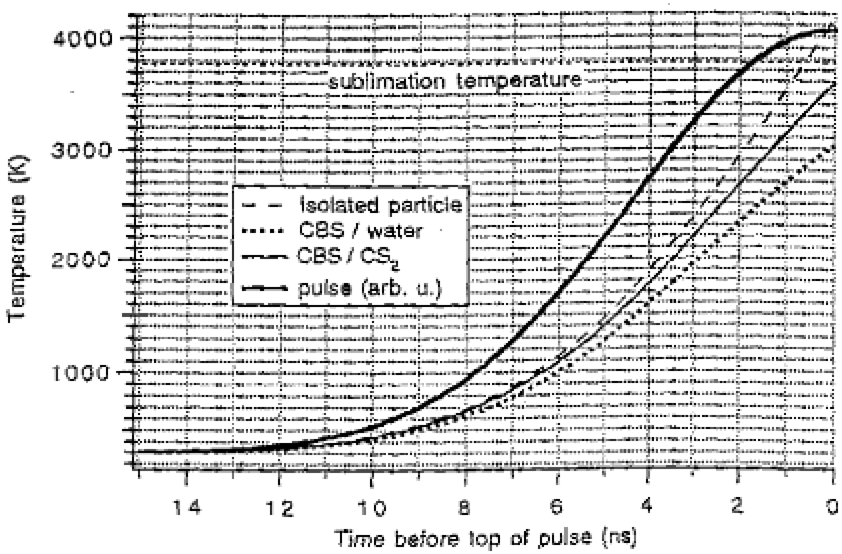

- Thermodynamic model for CBS
- Two threshold behavior: nanobubbles of evaporated liquid, then sublimation of particles. (Water only exhibits a sublimation threshold.)
- Attribute white light to carbon incandescence

✓ I adopted the underpinnings of this thermodynamic model into the modeling in this dissertation

K. J. McEwan, P. K. Milsom and D. B. James, presented at the Nonlinear Optical Liquids for Power Limiting and Imaging. San Diego, CA, 1998.

- Thermodynamic model
- Proposed mechanism: heating of particles by absorbed light and subsequent bubble formation
- Simple beam propagation model: Assumes digital character to Beer-Lambert Law extinction coefficient (one for the linear state, one for the scattering state)

$$T = e^{-\alpha L}$$

✓ I adopted this digital extinction coefficient approach to model beam attenuation

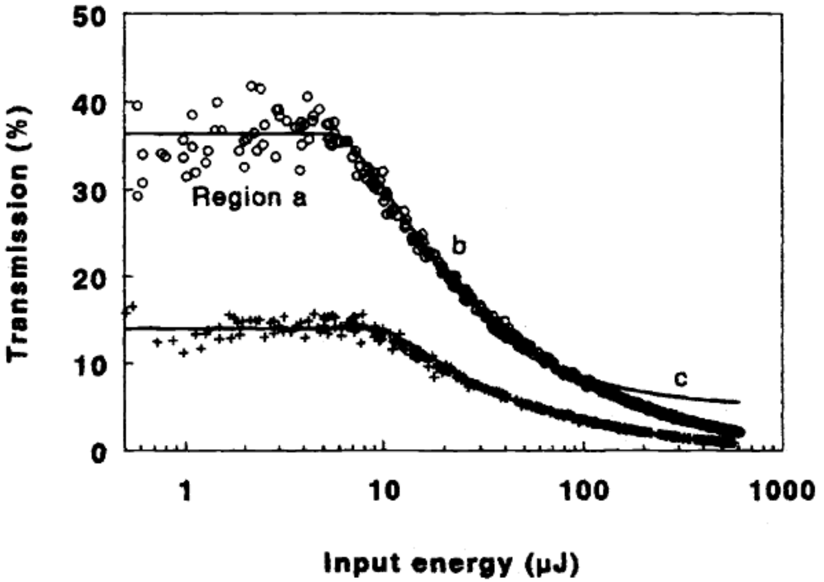

Figure 9: Comparison between simulated response (solid-line) and experimental data for two carbon black suspensions in water with different initial transmissions

H. W. Kroto, J. R. Heath, S. C. Obrien, R. F. Curl and R. E. Smalley, Nature 318 (6042), 162-163 (1985).

- Discovered C_{60}
- Suggested its structure
- Named it "Buckminsterfullerene"

During experiments aimed at understanding the mechanisms by which long-chain carbon molecules are formed in interstellar space and circumstellar shells[1], graphite has been vaporized by laser irradiation, producing a remarkably stable cluster consisting of 60 carbon atoms. Concerning the question of what kind of 60-carbon atom structure might give rise to a superstable species, we suggest a truncated icosahedron, a polygon with 60 vertices and 32 faces, 12 of which are pentagonal and 20 hexagonal. This object is commonly encountered as the football shown in Fig. 1. The C_{60} molecule which results when a carbon atom is placed at each vertex of this structure has all valences satisfied by two single bonds and one double bond, has many resonance structures, and appears to be aromatic.

Fig. 1 A football (in the United States, a soccerball) on Texas grass. The C_{60} molecule featured in this letter is suggested to have the truncated icosahedral structure formed by replacing each vertex on the seams of such a ball by a carbon atom.

L. W. Tutt and A. Kost, Nature 356, 225-226 (1992).

A. Kost, L. W. Tutt, M. B. Klein, T. K. Dougherty and W. E. Elias, Opt. Lett. 18 (5), 334-336 (1993).

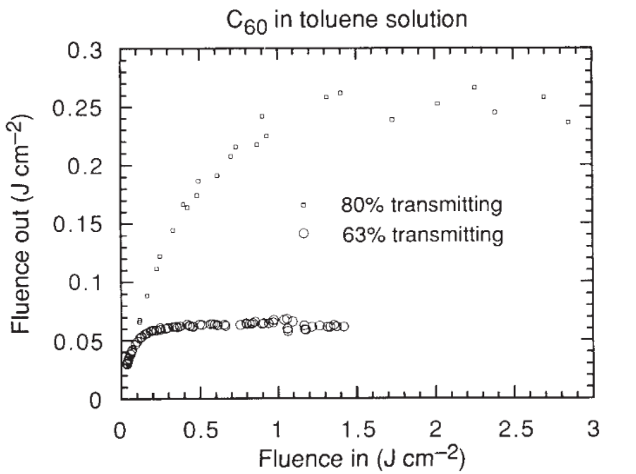

FIG. 1 Optical limiting response of 63% and 80% transmitting solutions of C_{60} in toluene to 7 ns, 532 nm optical pulses.

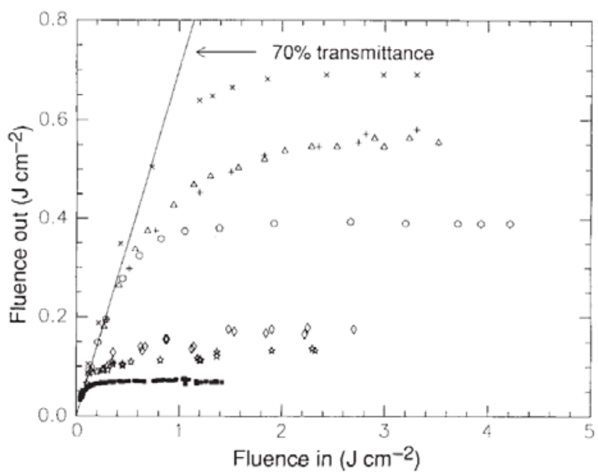

FIG. 2 Comparison of the optical limiting response of solutions of various reported optical limiters to C_{60} in toluene. All comparison solutions are 70% transmitting at 532 nm, and the solvent was methylene chloride, except with the two exceptions of chloroaluminum phthalocyanine, which was dissoved in methanol, and indanthrone, dissolved in dilute KOH. ○, $HFeCo_3(CO)_{10}(P(CH_3)_3)_2$; △, $HFeCo_3(CO)_{12}$; +, $(N(C_2H_5)_4)^+(FeCo_3(CO)_{12})^-$; ×, $HFeCo_3(CO_{10})(PPh_3)_2$; ◇, indanthrone; ☆, chloroaluminium phthalocyanine; ■, C_{60}.

- First reported optical limiting in C_{60} liquid solutions and solid hosts
- Pointed out that nonlinear scattering plays a role in C_{60}'s NLO response in liquids

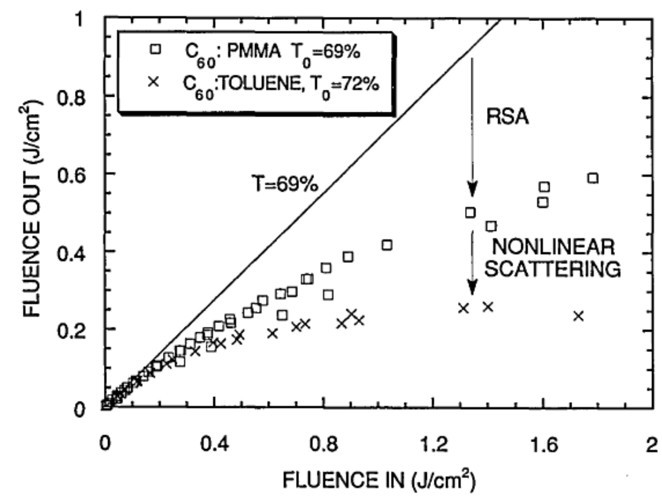

Fig. 3. Comparison of optical limiting for C_{60}:PMMA with C_{60}:toluene. The liquid appears to have an additional component from nonlinear scattering. RSA, reverse saturable absorption.

K. M. Nashold and D. P. Walter, Journal of the Optical Society of America B (Optical Physics) 12 (7), 1228-1237 (1995).

- Transmitted, scattered, and absorbed energy (total)
- Spatial distribution of scattered light
- Examined CBS and C_{60} in toluene
- CBS dominated by nonlinear scattering, but nonlinear absorption was also strong
- C_{60} in toluene dominated by nonlinear absorption, but there was significant nonlinear scattering (a ratio of 0.4 scattered to absorbed light)

✓ This work is the predecessor of the total scattering experiment in this dissertation, which I refined and extended to the study of C_{60} colloids.

CBS | C_{60} in Toluene

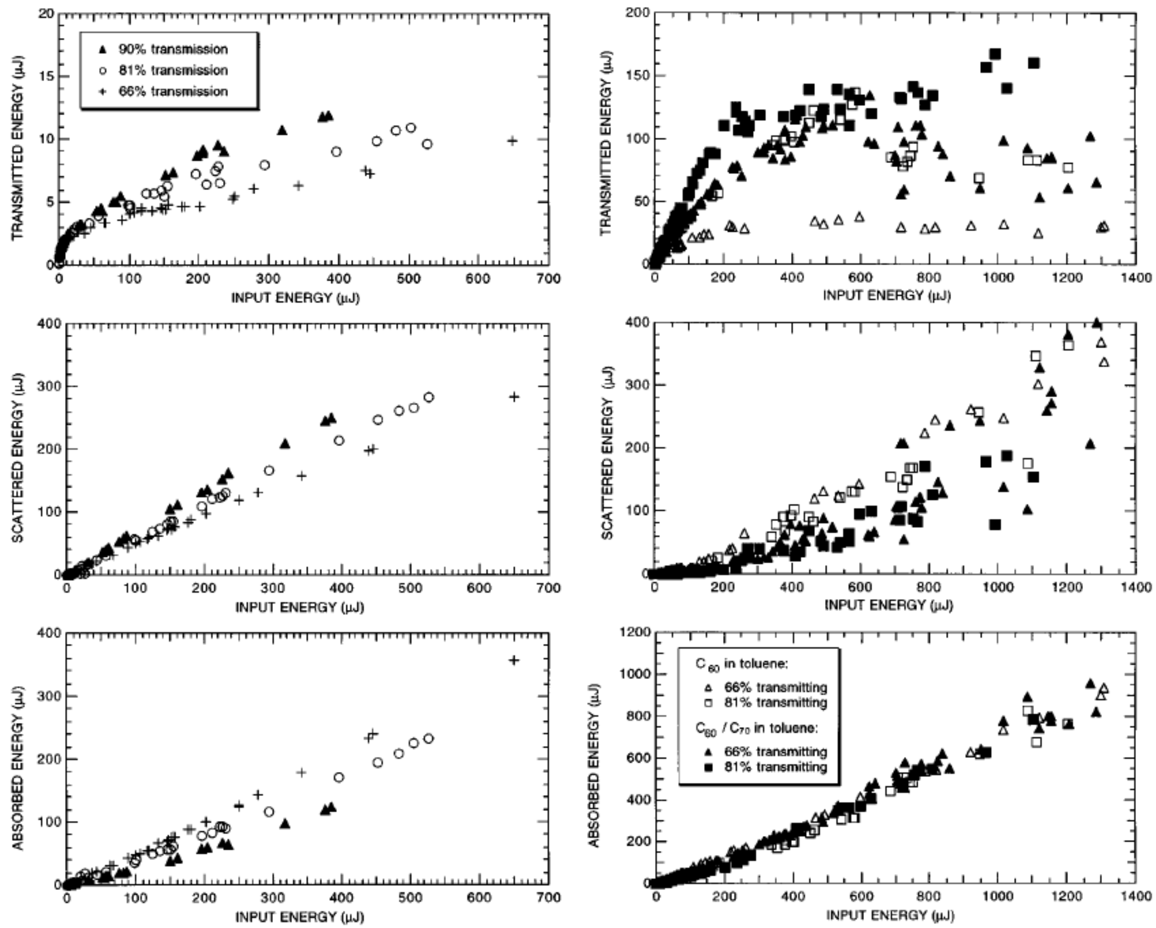

C_{60} Colloid Photophysics

Nanosecond Laser Flash Photolysis

D. M. Guldi, R. E. Huie, P. Neta, H. Hungerbühler and K.-D. Asmus, Chemical Physics Letters **223** (5-6), 511-516 (1994).

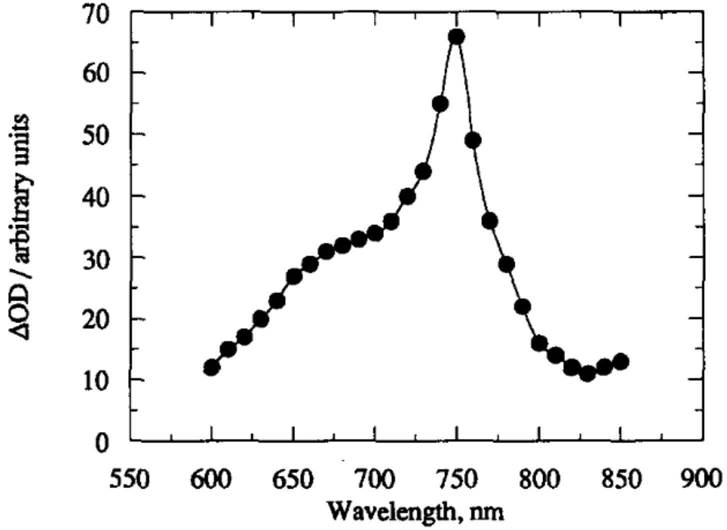

Fig. 1. Differential absorption spectrum obtained upon flash photolysis at 351 nm of 2.0×10^{-5} mol dm^{-3} C_{60}/triton X-100 (reduced form) in a nitrogen saturated aqueous solution.

M. Fujitsuka, H. Kasai, A. Masuhara, S. Okada, H. Oikawa, H. Nakanishi, A. Watanabe and O. Ito, Chem. Lett. (12), 1211-1212 (1997).

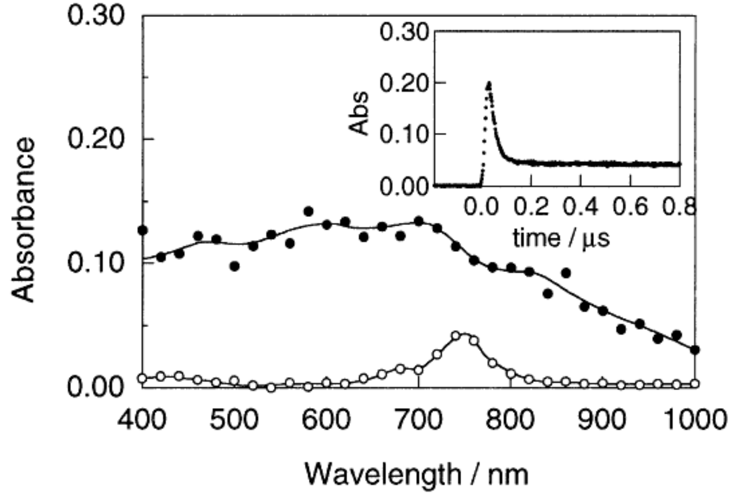

Fig. 4. Transient absorption spectra of C_{60}FP dispersed in ethanol at 50 ns (solid circle) and 500 ns (open circle) after 355 nm laser irradiation. Insert: absorption–time profile at 740 nm.

- ✓ I published C_{60} colloid photophysics on the femtosecond time scale in the course of this dissertation research, which was previously unreported.

A. Fein, Z. Kotler, J. Bar-Sagi, S. Jackel, P. Shaier and B. Zinger, presented at the FRISNO 3. 3rd French-Israeli Symposium on Nonlinear-Optics. Dead Sea, Israel. 6-10 Feb. 1994., 1995

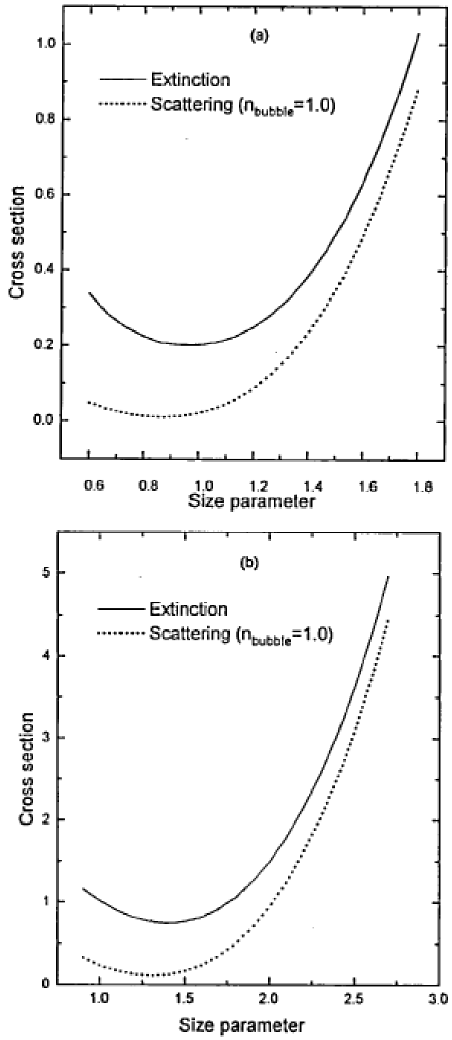

FIGURE 6 Plots of calculated extinction and scattering cross sections as a function of the size parameter $\chi(R) = 2\pi(a+R)/\lambda$ where a is the particle radius, R the bubble radius and λ the wavelength. Refractive indices of the liquid and vapor were 1.33 and 1 respectively. 6a shows the results for a particle radius of 0.1 μm[$\chi(0) = 0.6$], 6b shows the results for a particle radius of 0.15 μm[$\chi(0) = 0.9$].

- NLO threshold in CBS is strongly solvent dependent
- Nonlinear scattering in CBS is strongly solvent dependent
- Emittance is almost independent of solvent
- Proposed mechanism: Solvent boils to form nanobubbles around particles much below the plasma threshold
- Thermodynamic modeling to support proposed mechanism

O. Durand, V. Grolir-Mazza and R. Frey, Journal of the Optical Society of America B (Optical Physics) 16 (9), 1431-1438 (1999).

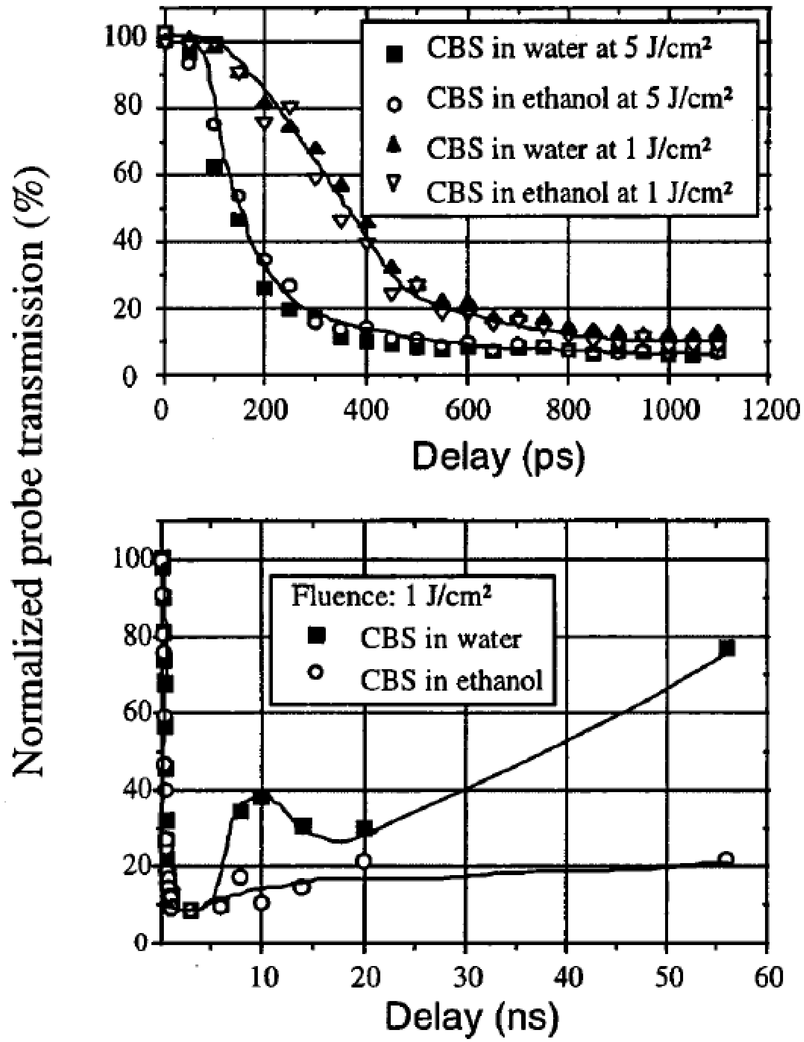

- Time-resolved scattering and pump-probe experiments
- Found that attenuation was only solvent dependent after the first 1-2 ns
- Proposed mechanism: Initial scattering by nanoplasmas followed by additional scattering from bubble growth in the liquid

I. M. Belousova, N. G. Mironova, A. G. Scobelev and M. S. Yur'ev, Opt. Commun. 235 (4-6), 445-452 (2004).

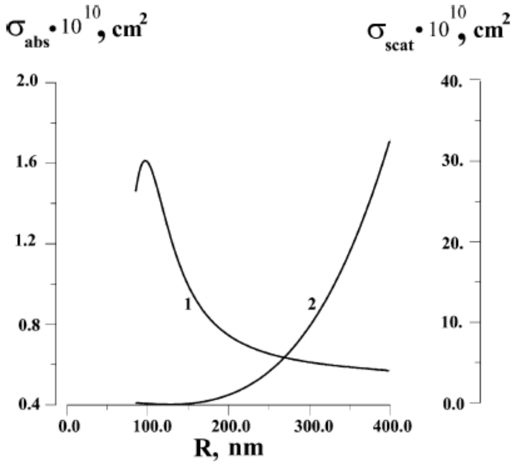

Fig. 3. Absorption (1) and scattering (2) cross-sections versus radius of the vapour shell, computed within the framework of the Mie theory with an effective refractive index, calculated using the Braggeman formulas. Incident wavelength is 1064 nm. Carbon particle radius is 85 nm.

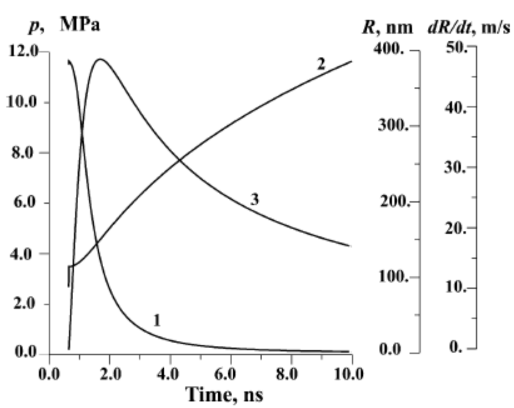

Fig. 4. Theoretical time dependencies of: (1) pressure inside the vapor shell; (2) radius of vapor shell and (3) the rate of its expansion in the front part of the cell. The input energy density is 0.4 J/cm^2, pulse duration is 10 ns, incident wavelength is 1064 nm, carbon particle radius is 85 nm.

- Thermodynamic model
- Proposed mechanism: heating of the particles by absorbed light, formation of a vapor shell by explosive boiling of the liquid surrounding the particle, and growth of this shell
- Qualitative agreement between model and experiment

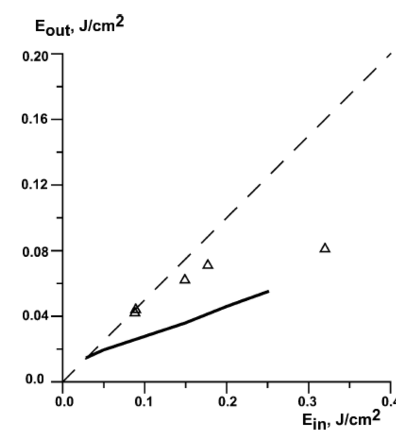

T. W. Ebbesen, K. Tanigaki and S. Kuroshima, Chemical Physics Letters 181 (6), 501-504 (1991).

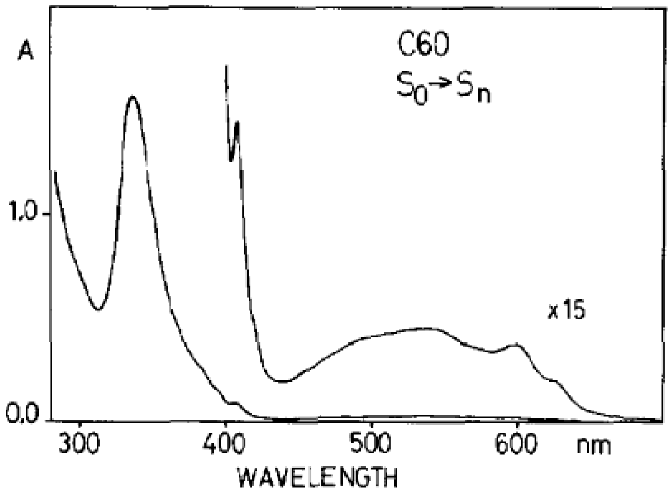

- Ground state absorption spectrum
- Singlet excited state absorption spectrum
- Triplet excited state absorption spectrum

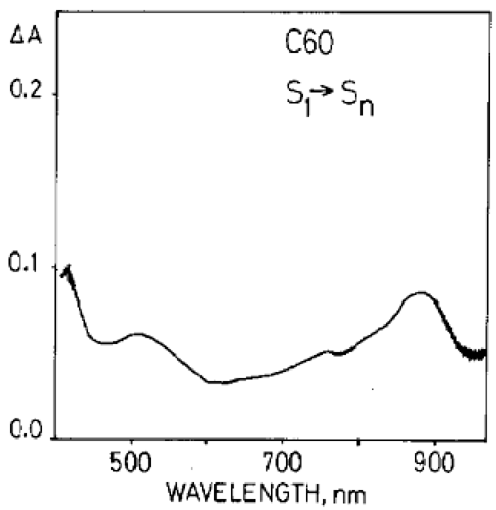

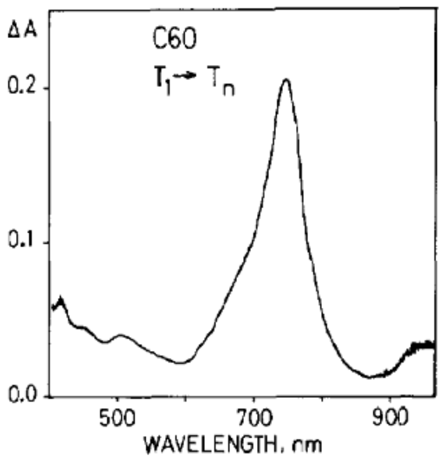

R. J. Sension, C. M. Phillips, A. Z. Szarka, W. J. Romanow, A. R. McGhie, J. P. McCauley, A. B. Smith and R. M. Hochstrasser, J. Phys. Chem. 95 (16), 6075-6078 (1991).

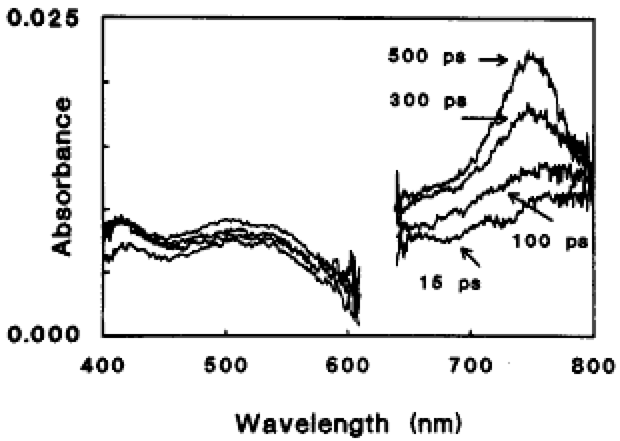

Figure 2. Transient absorption spectra of C_{60} in toluene obtained for delay times of 15, 100, 300, and 500 ps. The pump wavelength is 520 nm.

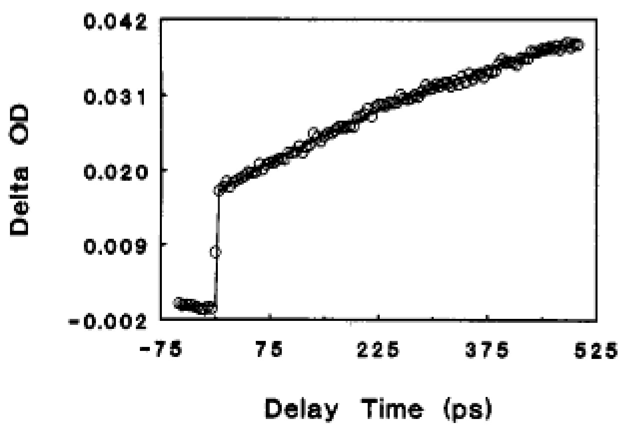

Figure 3. Transient absorption kinetics for C_{60} in toluene pumped at 520 nm and probed at 740 nm. An identical result was obtained when the sample was pumped at 312 or 624 nm. The solid line represents a fit of the data to the following functional form: $A_1 \exp(-t/650 \text{ ps}) + A_2[1 - \exp(-t/650 \text{ ps})]$. Additional data obtained for short delay times and using a smaller step size indicate that the initial rise is instrument limited where the instrument response function is ca. 500 fs.

- Transient absorption studies of C_{60}
- Reported rates corresponding to 5-level model

C. P. Singh and S. Roy, Optical Engineering 43 (2), 426-431 (2004).

- Applied C_{60} to all-optical switching

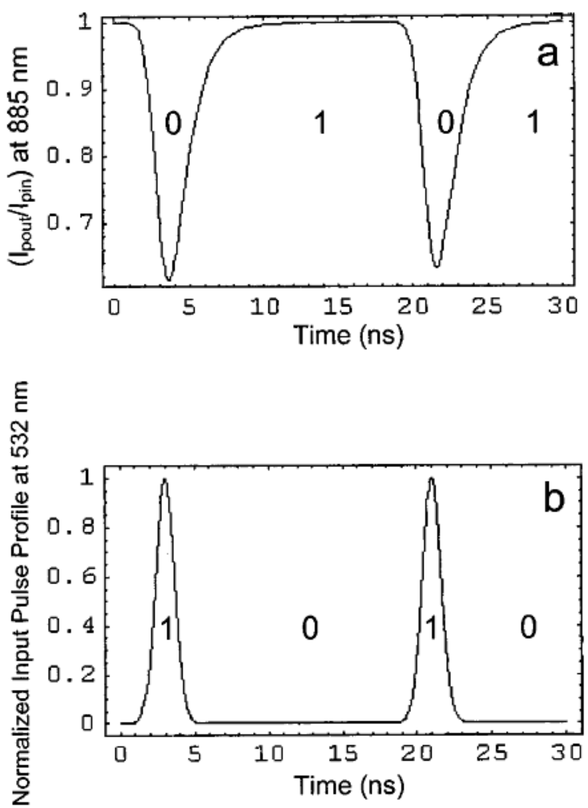

Fig. 7 All-optical inverter (NOT) logic gate (a) variation of normalized transmitted intensity of the probe beam (I_{pout}/I_{pin}) at 885 nm as output with time; (b) normalized input pulse profile at 532 nm.

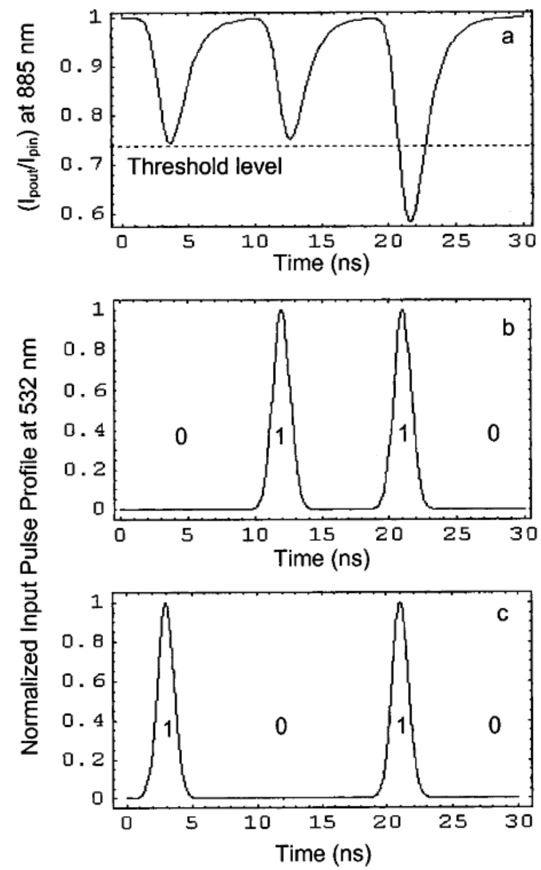

Fig. 8 All-optical logic operations: (a) NOR gate function (without threshold) and NAND gate function (with threshold), with variation of normalized transmitted intensity of the probe laser beam at 885 nm as output with time; (b) and (c) normalized pulse profiles of the two inputs1 and 2 at 532 nm.

C_{60} Colloid Syntheses

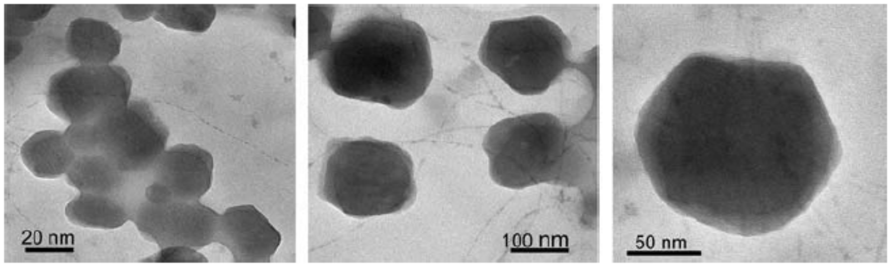

J. Brant, H. Lecoanet, M. Hotze and M. Wiesner, Environmental Science & Technology **39** (17), 6343-6351 (2005).

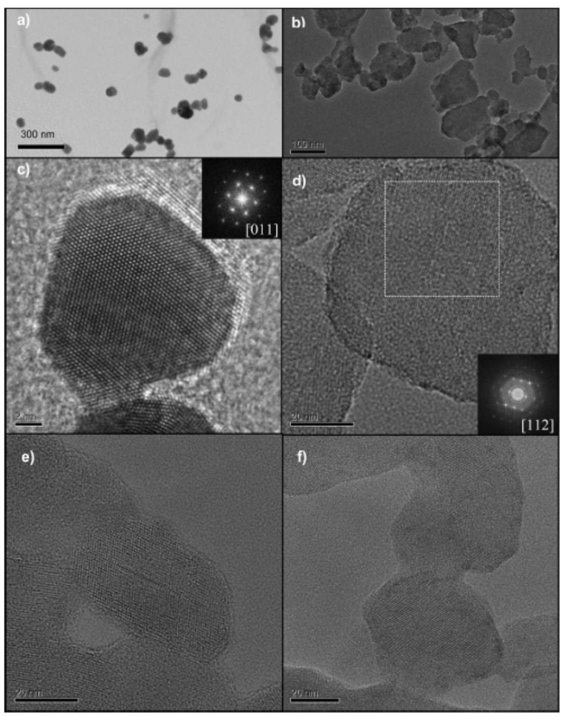

L. Duncan, J. Jinschek, P. Vikesland, Environmental Science & Technology **42** (1), 173-178 (2008).

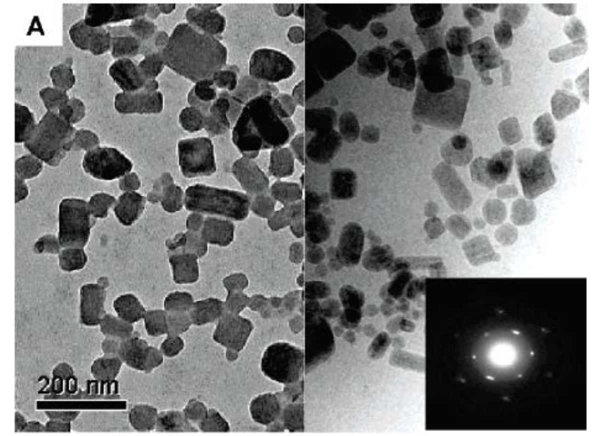

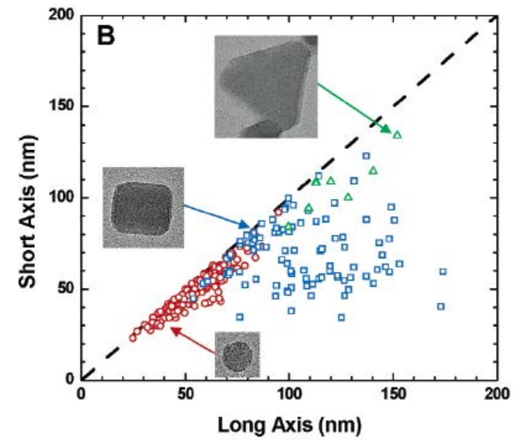

J. D. Fortner, D. Y. Lyon, C. M. Sayes, A. M. Boyd, J. C. Falkner, E. M. Hotze, L. B. Alemany, Y. J. Tao, W. Guo, K. D. Ausman, V. L. Colvin and J. B. Hughes, Environ. Sci. Technol. **39** (11), 4307-4316 (2005).

R. Goedert, R. Becker, A. Clements and T. Whittaker, J. Opt. Soc. Am. B-Opt. Phys. 15 (5), 1442-1462 (1998).

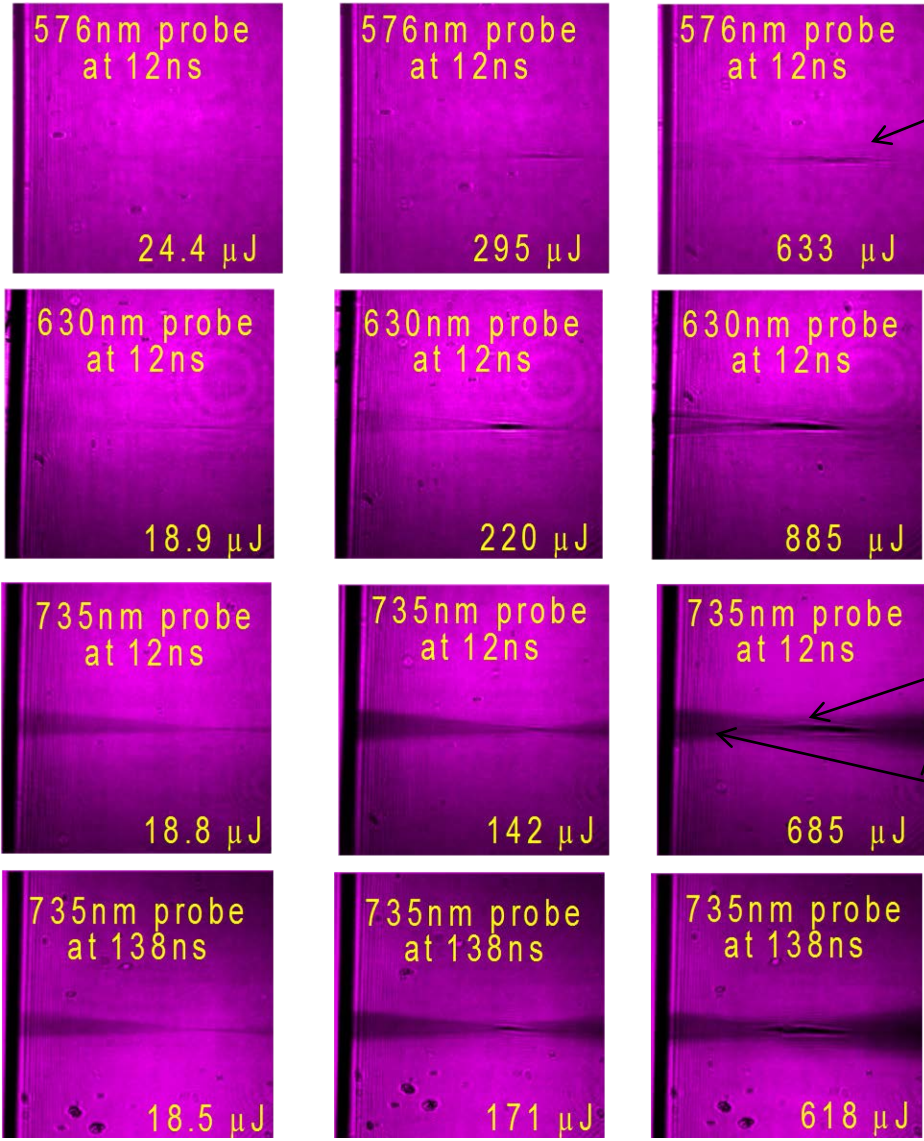

Purely refractive image: Gradient in PMMA refractive index

Refractive Index Gradient

Triplet Absorption

- Examined C60 in PMMA with shadowgraph technique
- Saw evidence of long-lived RSA as well as nonlinear refraction

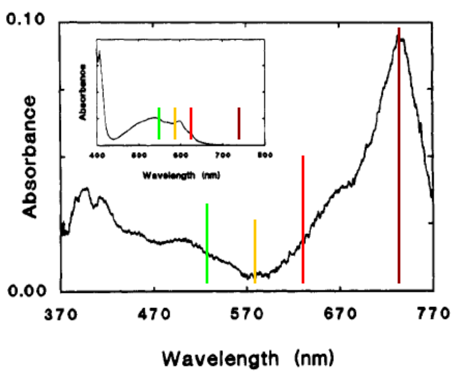

Triplet absorption spectrum of C60. (Inset, ground state absorption of C60.) Colored lines: shadowgraph probes and excitation wavelength..

DISSERTATION RESEARCH

C_{60}-1 Synthesis

C_{60}/Toluene solution

↓

Triton X-100 added

↓

Bubbled with Argon at 50° C to evaporate

↓

Dark brown residue
(C_{60} and Triton-X-100)

↓

De-ionized H_2O added incrementally
w/ sonication between additions

↓

Dark brown suspension

↓

Filtered 0.22 μm

↓

Dark brown suspension
(C_{60} Colloids in 15:85 Triton X-100: H_2O solution)

C_{60}-2 Synthesis

C_{60}/NMP solution

↓

Added dropwise to Triton X-100:H_2O solution while stirring

↓

Dialyzed against de-ionized water

↓

Freeze-dried

↓

Dark brown residue
(C_{60} and Triton-X-100)

↓

De-ionized H_2O added incrementally
w/ sonication between additions

↓

Dark brown suspension

↓

Filtered 0.22 μm

↓

Dark brown suspension
(C_{60} Colloids in 11:89 Triton X-100: H_2O solution)

Dynamic Light Scattering

- Brownian motion: Movement of suspended particles due to collisions with solvent molecules. Small particles move faster and farther than large particles.
- Velocity of Brownian motion related to particle size via the Stokes-Einstein equation.

$$d = \frac{kT}{3\pi\eta D}$$

- Laser light scattered from a collection of particles forms a speckle pattern, which fluctuates because the particles are always in motion.
- DLS instruments use autocorrelators to compare the irradiance signal from the scattered light with itself at different times. The signal stays correlated longer for large particles than small particles.
- Data presented in different bases:
  - Z-Average: Best single-exponential fit to the correlogram.
  - Intensity Distribution: Multiple-exponential fits build a distribution of sizes vs. the intensity of light scattered. Weighted to larger particles because the intensity scattered is proportional to the 6^{th} power of the radius.
  - Volume Distribution: Calculated from intensity distribution via Mie theory.
  - Number Distribution: Calculated from volume distribution via Mie theory. (How many particles there actually are of each size.)

Nanoparticle Tracking Analysis

- Light scattered from particles is focused to a CCD camera, forming bright dots, even though the particles are below optical resolution.
- Video is taken of the bright dots as the particles move under Brownian motion.
- Software tracks each particle individually and calculates the particle size distribution of the sample.

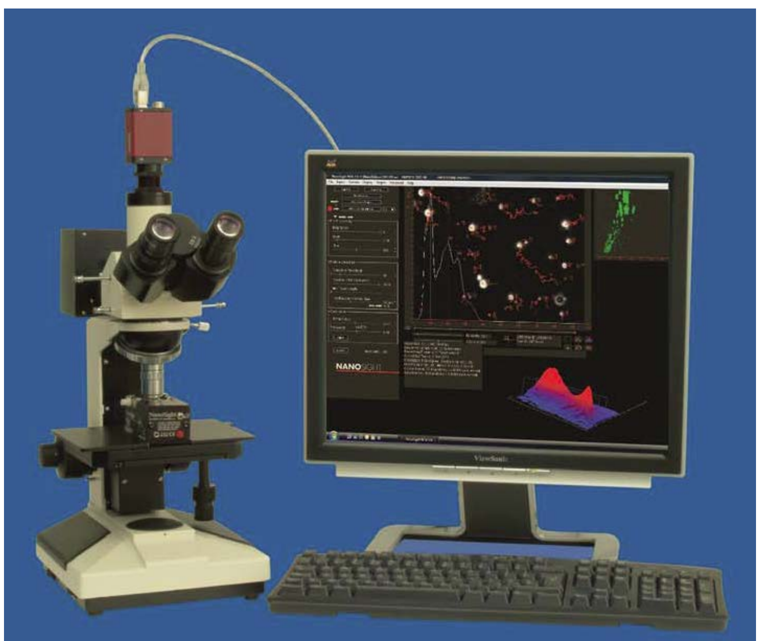

- Distributions are given in number density.
- Smaller sample volume than DLS.
- Difficulty with particles less than 50 nm diameter.

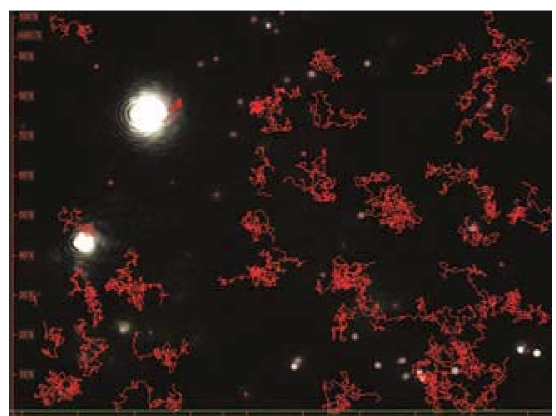

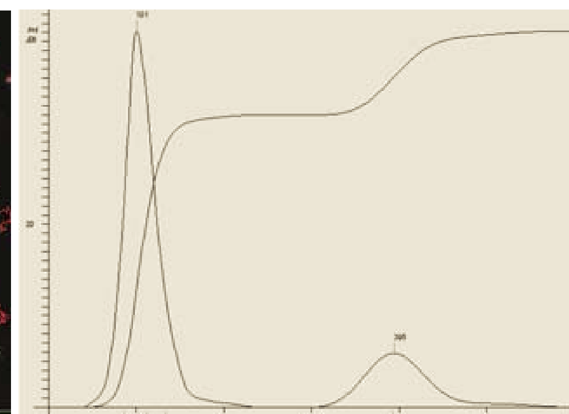

Images from www.nanosight.com

Modeling: Nonlinear Scattering Alternate Approach

Egerev gives the following equation to estimate the critical fluence for bubble formation:

$$F_c = \frac{\chi_l \tau_L}{\sigma_{abs}} \frac{4\pi R_{np} c_l \rho_l T_b}{\left\{1 + \frac{\xi_1}{\xi_2 - \xi_1} erfcx\left(\xi_2 \frac{\sqrt{\chi_l \tau_L}}{R_{np}}\right) - \frac{\xi_1}{\xi_2 - \xi_1} erfcx\left(\xi_1 \frac{\sqrt{\chi_l \tau_L}}{R_{np}}\right)\right\}}$$

where χ_l is the thermal diffusivity of the liquid, τ_L is the laser pulse length, c_l is the specific heat capacity of the liquid, ρ_l is the density of the liquid, and T_b is the boiling temperature of the liquid. The values for $\xi_{1,2}$ are given by:

$$\xi_{1,2} = \frac{3}{2}\left[\propto \mp \sqrt{\propto(\propto - 4/3)}\right]$$

where

$$\alpha = \frac{c_l \rho_l}{c_{np} \rho_{np}}$$

For short pulses ($\chi_l \tau_L << R_{np}^2$), the critical fluence relation simplifies to:

$$F_c = V_{np} c_{np} \rho_{np} T_b / \sigma_{abs}$$

where V_{np}, c_{np}, and ρ_{np} are the volume, specific heat capacity, and density of the nanoparticle.

For long pulses ($\chi_l \tau_L >> R_{np}^2$), the critical fluence relation simplifies to:

$$F_c = 4\pi R_{np} c_l \rho_l T_b \chi_l \tau_L / \sigma_{abs}$$

Modeling: Nonlinear Scattering Alternate Approach

Once the initial bubble radius was calculated, the model calculated the resulting extinction coefficients (scattering, absorption, and total) via Mie theory.
Two approaches were used in the Mie calculations:

1) Treating the scattering center as a bubble with a refractive index of 1.
2) Treating the scattering center as a bubble surrounding the nanoparticle (concentric spheres) using the Maxwell Garnett average dielectric function to calculate an effective complex refractive index.

The Maxwell Garnett average dielectric function is:

$$\epsilon_{av} = \epsilon_m \left[1 + \left\{3f\left(\frac{\epsilon_i - \epsilon_m}{\epsilon_i + 2\epsilon_m}\right) \Big/ \left[1 - f\left(\frac{\epsilon_i - \epsilon_m}{\epsilon_i + 2\epsilon_m}\right)\right]\right\}\right]$$

where f is the volume fraction of the inclusion(s), ε_i is the dielectric permittivity of the inclusion (particle), ε_m is the dielectric permittivity of the medium (vapor bubble), and ε_{av} is the dielectric permittivity of the entire structure treated as one effective spherical particle. The complex refractive index can then be determined by:

$$N = c\sqrt{\epsilon\mu} = n + ik$$

where N is the complex refractive index, c is the speed of light in vacuum, ε is the dielectric permittivity, μ is the magnetic permeability, n is the real part of the refractive index and k is the imaginary part of the refractive index.

Mie calculations were done via the BHMIE program published by Bohren & Huffman.

Modeling of Total Scattering Results for C_{60}-1

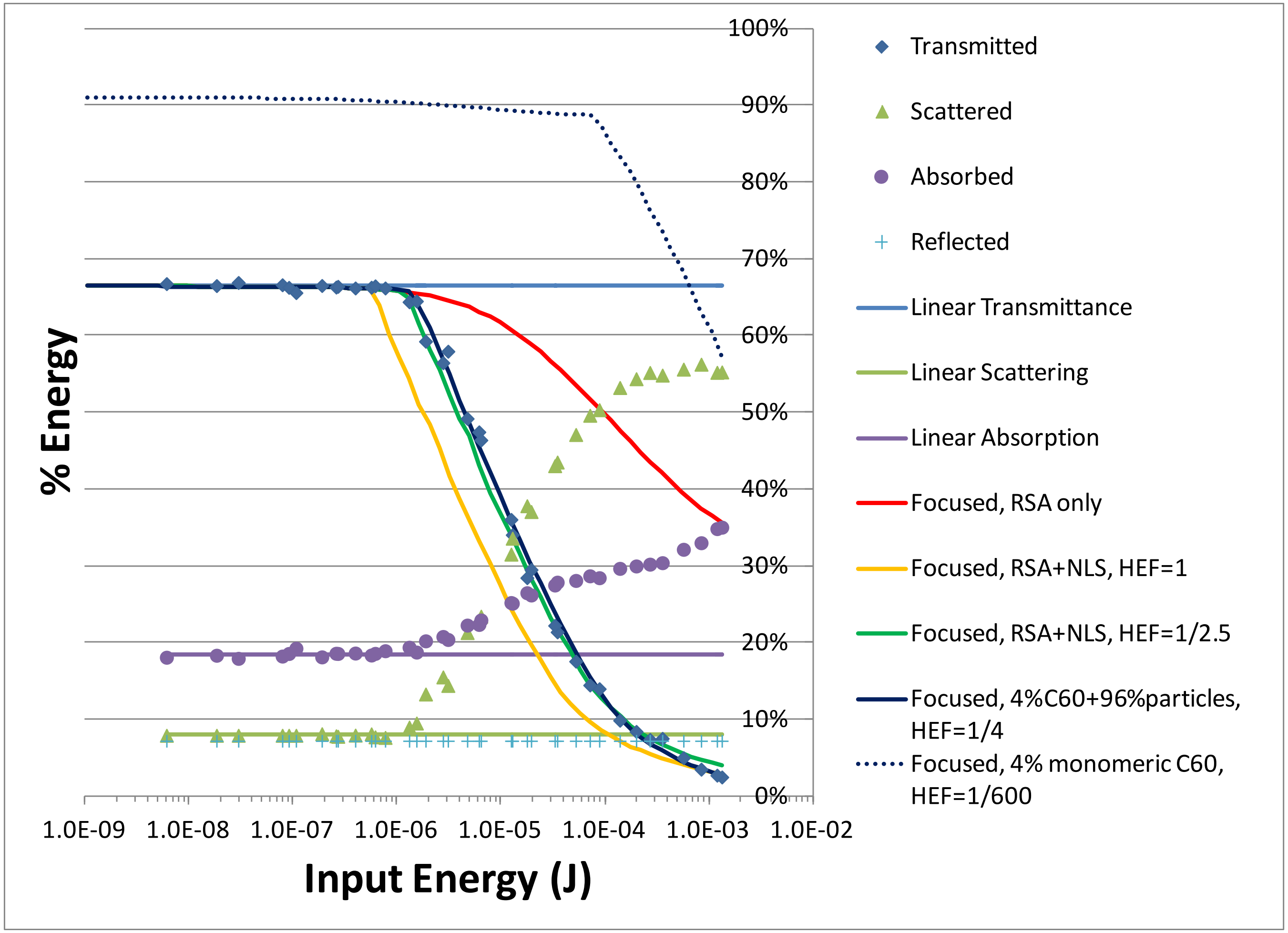

- The data can be interpreted either as 4% monomeric C_{60} providing RSA and 96% fully quenched colloid particles providing only NLS, or as all C_{60} molecules participating in RSA, but strongly quenched.

Modeling of Total Scattering Results for C_{60}-2

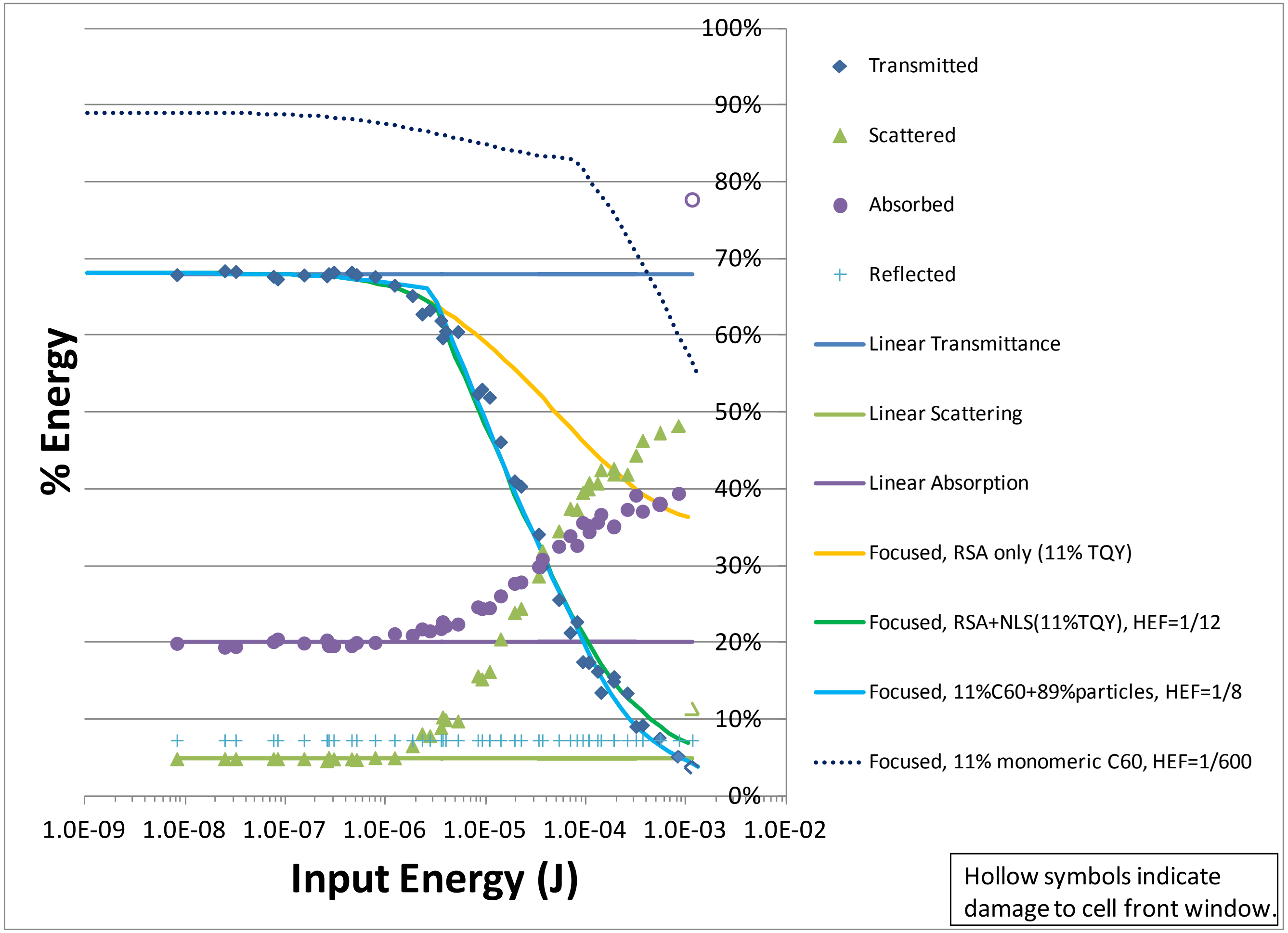

- The data fits better assuming that all C_{60} molecules are participating in RSA, but with significant quenching of the first excited singlet state than it does assuming that all RSA comes from monomeric C_{60} micelles and that colloid particles act only as scatterers.

Modeling of Total Scattering Results for C_{60}-2

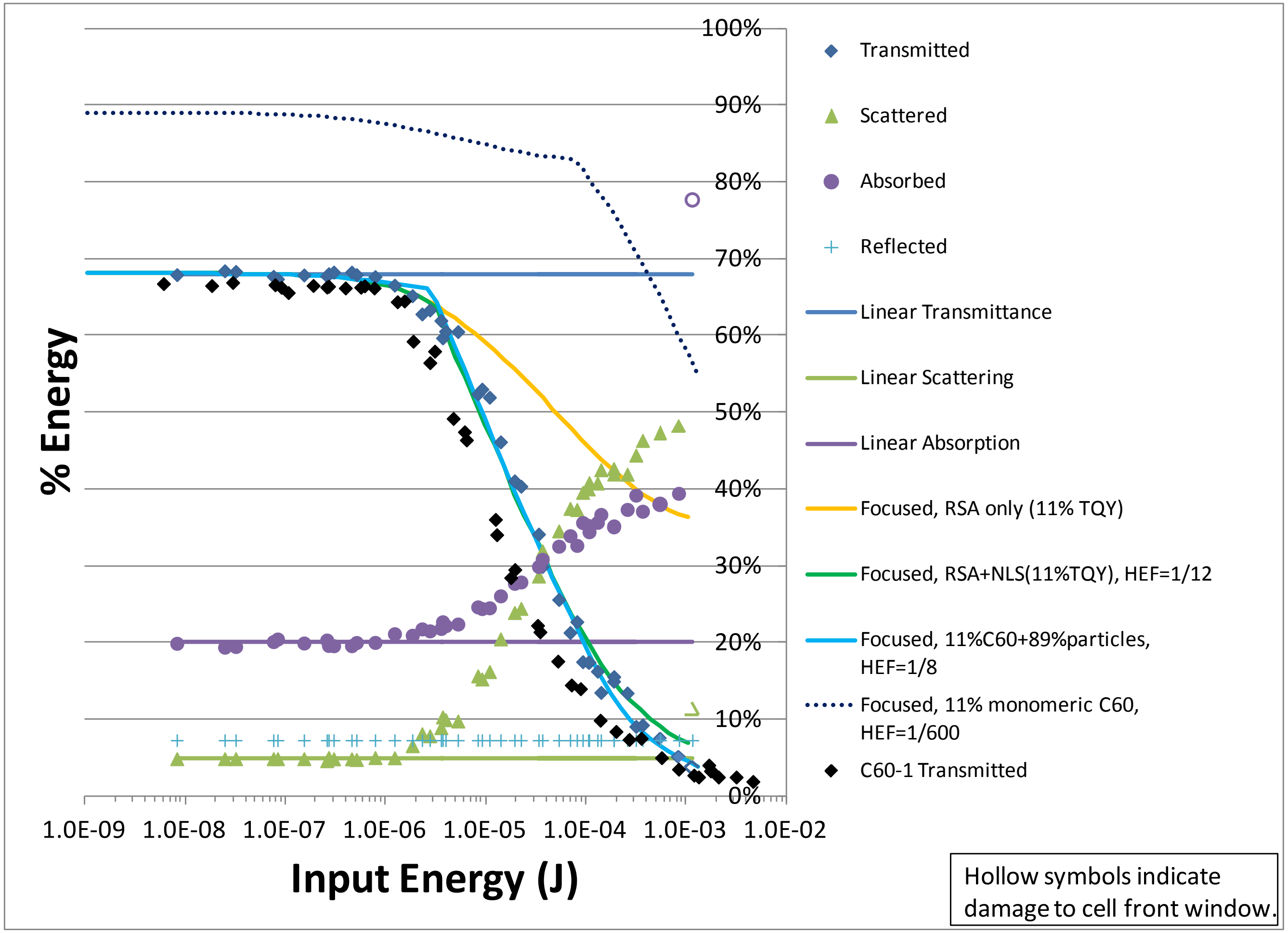

- C_{60}-2 has a higher NLS threshold than C_{60}-1. This implies that C_{60}-2 is less efficient at heating to sublimation. Since the particle size distributions are so similar, this difference in NLS threshold is not likely explained by particle size. Rather, it is more likely that the population in the triplet state contributes less to heating the particles. The triplet states are long-lived, so a portion of the energy is stored as electronic energy and cannot convert to heat until well after the input pulse.